

**Cultivation of Hepatitis B Virus Producing
Cell Line HepG2.2.15 on Microcarrier
and
Functional Characterization of the
Hepatitis B Virus Polymerase**

DISSERTATION

zur Erlangung des akademischen Grades
doctor rerum naturalium
(Dr. rer. nat.)
im Fach Biologie

eingereicht an der
Mathematisch-Naturwissenschaftlichen Fakultät I
der Humboldt-Universität zu Berlin

von
Dipl.-Ing. (FH) Joachim Lupberger
geboren am 3. Oktober 1974 in Ravensburg

Präsident der Humboldt-Universität zu Berlin
Prof. Dr. Christoph Marksches

Dekan der Mathematisch-Naturwissenschaftlichen Fakultät I
Prof. Dr. Christian Limberg

Gutachter: 1. Prof. Dr. Detlev Krüger, Charité, Berlin
2. Prof. Dr. Georg Pauli, Robert Koch-Institut, Berlin
3. Prof. Dr. Hans Will, Heinrich-Pette-Institut, Hamburg

eingereicht: 12. Dezember 2006

Datum der Promotion: 27. April 2007

ZUSAMMENFASSUNG

Hepatitis B Virus (HBV) Infektionen verursachen entzündliche Erkrankungen der Leber. Insbesondere die frühen Phasen des HBV Lebenszyklus sind noch nicht geklärt, so ist z.B. der Rezeptorkomplex an den HBV bindet unbekannt. Mittlerweile stehen neue Infektionsmodelle zur Verfügung um den HBV Lebenszyklus zu untersuchen. Dies erfordert eine effiziente Zellkultur basierende Methode um große Mengen infektiöser Partikel zu generieren. Ein Ziel der Arbeit war durch Kultivierung auf Mikrocarrier die HBV Produktion der Zelllinie HepG2.2.15 zu steigern. Die Analyse von Protein und HBV Sekretion, Infektiösität und MAP Signalübertragung ergab eine 18x höhere HBV Produktion bei einer reduzierten Sekretion von subviralen Partikeln durch HepG2.2.15 die auf Mikrocarrier kultiviert wurden. Der Anstieg der Virusproduktion korreliert mit einer verstärkten Aktivierung der MAP Kinase ERK-2, die mit HBV Replikation in Verbindung steht.

Ein weiterer wenig verstandener Teil des HBV Lebenszyklus ist der Kernimport des HBV Genoms. Spuren der viralen Polymerase finden sich im Zellkern von HBV infizierten Zellen. Ziel der Arbeit war, Motive in der HBV Polymerase zu finden, die in der Lage sind Zelllokalisierung zu beeinflussen. Durch Sequenzvergleich wurde eine konservierte zweiseitige Kernlokalisationssequenz im Terminalen Protein der HBV Polymerase identifiziert, die eine Proteinkinase CKII Erkennungsstelle enthält. Inhibition der CKII Aktivität in HBV infizierten primären Hepatozyten sowie die Zerstörung der CKII Erkennungsstelle im Terminalen Protein inhibieren die HBV Replikation. Die Funktionalität der Kernlokalisationssequenz wurde durch Fusion an GFP bestätigt und war Abhängig von CKII Aktivität in der Zelle. Dies wurde *in vitro* durch Bindung des Adapterproteins Karyopherin-alpha an CKII-phosphoryliertes Terminales Protein bestätigt. Die HBV Polymerase enthält eine konservierte zweiseitige Kernlokalisationssequenz deren Funktionalität durch CKII Phosphorylierung vermittelt wird.

SCHLAGWORTE: Mikrocarrier, HepG2.2.15, HBV, Virologie, Polymerase, CKII, NLS, Kernimport

ABSTRACT

Hepatitis B virus (HBV) infection causes acute and chronic liver inflammation. Especially the early phase of the HBV life cycle is not clearly understood. For example the receptor complex that mediates viral entry is not known. Novel infection models to study the HBV lifecycle are described that demand for a large amount of cell culture generated infectious HBV particles. One aim was to enhance HBV production of the cell line HepG2.2.15 by cultivation on microcarrier substrate. Analysis of protein and viral particle secretion, infectivity, and cellular MAP kinase signaling revealed an up to 18x increased HBV production and a decreased subviral particle secretion by HepG2.2.15 when cultivated on microcarrier. The observed effect was due to an enhanced phospho-activation of MAP kinase ERK-2 that is tightly associated with HBV replication.

Another poorly understood part of the HBV lifecycle is the mechanism that delivers the HBV genome into the nucleus. Traces of HBV polymerase can be found in HBV infected cells. The second objective was to identify motifs on the HBV polymerase that determine its subcellular localization. By sequence alignment a conserved bipartite nuclear localization signal was found in the terminal protein of the HBV polymerase encompassing a protein kinase CKII recognition site. Inhibition of CKII kinase in infected primary hepatocytes and destruction of the identified CKII recognition site in the viral polymerase impaired virus production. The functionality of the putative nuclear localization signal was confirmed by fusion to GFP. Moreover, its functionality was depended on CKII activity that was verified by *in vitro* binding experiments of terminal protein to the import adaptor karyopherin-alpha. This data identified a nuclear localization signal in the HBV polymerase, which functionality is mediated by CKII phosphorylation.

KEYWORDS: microcarrier, HepG2.2.15, HBV, virology, polymerase, CKII, NLS, nuclear, import

TABLE of CONTENT

ZUSAMMENFASSUNG	2
ABSTRACT.....	3
TABLE of CONTENT	4
LIST of ABBREVIATIONS	8
LIST of FIGURES	10
LIST of TABLES	12
1 INTRODUCTION	14
1.1 Hepatitis B	14
1.1.1 Disease	14
1.1.2 HBV epidemiology	14
1.1.3 Prevention and treatment.....	16
1.2 Hepatitis B virus	16
1.2.1 Genome organization and structure.....	16
1.2.2 HBV species and subtypes	19
1.3 HBV lifecycle	21
1.4 HBV regulatory proteins.....	24
1.5 Infection models.....	25
1.6 HBV particles for infection models	26
1.7 HBV polymerase.....	27
1.8 Nuclear import mechanism	28
1.9 Nuclear localization signals	29
1.10 Regulation of nuclear import	33
1.10.1 Proteolysis.....	34
1.10.2 NLS masking.....	34
1.10.3 Phosphorylation	34
2 THESIS OBJECTIVES.....	36
2.1 Upscale of HBV production.....	36
2.2 Subcellular localization of the HBV polymerase	36
3 MATERIALS	37
3.1 Viruses, cells and animals	37
3.1.1 Viruses	37
3.1.2 Bacterial strains.....	37
3.1.3 Cell lines	37

3.1.4	Animals	38
3.2	Chemicals.....	38
3.2.1	Plasmids	38
3.2.2	Synthetic Oligonucleotides	39
3.2.3	Molecular Weight Calibrators.....	39
3.2.4	Antibodies	40
3.2.5	Enzymes.....	40
3.2.6	Radiochemicals	41
3.2.7	Reagents for cell culture.....	41
3.2.8	Inhibitors	42
3.2.9	Fine chemicals.....	42
3.2.10	Drugs.....	43
3.2.11	Membranes and relevant plastic ware	43
3.3	Buffers and solutions	44
3.4	Kits.....	44
3.5	Devices.....	44
3.5.1	Chromatography.....	44
3.5.2	Electrophoresis.....	44
3.5.3	Microscopy.....	45
3.5.4	PCR cycler	45
3.5.5	Imaging	45
3.5.6	Centrifugation	45
3.5.7	Other devices.....	46
4	METHODS	47
4.1	Cell culture.....	47
4.1.1	Prokaryotic cell culture and protein expression	47
4.1.2	Eukaryotic cell culture	47
4.1.3	Adherent cell culture on microcarrier	48
4.1.4	Cell trypsination.....	48
4.1.5	Collagen coating	48
4.1.6	Silane coating.....	49
4.1.7	Cell counting.....	49
4.1.8	Transfection of hepatoma cells	49
4.1.9	Preparation of primary hepatocytes.....	49
4.2	RNA and DNA manipulation.....	51
4.2.1	RNA preparation.....	51
4.2.2	Virus DNA preparation.....	51
4.2.2.1	Adsorber method	51
4.2.2.2	Phenol/chloroform method.....	51
4.2.3	Restriction enzyme reaction.....	51

4.2.4	Dephosphorylation of vector DNA	52
4.2.5	Ligation of DNA	52
4.2.6	Transformation of DNA	52
4.2.7	Plasmid extraction	52
4.2.8	Polymerase chain reaction (PCR)	53
4.2.8.1	Standard PCR	53
4.2.8.2	Quantitative PCR.....	53
4.2.8.3	Site directed mutagenesis	54
4.2.9	Agarose electrophoresis	54
4.2.10	DNA extraction from agarose gels.....	55
4.2.11	Sequencing and sequence analysis.....	55
4.2.12	Northern blot.....	55
4.2.13	Southern blot.....	56
4.2.14	Endogenous Polymerase Assay (EPA).....	56
4.3	Cell lysis	56
4.3.1	Enzymatic cell lysis.....	56
4.3.2	Cell lysis using detergent	57
4.3.3	French Press	57
4.4	Protein chemistry	58
4.4.1	Protein quantification	58
4.4.1.1	Optical density.....	58
4.4.1.2	Bradford assay.....	58
4.4.2	SDS-PAGE electrophoresis.....	58
4.4.3	Silver staining	59
4.4.4	Western blot	59
4.4.5	Immuno-histology	60
4.4.6	In vitro phosphorylation.....	60
4.5	Microscopy	61
4.5.1	Confocal laser scanning microscopy.....	61
4.5.2	Electron microscopy.....	61
4.6	Antibody generation.....	61
4.7	Protein purification	62
4.7.1	Nickel-chelating chromatography	62
4.7.2	Cationic exchange chromatography	64
4.7.3	Gel filtration.....	64
4.7.4	Ammonium sulfate precipitation.....	64
4.7.5	Antibody affinity purification	65
4.7.6	TP binding partner fishing	66

5	RESULTS	68
5.1	Cultivation of HepG2.2.15 on Cytodex-3	68
5.1.1	Identification of the optimal cell density	68
5.1.2	HBV production and antigen secretion	70
5.1.3	Virus infectivity	72
5.1.4	Effect on cellular signaling	74
5.2	Generation and purification of P directed antibodies	76
5.2.1	Purification and immobilization of recombinant TP and S domain	76
5.2.2	TP and S directed antibody	76
5.3	Nuclear import of the HBV polymerase	81
5.3.1	Identification of conserved motifs on the HBV polymerase	81
5.3.2	TP domain is phosphorylated by protein kinases PKC and CKII	82
5.3.3	PKC and CKII phosphorylation affect HBV replication.....	83
5.3.4	P protein harbors a functional bipartite NLS, which depends on phosphorylation ...	87
5.3.5	Binding of karyopherin- α 2 to TP depends on CKII mediated phosphorylation	89
5.3.6	Ab initio modeling of the TP domain tertiary structure	90
6	DISCUSSION.....	92
6.1	Cultivation of HepG2.2.15 on microcarrier increases HBV replication	92
6.2	PKC phosphorylation of HBV polymerase impairs virus replication	94
6.3	Nuclear import of the HBV polymerase is mediated by a bipartite NLS and depends on CKII phosphorylation.....	95
	REFERENCES.....	100
	APPENDIX 1.....	109
	APPENDIX 2.....	112
	ACKNOWLEDGEMENT.....	113
	ASSURANCE of RESEARCH	115
	CURRICULUM VITAE.....	116
	PUBLICATIONS	119

LIST of ABBREVIATIONS

6-FAM	6-Carboxyfluorescein
ATP	Adenosine triphosphate
AU	Absorption unit
BSA	Bovine serum albumin
cccDNA	Covalently closed circular DNA
CKII	Protein kinase CKII (formerly known as casein kinase II)
cv	Column volume
DAPI	2-(4-Amidinophenyl)-6-indolecarbamide dihydrochloride
DHBV	Duck hepatitis B virus
DMAT	2-Dimethylamino-4,5,6,7-tetrabromo-1H-benzimidazole
DMSO	Dimethyl sulfoxide
DR	Direct repeat
dw	Dry weight
EDTA	Ethylenediaminetetraacetic acid
EGTA	Ethylene glycol-bis(2-aminoethylether)- <i>N,N,N',N'</i> -tetraacetic acid
ELISA	Enzyme-linked immunosorbent assay
EPA	Endogenous polymerase assay
ERK	Extracellular signal-regulated kinase
FCS	Fetal calf serum
GE	Genome equivalent
GFP	Green fluorescent protein
GTP	Guanosine 5'-triphosphate
HBeAg	Hepatitis B virus early antigen
HBsAg	Hepatitis B virus surface antigen
HBV	Hepatitis B virus
HCC	Hepatocellular carcinoma
IPTG	Isopropyl β -D-1-thiogalactopyranoside
LHBsAg	Large hepatitis B virus surface antigen
Mab	Monoclonal antibody

MAP	Mitogen-activated protein
MHBsAg	Middle hepatitis B virus antigen
mRNA	Messenger RNA
MW	Molecular weight
MWCO	Molecular weight cut off
NHS	N-Hydroxysuccinimide
NLS	Nuclear localization signal
NPC	Nuclear pore complex
NTA	Nitrilotriacetic acid
NTP	Nucleotide triphosphate
ORF	Open reading frame
P	Hepatitis B virus polymerase
Pab	Polyclonal antibody
PAGE	Polyacrylamide
PCNA	Proliferating cell nuclear antigen
PCR	Polymerase chain reaction
pgRNA	Pre-genomic RNA
PKC	Protein kinase C
PML	Promyelocytic leukemia bodies
REM	Raster electron microscopy
rpm	Rotation per minute
RT	Reverse transcriptase
S (context HBsAg)	S reading frame of hepatitis B virus genome
S (context P)	Spacer domain of hepatitis B virus polymerase
SDS	Sodium dodecyl sulfate
SHBsAg	Small hepatitis B virus surface antigen
siRNA	Small interfering RNA
TAMRA	Carboxytetramethylrhodamine
TP	Terminal protein domain of the hepatitis B virus polymerase
UV	Ultraviolet
WHBV	Woodchuck hepatitis B virus

LIST of FIGURES

Figure 1:	Worldwide prevalence of chronic hepatitis B.....	15
Figure 2:	HBV genome organization.....	17
Figure 3:	HBV structure.....	18
Figure 4:	Electron microscopy of HBV particles.....	19
Figure 5:	Phylogenetic relationship of HBV genotypes.....	20
Figure 6:	Scheme of the HBV lifecycle within a hepatocyte.....	22
Figure 7:	Large asian tree shrew (<i>Tupaia belangeri</i>).....	26
Figure 8:	Scheme of the HBV polymerase (ayw).....	27
Figure 9:	Karyopherin- α mediated shuttling of cargo into the nucleus.....	29
Figure 10:	Crystal structure of karyopherin- α 2 (<i>Saccharomyces cerevisiae</i>) binding a bipartite NLS from nucleoplasmin (<i>Xenopus laevis</i>).....	33
Figure 11:	Collagenase perfusion of <i>Tupaia</i> liver tissue.....	50
Figure 12:	Scheme of a semi-dry blotting stack.....	59
Figure 13:	Generation of an antigen-adjuvant emulsion.....	62
Figure 14:	Purification principle of nickel-chelating chromatography.....	63
Figure 15:	Immobilization and subsequent <i>in vitro</i> phosphorylation of TP domain on Ni-NTA Superflow.....	67
Figure 16:	Optimal cell density for HBV production and cell attachment of HepG2.2.15 on Cytodex-3 after 48 h.....	69
Figure 17:	Comparison of HepG2.2.15 virus production on Cytodex-3 (dark bars) versus stationary culture flask (striped bars) over 72 h.....	71
Figure 18:	Analysis of cell number and cell differentiation of HepG2.2.15 cells grown on microcarrier or stationary culture.....	72
Figure 19:	Comparative quantification of viral particles secreted from HepG2.2.15 grown on microcarrier and in stationary culture.....	74

Figure 20:	Comparison of cell proliferation and MAP kinase signaling activation in HepG2.2.15 grown on microcarrier versus stationary culture.	75
Figure 21:	Isolation of highly purified terminal protein and spacer domain.	76
Figure 22:	Coupling efficiency of TP and S domain to NHS-activated sepharose.	77
Figure 23:	Determination of the sensitivity of the purified TP- and S-specific antisera.	77
Figure 24:	Immuno-precipitation of HBV P protein by the generated antibodies.	78
Figure 25:	Immuno-fluorescence analysis of HBV P expressing S ₉ cells with purified P directed antibodies.	79
Figure 26:	Immuno-fluorescence analysis of HBV P expressing huh-7 cells with purified P directed antibodies.	79
Figure 27:	Sequence alignment of the HBV polymerase (P) from various virus genotypes and species.	81
Figure 28:	<i>In vitro</i> phosphorylation of recombinant TP domain by protein kinases CKII and PKC.	82
Figure 29:	Effect of CKII inhibition on HBV secretion of infected hepatocytes.	84
Figure 30:	Effect of PKC inhibition on HBV secretion of infected hepatocytes.	85
Figure 31:	Effects of the identified motifs on virus replication.	86
Figure 32:	Subcellular localization of NLS-GFP fusion proteins.	88
Figure 33:	Binding of karyopherin- α 2, PKC, and CKII to immobilized TP domain.	89
Figure 34:	<i>Ab initio</i> modeling of TP domain (amino acid 1-181).	91

LIST of TABLES

Table 1:	Subtype (serotype) distribution in HBV genotypes.	21
Table 2:	Monopartite nuclear localization signals in nuclear proteins.	30
Table 3:	Bipartite nuclear localization signals in nuclear proteins.	31
Table 4:	Plasmids and vectors.	38
Table 5:	Synthetic Oligonucleotides.	39
Table 6:	Antibodies.	40
Table 7:	Inhibitors.	42
Table 8:	PCR reaction mixtures.	53
Table 9:	Typical time course for the immunization of rabbits.	62

Dem Zweiten Bildungsweg

1 INTRODUCTION

1.1 Hepatitis B

Hepatitis is an inflammatory liver disease. It can be caused by radiation, contusion, drugs, toxins or pathogens like bacteria, parasites or viruses. Most cases of hepatitis are due to virus infections. The known hepatitis viruses are classified in A, B, C, D, E and G and are non-related (beside C and G). Also some herpes viruses, Coxsackie virus, yellow fever virus, adenovirus, paramyxovirus and rubella virus can cause a hepatitis phenotype [Gerok, et al., 2000].

1.1.1 Disease

A hepatitis B virus (HBV) infection can be acquired by sexual contact and through body fluid transmission with blood contact, e.g. over lesions. The clinical symptoms of acute hepatitis are weariness, adynamia, headache, nausea, loss of appetite, elevated blood levels of transaminases, and symptoms of disturbed liver metabolism including icterus, cholestase, portal hypertension and dark urine [Gerok, et al., 2000]. In some cases the infection leads to fulminant hepatitis with severe complications including liver failure. Chronic hepatitis B is defined if the infection persists for more than 6 month. It can be asymptomatic although the viral surface antigen (HBsAg) is detectable in the blood of the patient. About 10 % of acutely HBV infected adults and 90 % of acutely infected children become chronically infected [de Franchis, et al., 2003]. Chronic hepatitis B infection can lead to liver cirrhosis and hepatocellular carcinoma [Gerok, et al., 2000].

1.1.2 HBV epidemiology

It is estimated that 2 billion people worldwide have come into contact with HBV (positive for antibodies directed against viral core protein) and 400 million people are chronically infected with HBV [Buster and Janssen, 2006]. In the year 2000 about

250,000 incidences of hepatocellular carcinoma (HCC) were diagnosed worldwide in HBV carriers [Lupberger and Hildt, in press].

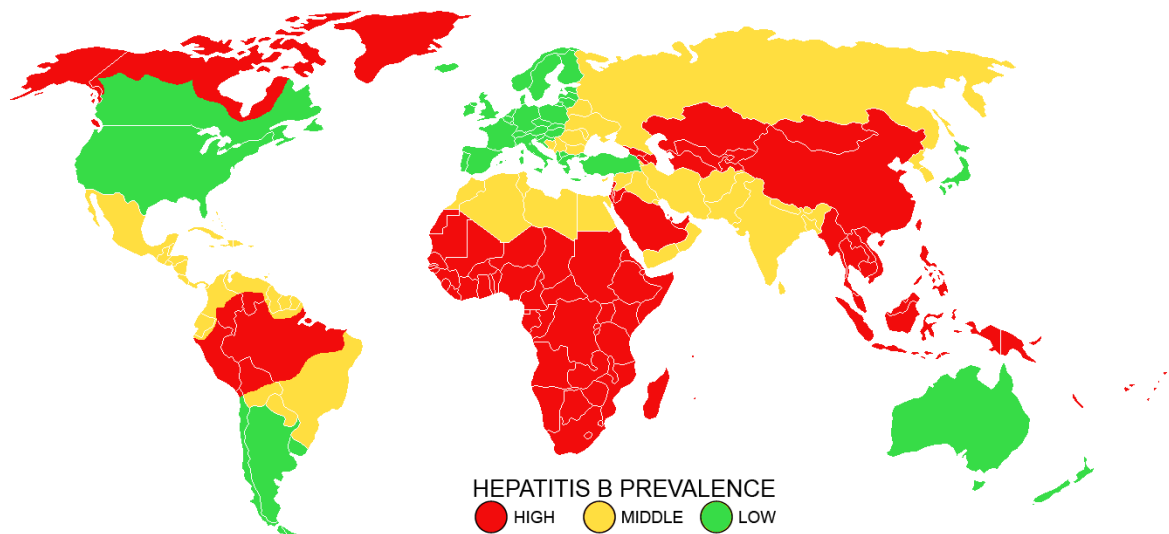


Figure 1: Worldwide prevalence of chronic hepatitis B. >8 % high prevalence (red), 2-8 % middle prevalence (yellow), <2 % low prevalence (green). Data based on WHO [Hollinger and Liang, 2001].

Regions with a chronic hepatitis B prevalence of 8-20 % of the population are defined as high endemic regions (Fig. 1, red). They include the population of Alaskan and Greenland Indians, the Amazon basin, sub-Saharan Africa, parts of the Middle East, Central Asian republics, Southeast Asia, and the Pacific basin (excluding Japan, Australia, and New Zealand) [Hollinger and Liang, 2001]. In China, Senegal, and Thailand the infection rate in infants exceeds 25 %. In Panama, New Guinea, Solomon Islands, Greenland, and in the population of Alaskan Indians the infection rates in infants are relatively low but increase rapidly during early childhood. [Hollinger and Liang, 2001]. In high endemic regions, about 70-90 % of the population becomes HBV infected before the age of 40.

Areas with a chronic hepatitis B prevalence of less than 2 % of the population are defined as low endemic regions (Fig. 1, green). They include North and parts of South America, Western and Central Europe, Turkey, Japan, Australia, and New Zealand. In these regions less than 20 % of the population becomes HBV infected before the age of 40 [Hollinger and Liang, 2001].

The rest of the world falls under intermediate endemic regions (Fig. 1, yellow) with a chronic hepatitis B prevalence of 2-8 % of the population [Hollinger and Liang, 2001].

1.1.3 Prevention and treatment

Immunization with recombinant HBV surface antigen has been available since 1986. An acute infection is usually not treated but monitored. The major target of the current treatment for chronic hepatitis B is the HBV polymerase. Its activity can be inhibited by nucleoside analogs (e.g. Lamivudine, Entecavir) and nucleotide analogs (e.g. Adefovir). But after long-term application of nucleos(t)ide-analogs the incidence of drug resistant escape mutants is high [Buster and Janssen, 2006]. Nucleos(t)ide-analogs are usually applied in combination with pegylated interferon-alpha, which stimulates the antiviral response of the host immune system [Buster and Janssen, 2006]. Nevertheless, there is a low chance for successful cure of a chronic HBV infection.

1.2 Hepatitis B virus

1.2.1 Genome organization and structure

The hepatitis B virus belongs to the family *hepadnaviridae* that is subdivided into the genus *avihepadnavirus* (bird HBV e.g. Shanghai duck HBV, Ross goose HBV, China duck HBV, Heron HBV) and *orthohepadnavirus* (mammalian HBV e.g. human HBV, ground squirrel HBV, woodchuck HBV). It has a partially double-stranded 3.2 kb DNA genome, in which coding sequences are organized into four overlapping and nested open reading frames (ORF) coding for seven viral proteins. All coded proteins are translated from 3-4 RNA transcripts (Fig. 2).

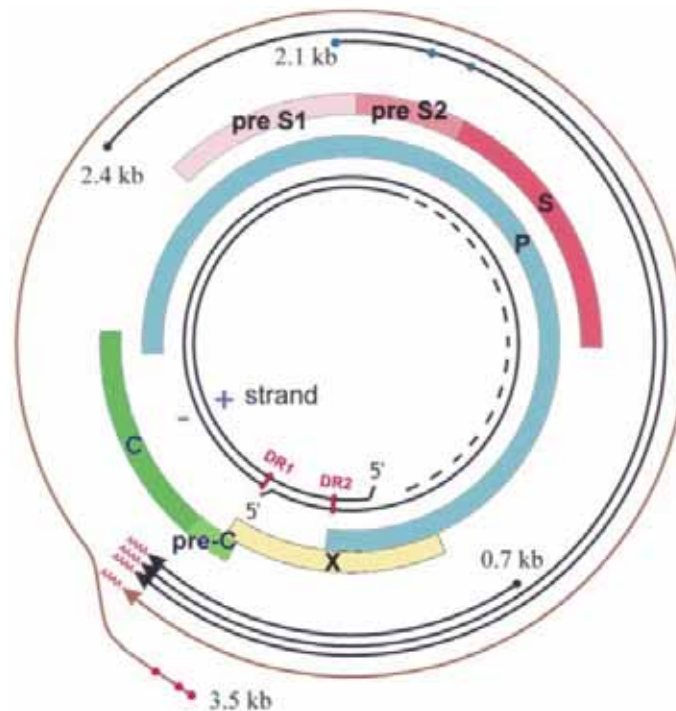


Figure 2: HBV genome organization. The 3.2 kb partial double-stranded DNA genome (center) harbors 7 overlapping and nested open reading frames: polymerase (P), X protein (X), core (C), E (Pre-C+C), large surface protein (PreS1+PreS2+S), middle surface protein (preS2+S), and small surface protein (S). The four viral mRNA transcripts are indicated with the size in kb: 0.7 kb, 2.1 kb, 2.4 kb and 3.5 kb pregenomic RNA transcript, with a redundant region harboring two direct repeats (DR). Figure modified from original [Kidd-Ljunggren, et al., 2000].

The 3.5 kb pregenomic RNA (pgRNA) is an overlength transcript, which is an intermediate for virus replication and serves as a transcript for the translation of the 90 kDa viral polymerase (ORF P), the 21 kDa core protein (ORF C), and a 24 kDa precursor early antigen (ORF preC-C) (Fig. 2). The preC region of the precursor protein harbors a signal sequence that directs the chain into the secretory pathway, where it is cleaved to a 16 kDa early antigen (HBeAg) and secreted to the bloodstream. The function of HBeAg is not known and HBeAg negative mutants replicate well *in vitro* and arise frequently during natural infections [Takahashi, et al., 1983]. The surface antigens (HBsAg) are translated from the 2.4 kb and the 2.1 kb mRNAs into the 42 kDa large surface antigen (ORF PreS1-PreS2-S), 31 kDa middle surface antigen (ORF PreS2-S) and 24 kDa small surface antigen (ORF S) [Seeger and Mason, 2000]. The 0.7 kb mRNA is translated into the 16 kDa X protein, which is a regulatory protein [Twu and Schloemer, 1987; Wollersheim, et al., 1988]. The existence of the 0.7 kb mRNA has been verified in cell culture but not *in vivo*.

In the mature virus, the viral polymerase (P) is covalently attached to the 5'-end of the genome minus-strand. The P-genome complex is protected by an icosahedral capsid assembly consisting of the viral core protein (HBc). The HBV capsid is enveloped by host cell membrane, which is spiked with the small, middle, and large surface antigens (SHBsAg, MHBsAg, LHBsAg, respectively) [Seeger and Mason, 2000] (Fig. 3).

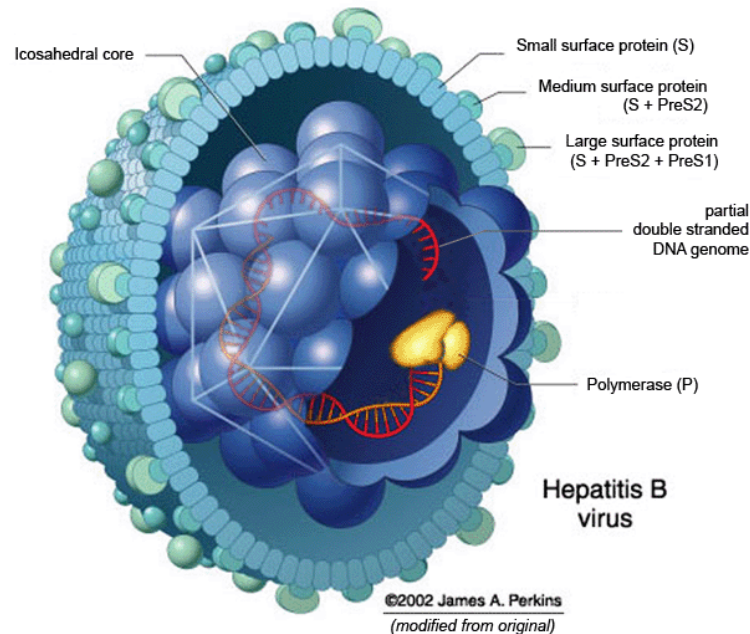


Figure 3: HBV structure. A partial double-stranded DNA genome is bound covalently to the viral polymerase (P). The P-genome complex is enclosed by an icosahedral capsid consisting of core protein monomers. The viral capsid is enveloped by host membrane from the pre-Golgi compartment spudded with the viral surface proteins LHBsAg, MHBsAg, and SHBsAg. Image modified from James A. Perkins.

In the blood of infected patients 42 nm infectious virus particles (Dane particles) are found together with an approximate 1000 fold excess of 22 nm sized subviral particles (SVPs) [Ganem, 1991] (Fig. 4). These spherical and filamentous structures consist only of HBsAg spiked viral envelope. The role of SVPs during infection remains unclear but it is speculated that the vast excess of SVPs compared to Dane particles is a kind of decoy that helps to mislead the immune system. Furthermore, it was suggested that SVP binding to the infected hepatocyte enhances viral replication due to a short-term transactivation of intracellular signaling [Bruns, et al., 1998].

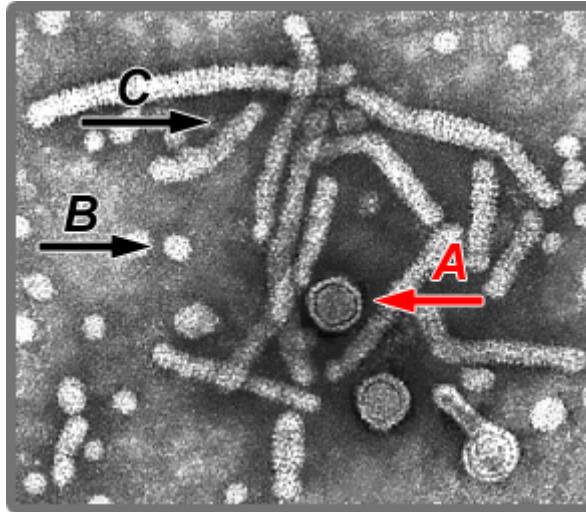


Figure 4: Electron microscopy of HBV particles. *A* = 42 nm Dane particle, *B* = 22 nm spherical subviral particle, *C* = 22 nm filamentous subviral particle (Image from Linda Stannard, University of Cape Town, South Africa).

1.2.2 *HBV species and subtypes*

Most viruses are able to adapt quickly to changing environments. Due to a lack of proofreading activity of the HBV polymerase the nucleotide substitution rate, per site and per year, is nearly as high as in retroviruses (10^{-5}), but is 10^4 times higher than in DNA virus genomes [Orito, et al., 1989]. The HBV genotypes are defined as having sequence divergence of more than 8 % of the whole genome and at least 4 % divergence within the HBsAg reading frame. In early studies four major genotypes were described (A-D). During the last 15 years four additional genotypes (E-H) were postulated [Kramvis, et al., 2005]. The worldwide distribution of HBV genotypes and their phylogenetic relationship is shown in Fig. 5.

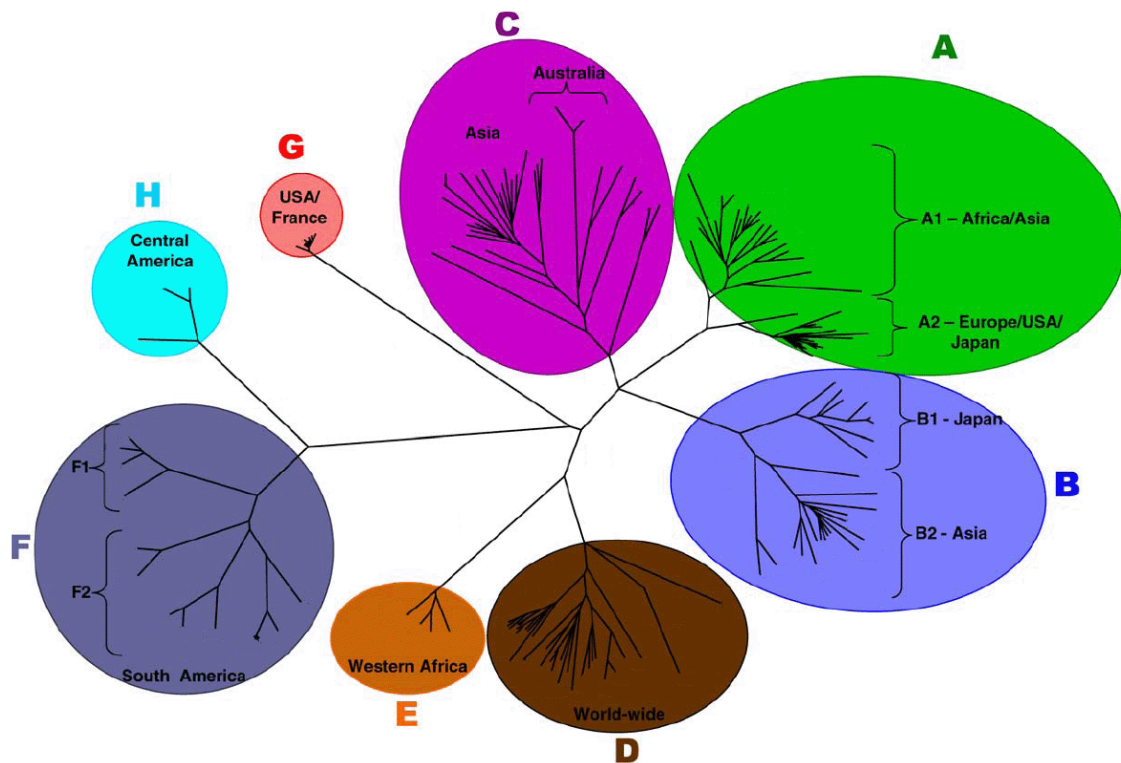


Figure 5: Phylogenetic relationship of HBV genotypes. 175 published HBV genomes are compared by neighbor-joining and are pictured as a single phylogenetic branch. Genotypes and their worldwide distribution are indicated: A (green) Asia, Japan, Africa, Europe, USA; B (light blue) Asia, Japan; C (purple) Asia, Australia; D (dark brown) worldwide; E (light brown) Western Africa; F (dark blue) South America; H (turquoise) Central America; G (pink) USA, France. Image modified from original [Kramvis, et al., 2005].

The treatment of HBV can promote the appearance of “quasispecies” [Kramvis, et al., 2005]. For example the use of nucleos(t)ide-analogs can cause drug resistant polymerase mutations that can also effect the overlapping HBsAg reading frame [Allen, et al., 1998]. Furthermore, it is described that selective pressure due to HBV vaccination can cause HBsAg mutations that escape the neutralization by vaccine-induced antibodies [Wilson, et al., 1999].

The viral surface antigen is exposed to the humoral immune response. The coding region of HBsAg is the most variable part of the viral genome due to the high selective pressure. Therefore, HBV is further classified in serotypes based on the heterogeneity of the HBsAg. Four serological subtypes (serotypes) were identified initially: ayw, adr, ayr and adw and have been expanded with the identification of further sub-determinants within the HBsAg [Kramvis, et al., 2005]. The predominant distribution of serotypes within the HBV genotypes and the consequence to the HBV polymerase ORF is shown in Table 1.

Table 1: Subtype (serotype) distribution in HBV genotypes. [Schaefer, 2005].

Genotype	Predominant subtype	Genome length (bp)	ORF-differences	Length of polymerase
A	adw2 (ayw1)	3221	Insertion of aa 153 and 154 in HBc	845 aa
B	adw2 (ayw1)	3215		843 aa
C	adr and ayr	3215		843 aa
D	ayw1,2,3	3182	Deletion of aa 1–11 in preS1	832 aa
E	ayw4 (adw2)	3212	Deletion of aa 11 in preS1	842 aa
F	adw4	3215		843 aa
G	adw2	3248	Insertion of 12 aa in HBc deletion of aa 11 in preS1	842 aa
H	adw4	3215		843 aa

1.3 HBV lifecycle

HBV productively infects only hepatocytes although it is discussed that it can enter bile ductule epithelium cells, some cells from the pancreas, kidneys, and from the lymphoid system presumably to ensure viral persistence [Seeger and Mason, 2000]. HBV has a non-lytic lifecycle and enters the hepatocyte by endocytosis mediated by the binding of the LHBsAg to an unknown receptor complex (Fig. 6). Inside the endosome the viral surface protein is probably cleaved by an unknown protease. This leads to a high density exposure of a cell permeable motif (TLM) within the PreS2 region of the LHBsAg that mediates the passage of the whole virus through the endosomal membrane [Stoeckl, et al., 2006].

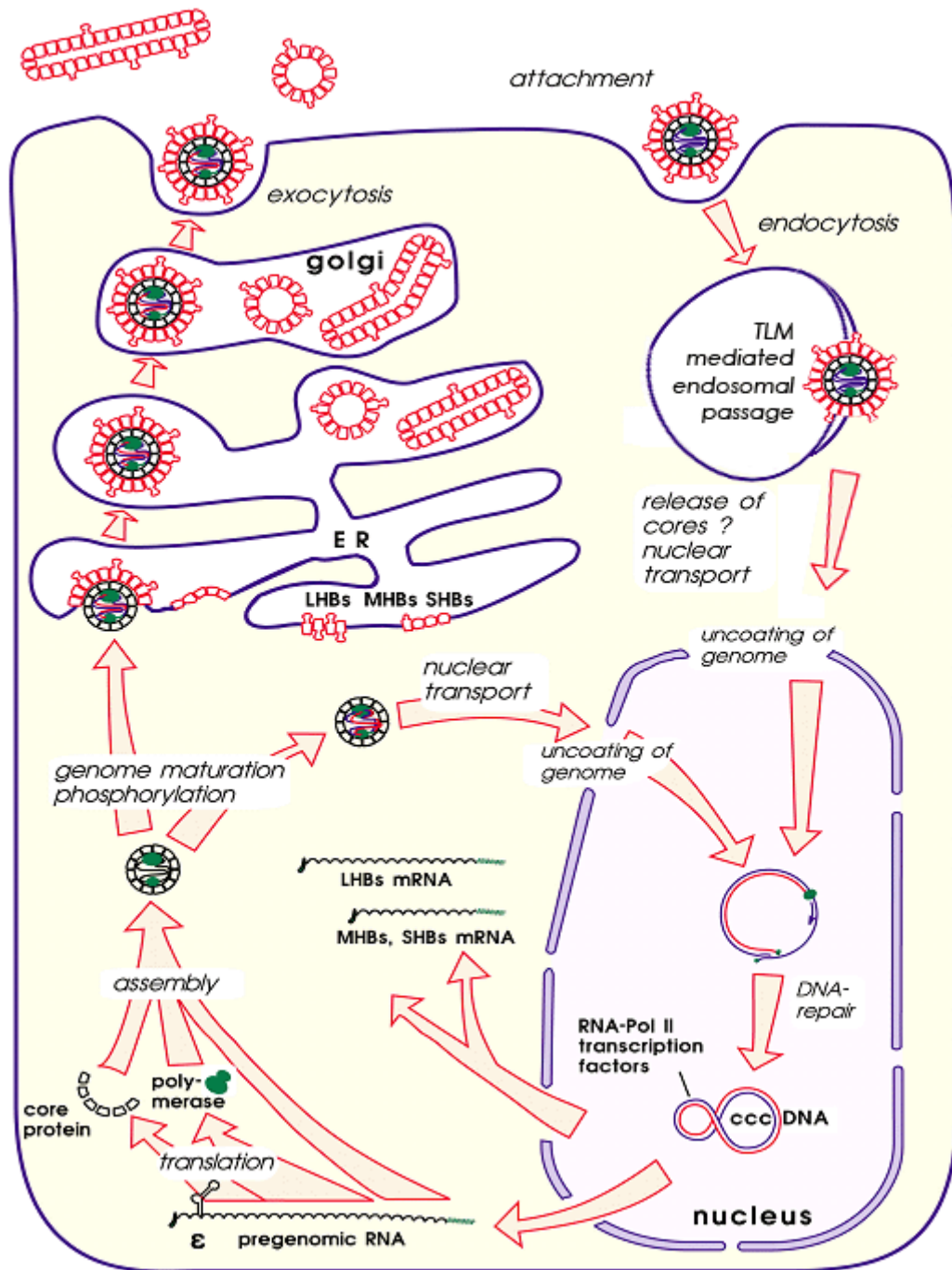


Figure 6: Scheme of the HBV lifecycle within a hepatocyte. Image modified from original [Kann, et al., 1995].

The endosomal processing and the reducing conditions probably lead to the uncoating of the envelope in the cytoplasm. It is discussed whether the P-genome complex is delivered into the nucleus by the intact nucleocapsid [Rabe, et al., 2003] or if a partial disassembly of the capsid within the nuclear pore complex or in a perinuclear domain leads to a release of the genome and its import into the nucleus [Brandenburg, et al., 2005].

In the nucleus presumably the host DNA polymerases and repair mechanisms form a very stable non-integrated HBV mini-chromosome (cccDNA) [Zoulim, 2005]. cccDNA serves as a template for the host RNA polymerase II that transcribes the viral mRNAs (Fig. 2 & 6) that are transported to the cytoplasm where the viral proteins are translated.

Upon steric activation by host chaperones Hsp90, Hsp70, Hsp40, Hop, and possible additional factors, the P protein binds to a secondary structure (ϵ) at the 5'-end of the pgRNA [Hu, et al., 2002]. A tyrosine residue of the polymerase serves as a protein primer that initiates reverse transcription, using a bulge within ϵ to initiate synthesis of the first 3-4 nucleotides of the minus-strand DNA [Wang and Seeger, 1993; Zoulim and Seeger, 1994]. The P protein serves as a reverse transcriptase and stays covalently attached to the nascent minus-strand of the HBV genome. The ϵ -structure recognition by P and the encapsidation by core protein oligomers are tightly coupled events [Bartenschlager, et al., 1990; Hirsch, et al., 1990].

For HBV nucleocapsid maturation phosphorylation [Melegari, et al., 2005] and dephosphorylation [Perlman, et al., 2005] of the viral core protein is required. The involvement of several cellular kinases are discussed, for example cdc2 [Liao and Ou, 1995], SPRK1 and SRPK2 [Daub, et al., 2002], and an unknown 46 kDa protein which has yet to be characterized [Kau and Ting, 1998]. At least one molecule of protein kinase C (PKC) has been detected inside mature HBV virions [Kann, et al., 1993]. PKC phosphorylation of the core protein is proposed to be responsible for the docking of the capsid to the nuclear core complex during HBV infection [Kann, et al., 1999].

It is assumed that in the early stage of infection with low intracellular HBsAg levels the majority of mature capsids are directed to the nucleus to amplify the intranuclear cccDNA level to 10-50 molecules per cell [Newbold, et al., 1995]. In a latter phase mature HBV capsids are enveloped at a pre-Golgi compartment mediated by membrane associated viral surface proteins [Bruss, 2004] and secreted by the Golgi secretory pathway (Fig. 6).

1.4 HBV regulatory proteins

Various regulatory functions are discussed for the HBV X protein [Bouchard and Schneider, 2004]. The integrity of X is essential for WHBV replication in woodchucks [Zoulim and Seeger, 1994] but not for HBV replication in the hepatoma cell line HepG2 [Bouchard, et al., 2001]. HBx is a transcriptional activator that stimulates gene expression by several transcriptional factors e.g. NF- κ B, AP-1, AP-2, ATF/CREB or the calcium activated factor NF-AT [Bouchard and Schneider, 2004]. Two major mechanisms of stimulation are described: (i) by direct binding of HBx to various members of the transcriptional machinery and e.g. enhancing DNA binding activity of transcriptional factor CREB or (ii) by stimulation of cytoplasmic signal transduction pathways. For example, it is found that HBx causes calcium release from the mitochondria leading to a subsequent activation of focal adhesion kinase (FAK), proline-rich tyrosine kinase (Pyk2), and Src kinases which results in a Ras-dependent activation of the mitogen-activated protein (MAP) kinase pathways c-Raf/MEK/ERK and MEKK-1/JNK [Bouchard and Schneider, 2004]. The stimulated MAP kinase pathways inhibit apoptosis and stimulate cell proliferation which results in enhanced HBV gene transcription in HBV infected cells [Peyssonnaud and Eychene, 2001].

The PreS2 region of the large and of the C-terminally truncated middle surface antigens has also a transcriptional activator function [Hildt, et al., 1996; Kekule, et al., 1990] that requires the integrity of the PreS2 domain and its cytoplasmic orientation as is given for a fraction of the large surface antigen [Bruss, et al., 1994]. PreS2 activates the c-Raf/MEK/ERK pathway in a PKC-dependent Ras-independent manner that enhances gene transcription [Hildt, et al., 2002].

It was shown that the integrity of the c-Raf/MEK/ERK pathway is crucial for HBV replication and that HBx and PreS2 can replace each other in respect to c-Raf/MEK/ERK pathway activation [Stockl, et al., 2003].

1.5 Infection models

As already mentioned the receptors that trigger viral entry upon HBV binding are not identified yet. Immortalized hepatocyte cell lines are widely used for studying the mechanisms of HBV replication but the virus uptake during the early phase of HBV infection is blocked due to unknown reasons. Only a few infection models are available to study HBV infection because HBV is very tissue and species specific [Dandri, et al., 2005]. Infection of primary human hepatocytes would be the most appropriate model but human liver tissue is only seldom available and the preparation of a sufficient amount of susceptible hepatocytes from a tissue sample is difficult. Another possibility is to study HBV infection in closely related viruses as the duck hepatitis B virus (DHBV) [Mason, et al., 1980], Heron hepatitis B virus (HHBV) [Sprengel, et al., 1988] or woodchuck hepatitis B virus (WHBV) [Aldrich, et al., 1989]. For example duckling liver tissue can be obtained easily and the preparation of hepatocytes by liver perfusion is more efficient.

Chimpanzees can be infected by human HBV but this is controversial in an ethical point of view and the maintenance of the animals is extremely expensive. A few years ago it was found that HBV can infect and replicate in primary hepatocytes from the Asian tree shrew *Tupaia belangeri* [Kock, et al., 2001; Walter, et al., 1996] (Fig. 7). Furthermore, a HBV susceptible hepatoblastoma cell line was described that can be infected in the presence of corticoids and dimethyl sulfoxide [Gripon, et al., 2002]. All of these model systems require a large amount of human HBV with a defined genome to perform reproducible experiments.



Figure 7: Large asian tree shrew (*Tupaia belangeri*).
Photo copyright Alan Hill (1@alan-hill.freerve.co.uk).

1.6 HBV particles for infection models

Stably HBV genome transfected liver cell lines HepG2.2.15 [Sells, et al., 1987] or HepAD38 [Ladner, et al., 1997] continuously produce infectious human HBV particles, which can be used to study the HBV lifecycle in the current infection models. The conventional scale up of adherent mammalian cells in cell culture flasks is cost and space intensive. An efficient alternative is the cultivation of adherent cells on microcarrier, which are small particles floating in a cell culture suspension. It has been shown recently for retroviruses, adenoviruses [Wu, et al., 2002], and flaviviruses [Wu and Huang, 2002] that host cell cultivation on microcarrier can lead to a decrease or an increase of replication depending on the virus. The cultivation of adherent cells on microcarrier offers an advantageous cost-value ratio and less space consumption in comparison to conventional stationary culture flasks. If an intracellular product is targeted the removal of the cells from the substrate e.g. by trypsination or scraping is, depending on the carrier system, often not necessary. For example Cytodex-3 can be disrupted together with the cells and separated by centrifugation. Gong et al. (1998) cultured immortalized liver cells on Cytodex microcarrier and infected them with HBV

enriched patient serum *in vitro*. 58 days after infection they observed an up to 3.5 fold increase of extracellular HBV DNA compared to the initial HBV DNA level in the virus inoculum [Gong, et al., 1998].

1.7 HBV polymerase

No crystal structure of the HBV polymerase (P) is available, yet a 3D model of the C-terminal part was calculated according to structural similarities with the HIV and MMLV reverse transcriptases [Lin, et al., 2001]. The molecular weight of P is about 90 kDa and it consists of three major domains (Fig. 8). The terminal protein (TP) domain is connected by a protein spacer (S) to the reverse transcriptase (RT) domain and the RNaseH domain at the C terminal end. The RT domain displays a reverse transcriptase activity and is functionally coupled to the RNaseH domain that degrades the RNA strand of a DNA/RNA hybrid. No enzymatic activity can be detected in the TP domain and the spacer, but tyrosine Y63 in TP acts as a protein primer during reverse transcription and stays covalently attached to the minus-strand within mature capsids.



Figure 8: Scheme of the HBV polymerase (ayw). Amino acid positions are indicated above: 1-181 terminal protein domain (TP), 181-335 spacer (S), 335-681 reverse transcriptase domain (RT), 681-832 RNaseH domain. Enzyme activities are only detectable of RT and RNase H.

The TP and RT domains harbor protein binding sites for at least Hsp90 [Cho, et al., 2000] and are important for ϵ -recognition and initiation of reverse transcription. ϵ -recognition and reverse transcription by the RT domain can be complemented by addition of recombinant TP domain and chaperones *in vitro*. Due to this finding it is concluded that the spacer has only minor relevance for the functionality of the P protein in HBV replication [Lanford, et al., 1999; Lanford, et al., 1997].

The fate of the polymerase during and after the nuclear delivery of the genome is not known. The majority of P is localized in the cytoplasm bound to an unknown structure

[Yao, et al., 2000]. But a small portion of P protein is found also in the nucleus of duck HBV infected cells [Yao, et al., 2000]. If overexpressed, some P protein was found colocalized with the p11 protein of nuclear PML bodies interestingly in the absence of other viral proteins [Choi, et al., 2003]. Last but not least, Kann and co-workers reported that the P protein alone is sufficient to shuttle the bound genome into the nucleus [Kann, et al., 1997].

1.8 Nuclear import mechanism

In eukaryotic cells intracellular trafficking between the cytoplasm and the nucleus is a highly regulated mechanism. The nucleus is separated from the cytoplasm by the nuclear membrane that is interspersed with specialized channels. Such a channel consists of several proteins that form a nuclear pore complex (NPC) [Allen, et al., 2000]. Molecules up to 9 nm (~20-40 kDa) can diffuse freely through the NPC in both directions. The passage of bigger molecules is either not possible or they are actively transported through the NPC [Goldfarb, et al., 2004; Mosammaparast and Pemberton, 2004]. The active passage is mediated by a cascade of intracellular receptor proteins that recognize a distinct nuclear localization signal (NLS) on the cargo protein (see chapter 1.6). Karyopherin- β binds to the cargo-NLS either directly or mediated by the adaptor protein karyopherin- α (Fig. 9a). The karyopherin-cargo complex interacts with NPC proteins (Fig. 9b) that mediate the passage of the complex into the nucleus (Fig. 9c). Within the nucleus the binding of Ran-GTP to karyopherin- β leads to a release of the cargo, and the adapter karyopherin- α form the ternary complex (Fig. 9d). The karyopherin- β -Ran-GTP complex is shuttled back to the cytoplasm, whereas karyopherin- α is recycled by forming another ternary complex with the karyopherin- α export receptors CAS and Ran-GTP (Fig. 9e). In the cytoplasm the Ran-GTPase activating protein (Ran-GAP) causes dephosphorylation of Ran-GTP to Ran-GDP that leads to the release of karyopherin- α and karyopherin- β from their binding partners (Fig. 9f).

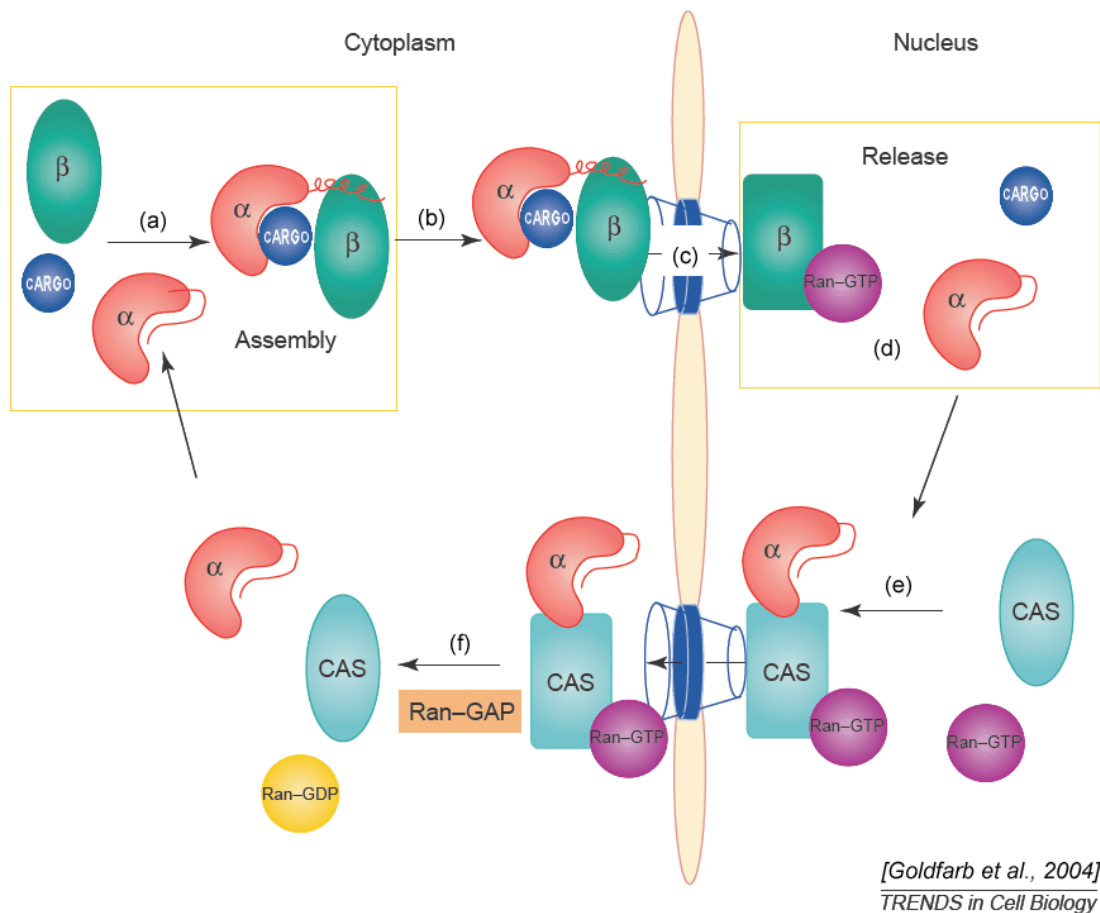


Figure 9: Karyopherin- α mediated shuttling of cargo into the nucleus. (a) The cargo protein (dark blue sphere) forms a ternary complex with karyopherin- α (red) and karyopherin- β (green) (b) the ternary complex binds to the NPC (c) and is actively transported into the nucleoplasm. The binding of terminator protein Ran-GTP (purple) to karyopherin- β leads to the release of karyopherin- α and its cargo (d). The karyopherin- β -Ran-GTP shuttles back to the cytoplasm. Karyopherin- α is recycled by binding to CAS-Ran-GTP that is exported to the cytoplasm (e) Dephosphorylation of Ran-GTP by Ran-GAP cause the release of the karyopherins into the cytoplasm. Image modified from original [Goldfarb, et al., 2004].

1.9 Nuclear localization signals

Nuclear import signals bind to intracellular receptor karyopherins that mediate the nuclear import of the NLS-cargo. The best characterized NLS is derived from the large tumor antigen (T-ag) of the simian virus 40 (SV40) [Kalderon, et al., 1984], but various other motifs responsible for nuclear import were identified in other nuclear proteins (Tab. 2). Although a general hydrophilicity and some lysine/arginine rich cluster can be observed in motifs that binds to karyopherins, no general consensus sequence can be derived for monopartite NLS.

Table 2: Monopartite nuclear localization signals in nuclear proteins. The amino acid position of the NLS are indicated in superscript [Jans and Hubner, 1996].

Protein	NLS
SV40 large tumor antigen	PKKKRKV ¹³²
Polyoma T	VSRKRPRP ¹⁹⁶ PPKKARED ²⁸⁶
Lamin L ₁	VRTTKGKRKRIDV ⁴²⁰
Lamin A/C	SVTKKKRKL ⁴²²
Cofilin	PEEVKKRKKAV ⁷³⁶
Human <i>c-myc</i>	PAAKRVKLD ³²⁸ RQRRNELKRFS ³⁷⁴
Ad7 E1a	KRPRP ²⁸⁹
SV40 VP1	APTKRKGS ⁸
SV40 VP2/3	PNKKKKR ³²³
Human p53	PQPKKKPL ³²³
NFκB p50	QRKRQK ³⁷²
NFκB p65	EEKRKR ²⁸⁶
Chicken <i>v-rel</i>	KSKKQK ²⁹⁵
Mouse <i>c-abl</i> IV	SALIKKKKKMAP ⁶³¹
Influenza virus NS1	DRLRR ³⁸ PKQKKR ²²¹
Hepatitis virus delta antigen	RKLKKIKKL ⁴⁴ PRKR ⁸⁹
chicken <i>c-ets-1</i>	GKRKKNPK ³⁸³
<i>v-jun</i>	KSRKRKL ²⁵³
Ribosomal protein L29	KTRKHRG ¹² KHKHHPG ²⁹
Human DNA ligase I	PKRRTARKQLPKRT ¹³²
Human hnRNP B1	KTLETVPLERKKREK ¹⁷
Human hnRNP A1	NDFGNYNQSSNFGPMKGGNFGGRSSGPY ²⁸⁹
Yeast histone 2B	GKKRSKAK ³⁶
Monkey <i>v-sis</i>	RVTIRTVRRRPPKHKHRK ²⁵⁵
Human PDGF-A (longer form) ^c	RESGKKRKRKRLKPT ²⁰⁷
Mouse Mx1	REKKKFLKRR ⁶¹⁵
Prothymosin α	TKKQKT ¹⁰⁷
VirD2 protein (octopine, <i>Agrobacterium tumefaciens</i>)	EYLSRKGKLEL ³⁸
Maize R protein	GDRRAAPARP ¹⁰⁹ MSERKRREKL ²⁴⁸ MISESLRKAIGKR ⁶¹⁰
MyoD	CKRKT TNADRRK ¹¹² CVNEAFETLKRC ¹³⁵
Serum response factor	RRGLKR ¹⁰⁰
CaM δB ^f	AKKPDGVKKRKS ³³²
Yeast Matα2	NKIPIKDLLNPQ ¹³ VRILESWFAKNIENPYLDT ¹⁵⁹
Influenza virus nucleoprotein	AAFEDLRVLS ³⁴⁵
Hepatitis B virus core protein	SKCLGWLWG ²⁹

Some proteins, e.g. polyoma T protein, influenza virus NS1 or Maze R protein harbor more than one NLS that are required in concert (Tab. 3). This increases the efficiency of the nuclear import and is needed especially to achieve complete nuclear localization of weak NLS [Shieh, et al., 1993]. A higher number of NLS in a protein seems to increase the import efficiency [Dworetzky, et al., 1988].

A special variation of this multiple monopartite NLS are the bipartite class of NLS consisting of two series of basic clusters that are divided by a spacer of 10-12 amino acids (Tab. 3). The functionality of a prototype NLS sequence that was discovered within the nuclear chaperon nucleoplasmin in *Xenopus laevis* has been well characterized [Robbins, et al., 1991].

Table 3: Bipartite nuclear localization signals in nuclear proteins. The amino acid position of the NLS are indicated in superscript [Jans and Hubner, 1996].

Protein	NLS
Human	
Poly(ADP-ribose) polymerase	KRKGDEV DGVDEVAKKKS²²⁶
c-fos	KRRIRRERNKMAAAKCRNKRRRL¹⁶¹
SRY	KRPMNAFVWSRDQRRK⁷⁷
HSF2	KRKVSSSKPEENKIR¹²² KRKRPLLNTNGAQKK²¹⁰
Steroid hormone receptors (human)	
Glucocorticoid	RKCLQAGMNLEARKTKK⁴⁹⁵
Progesterone	RKCCQAGMVLGGGRKFKK⁴⁹⁵
Androgen	RKCYEAGMTLGARKLKK⁴⁴⁸
Estrogen	RKCYEVGMMKGGIRKDR⁴⁹⁵
Erb-A	RKLAKRKLIEENREKRR¹⁹⁶
Thyroid β	KRLAKRKLIEENREKRR¹⁰⁶
Mouse	
p110 ^{RB1}	KRSAEGGNPPKPLKKLR⁸⁶⁹
FGF3	RLRRDAGGRGGVYEHLGGAPRRRK^{76/47}
Chicken	
Nucleolin	KRKKEMANKSAPEAKKKK²⁷³
Xenopus	
NO38	KRAAPNAASKVPLKKTR¹⁵³
Nucleoplasmin	KRPAATKKAGQAKKKKL¹⁷¹
N1/N2	RKKRKTEESPLKDKDAKKSQEP⁶⁵⁴
xnf7 ^d	KRKIEPEPEPKKAKV¹²¹
Viral	
Herpes ICP-8	RKRAFHGDDPFGEPPDKK¹¹⁸⁸
Saccharomyces cerevisiae	
SWI5	KKYENVVIKRSRKRGRPRK⁶⁵⁵
GCN4	KRARNTAARRSRARK²⁴⁵
Plants	
TGA-1A (tobacco)	KKLAQNREAAARKSRLRKK⁹²
TGA-1B (tobacco)	KKKARLVRNRESAQLSRQRKK³⁶⁴
Opaque-2 (maize)	RRKLEEDLEAFKMTR¹⁴³ RKRKESNRESARRSRYRK²⁴⁷
Agrobacterium tumefaciens^e	
VirD2 protein (octopine)	KRPRDRHDGELGGRRKRAR⁴¹³
VirD2 protein (nopaline)	KRPREDDDGEPSPDRKRER⁴³⁴
VirE2 protein	KLRPEDRYIQTEKYGRREIQKR²⁴⁹ RAIKTKYGS DTEIKLKS³⁰⁹
Consensus	K/R-K/R-10-12 amino acid spacer-K/R-K/R-K/R

A general consensus sequence was derived from nuclear proteins that harbor a functional bipartite NLS (K/R-K/R-(10-12 amino acid spacer)-K/R-K/R-K/R) (Tab. 3). The length of the amino acid spacer seems to have only minor effects on NLS

functionality although an increased hydrophobicity clearly reduces the nuclear import efficiency [Robbins, et al., 1991].

Bipartite nuclear localization signals usually bind karyopherin- α . The complex of a bipartite NLS and karyopherin- α was crystallized by Conti and co-workers in 2000 [Conti and Kuriyan, 2000] (Fig. 10). The NLS binding domain is slug-like shaped and consists of ten helical repeat motifs (ARM).



Figure 10: Crystal structure of karyopherin- α 2 (*Saccharomyces cerevisiae*) binding a bipartite NLS from nucleoplasmin (*Xenopus laevis*). Green = karyopherin- α 2, blue = two basic clusters of the bipartite NLS separated by a 10 amino acid spacer (red). Image generated with PyMol from published PDB coordinates [Conti and Kuriyan, 2000].

1.10 Regulation of nuclear import

Some proteins like histones are constitutively targeted to the nucleus, whereas others like transcription factors remain in the cytoplasm until a distinct triggering event. Such regulation of subcellular localization was described and characterized e.g. for the glucocorticoid receptor, transcription factor NF- κ B, sterol regulatory element binding protein SREBP-1, the yeast transcription factors xnf7 and SW15, and for the T-ag of simian virus 40. Various mechanisms by which the subcellular localization of proteins is regulated have been characterized.

1.10.1 Proteolysis

Proteolysis of carrier proteins or binding partners can reveal a blocked NLS or remove an NLS dominant subcellular anchor. For example a 125 kDa precursor protein of SREBP-1 is C-terminally anchored to the ER and the nuclear envelope. Cleavage by a calpain like protease leads to the nuclear import of the N-terminal 68 kDa fragment mediated by the exposed NLS [Wang, et al., 1994]. Another example is the binding of I κ B to transcription factor NF- κ B, which overlaps (masks) the NLS of NF- κ B and retains the protein in the cytoplasm. A phosphorylation of I κ B triggers its proteolytic degradation and the exposure of the NLS of NF- κ B that subsequently leads to its nuclear import [Lin, et al., 1995].

1.10.2 NLS masking

Masking is defined as a blockade of a functional NLS by an interaction with another binding factor or a binding of another part of the molecule due to a conformational change. For example the NLS of the glucocorticoid receptor (GR) is blocked by an Hsp90 chaperone complex that retains the receptor in the cytoplasm [Picard, et al., 1990]. GR is released if the corresponding hormone binds to the receptor. The subsequent exposure of the NLS triggers the binding of karyopherins that mediate nuclear import.

1.10.3 Phosphorylation

Protein phosphorylation is one of the main mechanisms to regulate subcellular localization. The best characterized example is the CcN motif of the T-antigen of simian virus 40 [Jans, et al., 1991; Jans and Jans, 1994]. Phosphorylation of the cell cycle dependent kinase cdc2 adjacent to the monopartite NLS of T-antigen inhibits nuclear import [Jans, et al., 1991], whereas phosphorylation upstream of the NLS by protein kinase CKII enhances nuclear import 40 fold [Jans and Jans, 1994]. This CcN motif is often found in proteins which are required in the nucleus at a distinct phase of the cell cycle. Beside CKII and cdc2, various other kinases are described to influence NLS

functionality, including PKC (lamin-B) or PKA (c-rel) [Jans and Hubner, 1996]. Bipartite NLS are also influenced by phosphorylation. In the case of nucleoplasmin, an upstream protein kinase CKII site of the bipartite NLS enhances the nuclear import of nucleoplasmin [Jans and Hubner, 1996; Vancurova, et al., 1995]. Immediate phosphorylation of one or two amino acids upstream of the crucial amino acid of classical monopartite NLS seems to have inhibitory effects on karyopherin binding due to a disturbance of the NLS basicity [Harreman, et al., 2004]. In the case of bipartite NLS this correlation is not evident. For example the spacer of the bipartite NLS of the *Agrobacterium tumefaciens* protein nopaline contains four negatively charged aspartates, one located immediately at the downstream basic cluster [Howard, et al., 1992]. In the other hand an increase of the hydrophobicity of the 10-12 amino acid spacer seems to decrease its functionality [Robbins, et al., 1991].

2 THESIS OBJECTIVES

2.1 Upscale of HBV production

Recently, novel infection models for studying the human HBV lifecycle have emerged [Gripon, et al., 2002; Kock, et al., 2001] demanding for large amounts of infectious HBV particles with a defined genome. Studies with various viruses infected cell lines have shown that variation of the cultivation substrate can alter virus replication and secretion [Wu and Huang, 2002; Wu, et al., 2002]. One aim of this study was to optimize HBV production by cultivation of the cell line HepG2.2.15 on spherical microsubstrate Cytodex-3 and to characterize the effects of this cultivation method on cellular signaling.

2.2 Subcellular localization of the HBV polymerase

The HBV polymerase is predominantly located in the cytoplasm but a small portion is also found in the nucleus of DHBV infected duck hepatocytes [Yao, et al., 2000]. Even in the absence of the viral core protein a small portion of the HBV P protein is found colocalized with PML bodies in the nucleus [Choi, et al., 2003]. Furthermore, P is sufficient for the import of the covalently attached HBV genome into the nucleus of digitonin permeabilized hepatocytes [Kann, et al., 1997]. Due to the fact that P is too big for free diffusion through the nuclear pore complex the second objective of this study was to identify motifs on the HBV polymerase, which determine the subcellular localization of the P protein during viral lifecycle.

3 MATERIALS

3.1 Viruses, cells and animals

3.1.1 Viruses

AcNPV::HBV P Modified *Autographa californica* nuclear polyhedrosis virus for the expression of HBV polymerase [Lanford, et al., 1995]

3.1.2 Bacterial strains

Following *Escherichia coli* K12 strains were used in this study:

DH5 α Adjusted for molecular cloning purposes; recombinase A and endonuclease A deficient strain (DSMZ #6897).

BL21 Adjusted for protein expression; deficient for proteases OmpT and Lon (Qiagen, Hilden).

M15 (pREP4) Optimized for expression of toxic proteins; plasmid pREP4 prevents promoter leakage prior to induction by overexpression of the coded *lac* repressor (Qiagen, Hilden).

3.1.3 Cell lines

Huh-7 Human hepatoblastoma cell line [Nakabayashi, et al., 1982].

HepG2.2.15 Human hepatoblastoma cell line harbors a 2.15 fold HBV genome (serotype ayw, genotype D) integrated into the chromosome [Sells, et al., 1987].

HepAD38 Inducible human hepatoblastoma cell line harbors a integrated tetracycline responsive 1.2 fold HBV genome (serotype ayw, genotype D) [Ladner, et al., 1997].

Sf9 Derived from pupal ovarian tissue of *Spodoptera frugiperda* (DSMZ #ACC 125).

3.1.4 Animals

Asian tree shrew (*Tupaia belangeri*) were obtained from the German Primate Center in Göttingen, Germany and maintained in the animal facility of the University of Freiburg.

Rabbit (*Oryctolagus cuniculus*) were obtained and maintained by the Bundesinstitut für Risikobewertung (BfR), Marienfelde, Berlin.

3.2 Chemicals

3.2.1 Plasmids

Table 4: Plasmids and vectors.

Plasmid	Description	Reference or source
peGFP-N1	27 kDa enhanced green fluorescent protein	Invitrogen, Karlsruhe
pcDNA3.1(-)	eukaryotic expression vector	Invitrogen, Karlsruhe
pSM2	2.5 fold HBV genome, serotype ayw, genotype D	(Sells et al. 1987)
pRV(P-)	1.2 fold HBV genome, serotype adr, P protein negativ	Pairan A, unpublished
pQE60	bacterial expression vector, C-terminal (His) ₆ -tag	Qiagen, Hilden
pJo2	pQE60::TP domain (amino acid 1-181) of HBV P (ayw)	this study
pJo3	pQE60::S domain (amino acid 182-340) of HBV P (ayw)	this study
pJo19	1.2 fold HBV genome, serotype ayw, genotype D	this study
pJo20	pJo19; P protein [T100I]	this study
pJo21	pJo19; P protein [T53I]	this study
pJo22	pJo19; P protein [T100I, T53I]	this study
pJo23	pEGFP-N1, Δa1 of start codon eGFP	this study
pJo37	pJo19; P protein [T53D]	this study
pJo40	pJo19; P protein [K105Q, K106S]	this study
pJo45	pJo19; P protein [T100D]	this study
pJo47	pJo19; P protein [T100D, T53D]	this study
pJo48	pJo23, <i>BamHI</i> cloned NLS of nucleoplasmin (K142-K158)	this study
pJo49	pJo23, <i>BamHI</i> cloned NLS of HBV P protein (K100-R106)	this study

3.2.2 Synthetic Oligonucleotides

Table 5: Synthetic Oligonucleotides. Nucleotide sequence starts at the 5'-end; bold indicated sequence is non-complementary to the template DNA; underlined sequence indicates relevant restriction sites. *6-FAM* = 6-carboxylfluorescein, *TAMRA* = carboxytetramethylrhodamine, *PH* = phosphate ester at the hydroxyl group of the 3'-end, Y = C/T. All synthetic oligonucleotides were synthesized by Tib-Molbiol, Berlin.

Primer	Sequence (5'-3')
(cloning)	
N-NLS-3b	TTTAGATCT TTTTACTTTTTTCTGTGG
N-NLS-3f	TTTAGATCT GTTTCAGGGCCAGTGC
pEGFP-3b	AGTCGCGGCCGCTTACTTGTACAG
TP_f	CCCGGATCC ATGCCCTATCCTATCAACAC
TP-NLS-3b	TTTAGATCT TCTTTTCTCATTAAGT
(mutagenesis)	
GFP Δ start_b	CCTCGCCCTTGCT CACCA TGGTGGCGACCCGGTGG
GFP Δ start_f	CCACCGTCGCC CACCA TGGTGAGCAAGGGCGAGG
N-NLS-4b	CCAGGGGCAGACCGCTTCC ATGGTGGCGAGATCT ACTTAAGAGTTTCACATCC
N-NLS-4f	GGATGTGAAACTCTTAAGT AGATCTCGCCACC ATGGGAAAGCGGTCTGCCCTGG
T100D_b	GGCAGGCATA AATTA ACTGCAATCTTCTTTTCTCATTAA CGTC GAGTGGGCCTACAACTG
T100D_f	CAGTTTGTAGGCCCACT GACG TAAATGAGAAAAGAAGATTGCA AATTA ATTATGCCTGCC
T100I_b	GGCAGGCATA AATTA ACTGCAATCTTCTTTTCTCATTAACTATGAGTGGGCCTACAACTG
T100I_f	CAGTTTGTAGGCCCACTCATAGTTAATGAGAAAAGAAGATTGCA AATTA ATTATGCCTGCC
T53D_b	GTAAAGTCCCCACCTTATGGT CCCAT GGAATACTAACATTGAGATT
T53D_f	GAATCTCAATGTTAGTATT CCATGGG ACCATAAAGGTGGGGAACTTTAC
T53I_b	GTAAAGTCCCCACCTTATGAAT CCAT GGAATACTAACATTGAGATT
T53I_f	GAATCTCAATGTTAGTATT CCATGG ATTTCATAAAGGTGGGGAACTTTAC
TP-NLS-5f	AAAAGATCTCGCCACC ATGGTGAATAAATGTGAACAGTTTGTAGG
Δ NLS_b	CAGGCATAATCAATTGCAATCTAGACTGCTCATTAACTGTGAGTGGGCC
Δ NLS_f	GGCCCACTCACAGTTAATGAGCAG TCT AGATTGCAATTGATTATGCCTG
(quantification)	
HBx_b	AGTCCAAGAGTYCTCTTATGYAAGACCTT
HBx_f	CCGTCTGTGCCTTCTCATCTG
HBx_sonde	6-FAM-CCGTGTGCACTTCGCTTCACTCTGC-TAMRA-T-PH

3.2.3 Molecular Weight Calibrators

(Protein markers)

Low molecular weight (LMW)

GE Healthcare, Freiburg

See blue Plus 2

Invitrogen, Karlsruhe

(DNA markers)

peqGold 100 bp DNA ladder PeqLab, Erlangen

peqGold 1 kb DNA ladder PeqLab, Erlangen

3.2.4 Antibodies

Table 6: Antibodies. Pab = polyclonal antibody; Mab = monoclonal antibody; HRP = horseradish peroxidase; Cy3 = cyanine 3; Cy5 = cyanine 5.

Antibody	Description	Reference or source
(primary)		
goat α -HBsAg	Pab, detects hepatitis B surface antigen	Dako, Hamburg
goat α -Hsp90- α	Pab, detects human heat shock protein 90 α isoform	Santa Cruz, USA
goat α -karyopherin- α 2	Pab (C-20), directed against importin- α 2	Santa Cruz, USA
mouse α -Pol (3552)	Mab (clone 3552), detects HBV polymerase	HPI Hamburg, unpublished
mouse α - β -actin	Mab (clone AC-74), detects human beta-actin	Sigma-Aldrich, Seelze
mouse α -CKII α	Mab, detects human protein kinase CKII α subunit	Calbiochem, Darmstadt
mouse α -PCNA	Mab (clone PC-10), detects human PCNA	Santa Cruz, USA
rabbit α -ACTIVE Mabk	Pab, detects phosphorylated form of human ERK	Promega, Mannheim
rabbit α - α -Fetoprotein	Pab, detects human α -Fetoprotein	Chemicon, Darmstadt
rabbit α -PKC α	Pab (C-20), detects human protein kinase C α subunit	Santa Cruz, USA
rabbit α -PolS1	Pab, detects S-domain of HBV polymerase	this study
sheep α -HBsAg	Pab, detects hepatitis B surface antigen	Uni Goettingen, unpublished
(secondary)		
donkey α -goat-Cy3	Pab, conjugated with Cy3 dye	Dianova, Hamburg
donkey α -goat-HRP	Pab, conjugated with horse raddish peroxidase	GE Healthcare, Freiburg
donkey α -rabbit-Cy5	Pab, conjugated with Cy5 dye	Dianova, Hamburg
donkey α -rabbit-HRP	Pab, conjugated with horse raddish peroxidase	GE Healthcare, Freiburg
goat α -rabbit-Cy3	Pab, conjugated with Cy3 dye	Dianova, Hamburg
sheep α -mouse-HRP	Pab, conjugated with horse raddish peroxidase	GE Healthcare, Freiburg

3.2.5 Enzymes

Antarctic phosphatase NEB, Frankfurt am Main

DNase I Sigma-Aldrich, Sleeze

DNase, RNase free Roche, Mannheim

LunaTaq hotstart polymerase Bioline, Luckenwalde

Lysozyme Carl-Roth, Karlsruhe

Protein kinase C (catalytical subunit) Calbiochem, Darmstadt

Protein kinase CKII	Calbiochem, Darmstadt
Restriction endonucleases	NEB, Frankfurt am Main
T4 DNA ligase	Roche, Mannheim
BIOTAQ polymerase	Bioline, Luckenwalde
<i>Pfu</i> Ultra hotstart polymerase	Stratagene, Netherlands

3.2.6 *Radiochemicals*

[γ 32P]ATP	Hartmann Analytics, Göttingen
[α 32P]dATP	GE Healthcare, Freiburg
[α 32P]dCTP	GE Healthcare, Freiburg

3.2.7 *Reagents for cell culture*

Collagenase CLSII	Biochrom, Berlin
Collagen G	Biochrom, Berlin
Dexamethasone	Sigma-Aldrich, Sleeze
L-glutamine	PAN Biotech, Aidenbach
Transferrin	Invitrogen, Karlsruhe
Sodium pyruvate	PAN Biotech, Aidenbach
Sodium selenite	Invitrogen, Karlsruhe
Bovine serum albumin	Invitrogen, Karlsruhe
DMEM medium (incl. L-glutamine)	PAN Biotech, Aidenbach
Trypsin / EDTA	PAA, Austria
Fetal calf serum (FCS)	PAA, Austria
G418	Sigma-Aldrich, Sleeze
Hydrocortisone	Sigma-Aldrich, Sleeze
Insulin	Sigma-Aldrich, Sleeze
Penicillin / Streptomycin	PAA, Austria
SFII900 insect cell medium	Invitrogen, Karlsruhe
Williams medium E (w/o L-glutamine)	Biochrom, Berlin

3.2.8 Inhibitors

Table 7: Inhibitors. Effective concentrations are cited in brackets; an asterisk indicates IC₅₀ concentrations.

Inhibitor	Target	Source
(Kinase inhibitors)		
Gö6976	PKC isoenzymes α (2.3 nM*), β (6.2 nM*)	Calbiochem, Darmstadt
DMAT	protein kinase CKII (150 nM*)	Calbiochem, Darmstadt
(Protease inhibitors)		
Leupeptin	serin-, cystein-proteases (4 μ M)	Sigma-Aldrich, Sleeze
Pepstatin	acid-, aspartatic-proteases (1 μ M)	Sigma-Aldrich, Sleeze
Aprotinin	serin-proteases (1 μ M)	Sigma-Aldrich, Sleeze
PMSF	serin-, cystein-proteases (1 mM)	Carl-Roth, Karlsruhe

3.2.9 Fine chemicals

All fine chemicals were purchased by Carl-Roth, Karlsruhe. Exceptions are listed below:

Aprotinin	Sigma-Aldrich, Sleeze
ATP	Sigma-Aldrich, Sleeze
GTP	Sigma-Aldrich, Sleeze
Bovine serum albumin (BSA)	PAA, Austria
Bradford reagent	Sigma-Aldrich, Sleeze
Cytodex 3	GE Healthcare, Freiburg
DAPI	Sigma-Aldrich, Sleeze
DEPC	Sigma-Aldrich, Sleeze
Dichlorodimethylsilane	Applichem, Darmstadt
DMAT	Calbiochem, Darmstadt
dNTP mix	Bioline, Luckenwalde
ECL peroxidase substrate	GE Healthcare, Freiburg
Ethanol amine	Sigma-Aldrich, Sleeze
Ethidium bromide	Applichem, Darmstadt
Freunds adjuvant	Sigma-Aldrich, Sleeze
Fugene 6 transfection agent	Roche, Mannheim

Gö6976	Calbiochem, Darmstadt
GTP	Sigma-Aldrich, Sleeze
Imidazole	Sigma-Aldrich, Sleeze
Leupeptin	Sigma-Aldrich, Sleeze
NHS-sepharose	GE Healthcare, Freiburg
Nickel-NTA Superflow	Qiagen, Hilden
NP-40	Sigma-Aldrich, Sleeze
Osmium tetroxide	Bal-Tec, Austria
Pepstatin	Sigma-Aldrich, Sleeze
Phalloidin-FITC	Sigma-Aldrich, Sleeze
Polyethylenimine (MW 25,000), linear	Polysciences, USA
Protein A/G agarose	Santa Cruz,, USA
Skim milk powder	Sigma-Aldrich, Sleeze
TEMED	Sigma-Aldrich, Sleeze
Triton X-100	Sigma-Aldrich, Sleeze
tRNA	Sigma-Aldrich, Sleeze
TriFast	Peqlab, Erlangen
Tween-20	Gerbu, Gaiberg

3.2.10 Drugs

Ketavet (ketamine hydrochloride)	Pharmacia & Upjohn, Erlangen
Rompun (xylazine hydrochloride)	Bayer, Leverkusen

3.2.11 Membranes and relevant plastic ware

Hybond-P	GE Healthcare, Freiburg
Hybond-N	GE Healthcare, Freiburg
T175 cm ² cell culture flasks	Greiner Bio-one, Frickenhausen
Cell strainer	BD Biosciences, USA
Abbocath 18 gauge catheter	Abbott, Ireland

3.3 Buffers and solutions

Buffers and solutions are summarized in APPENDIX 1

3.4 Kits

High Pure Viral Nucleic Acid Kit	Roche, Mannheim
NEBlot probe labeling kit	NEB, Frankfurt am Main
QIAGEN Plasmid Maxi Kit	Qiagen, Hilden
QIAprep Spin Miniprep Kit	Qiagen, Hilden
QIAquick Gel Extraction Kit	Qiagen, Hilden
Enzygnost HBeAG Monoclonal ELISA	Dade Behring, Marburg
Enzygnost HBsAG 5.0 ELISA	Dade Behring, Marburg

3.5 Devices

3.5.1 *Chromatography*

Äkta Purifier chromatography system	GE Healthcare, Freiburg
MonoS 5/50 GL cationic exchange column	GE Healthcare, Freiburg
MonoQ 5/50 GL anionic exchange column	GE Healthcare, Freiburg
HiTrap Desalting gel filtration column	GE Healthcare, Freiburg

3.5.2 *Electrophoresis*

Horizontal electrophoresis systems	GE Healthcare, Freiburg
GNA 100 and 200	
Vertical electrophoresis systems	GE Healthcare, Freiburg
SE 260 and 600	
Semi-dry blotting chambers	GE Healthcare, Freiburg

Semiphor and Multiphor II

Hofer Electrophoresis power supply 301

GE, Healthcare, Freiburg

*3.5.3 Microscopy*Confocal laser scanning microscope (Axioplan)
LSM510

Zeiss, Jena

Field emission scanning electron microscope LEO
1530

Carl Zeiss SMT, UK

3.5.4 PCR cyclers

Lightcycler 1.5

Roche, Mannheim

PegLab Primus 96

PegLab, Erlangen

Taqman Abi Prism 4000

Perkin-Elmer, Rodgau

3.5.5 Imaging

Image plate reader BAS-1500

Fujifilm, Düsseldorf

Intelligent Dark Box LAS-3000

Fujifilm, Düsseldorf

Image plate BAS MP 2040S

Fujifilm, Düsseldorf

BAS Cassette 2040

Fujifilm, Düsseldorf

AGFA CP-1000 film developer

AGFA, Köln

Biomax MR scientific imaging film

Kodak, Stuttgart

UV table UV-Biometra TB

Biometra, Göttingen

with camera BioToc

3.5.6 Centrifugation

Centrifuge 5415 R (refrigerated)

Eppendorf, Hamburg

Table centrifuge Biofuge fresco

Heraeus, Osterode

Sorvall Evolution RC with rotors SLA-1500 and SS-34	Sorvall Instruments, Bad Homburg
Beckmann L8-70 ultracentrifuge with rotors SW-28 and SW-41	Beckmann, USA
Amicon Ultra-15 centrifugal filter device MWCO 100 kDa	Millipore, Schwalbach
Amicon Centricon Ultracel YM-10 centrifugal filter device MWCO 10 kDa	Millipore, Schwalbach

3.5.7 *Other devices*

French Press Emulsi Flex C-5	Avestin, Canada
Homogenisator Sonoplus HD 2070	Bandelin, Berlin
Incubator	Heraeus, Osterode
pH meter 765 Calimatic	Knick, Berlin
Photometer Ultraspec 3300 pro	GE Healthcare, Freiburg
Satorius balance 1608 MP	Satorius, Göttingen
Satorius universal analytical balance	Satorius, Göttingen
Shaker Unitron	HT-Infors, Switzerland
Sterile bench HeraSafe	Kendro, Langenselbold
Thermomixer compact	Eppendorf, Hamburg
Vacuum dryer (Slap Dryer Model 443)	BioRad, USA
Vacuum pump	KNF Neuberger, Freiburg
Water bath GFL 1083	GFL, Burgwedel
CPB-303 Critical point dryer	Bal-Tec, Austria
Polaron E5100 Sputter Coater	Bal-Tec, Austria

4 METHODS

4.1 Cell culture

4.1.1 *Prokaryotic cell culture and protein expression*

E. coli K12 strains DH5 α , BL21 and M15 (pREP4) were cultivated in LB medium at 37 °C with agitation in baffled Erlenmeyer flasks. For protein expression the *E. coli* strains were cultivated in SB medium. The strain M15 (pREP4) was cultivated with an additional 40 μ g/mL kanamycin. Frozen stocks were stored in 25 % (v/v) glycerol at -80 °C.

Protein expression was induced within the logarithmic growth phase at an optical density of 0.5-0.6 at a wave length of 600 nm by addition of 1 mM IPTG to the growth medium. After additional cultivation for 2-3 h the bacteria were harvested by centrifugation for 15 min at 6000x g, 4 °C. Pellets were stored at -20 °C.

4.1.2 *Eukaryotic cell culture*

The cell lines huh-7 and HepG2.2.15 were cultivated in DMEM medium including 10 % (v/v) FCS, 0.1 U/mL penicillin, and 100 μ g/mL streptomycin. The cell line HepAD38 was cultivated with an additional 2.5 mg/L insulin, 50 μ M hydrocortisone, and 400 μ g/mL G418.

Primary hepatocytes of *Tupaia belangeri* were cultivated in Williams medium E, supplemented with 100 nM dexamethasone, 0.1 U/mL penicillin, 100 μ g/mL streptomycin, 2 mM glutamine, 10 mg/L insulin, 6.7 μ g/L sodium selenite, 5.5 mg/L transferrin, 110 mg/L sodium pyruvate, and 0.15 % (w/v) bovine serum albumin. All hepatocytes were cultivated attached to a collagen coated plastic surface at 37 °C in a water saturated atmosphere of 5 % (v/v) CO₂.

Spodoptera frugiperda (Sf9) derived cells were grown in suspension with SFII900 serum free insect cell medium at 27 °C and 135 rotations per minute.

4.1.3 *Adherent cell culture on microcarrier*

Cultures containing 6×10^6 – 2×10^7 cells per 20 mL were grown on 100 mg dw (dry weight) Cytodex-3 in a silanized 100 mL Erlenmeyer flask. The Cytodex-3 was equilibrated as suggested by the manufacturer except that the swollen microcarrier suspensions were not autoclaved. The microcarrier cultures were agitated by tilting 50 times in 3 min, followed by a 30 min brake. This cycle was repeated for 24 h followed by 48 h nonstop agitation with the same frequency. Sampling was performed every 24 h by replacing the half of the culture media with fresh medium. Before its analysis, the samples were precleared by centrifugation at 300x g for 15 min.

4.1.4 *Cell trypsination*

Passaging of adherent cells was performed using trypsin / EDTA at 37 °C. Prior trypsination the cells were carefully washed with PBS buffer to remove cell culture medium. After 2-5 min the treatment was stopped by addition of 10 mL culture medium including fetal calf serum. If necessary, cell aggregates were minimized by a repeated passage of the cell suspension through a 20 gauge injection needle. The cells were seeded in fresh culture medium to reach 30-50 % confluency.

4.1.5 *Collagen coating*

The growth surface of a sterile cell culture dish was rinsed with 100 µg/mL collagen G solution. The collagen layer was air dried for 1-2 days until usage.

4.1.6 *Silane coating*

A clean and dry 100 mL Erlenmeyer flask was rinsed with 5 % (v/v) dichlorodimethylsilane solution and baked for 1 h at 120 °C. The silanized glassware was rinsed with deionized water and autoclaved plugged with cellulose and aluminum foil.

4.1.7 *Cell counting*

Suspended eukaryotic cells were counted using a Neubauer chamber. The cells were diluted in 0.3 % (w/v) trypan blue to check for cell viability.

4.1.8 *Transfection of hepatoma cells*

For small scale transfections and endogenous polymerase assay analysis, huh-7 cells were transfected by lipofection using Fugene 6 according to the instructions of the manufacturer. For large scale transfections and if no further enzymatic reaction of extracellular products was necessary, cells were transfected using linear polyethylenimine (1 mg/mL) according to the manual of ExGene500 transfection agent (Fermentas, St. Leon-Rot).

4.1.9 *Preparation of primary hepatocytes*

Primary hepatocytes of *Tupaia belangeri* were isolated by liver perfusion with collagenase. Thereto, the animal was anaesthetized by injection of Ketavet (5 mg/100 mg body weight) and Rompun (1 mg/100 mg body weight) into the tail vein. After 10 min the animal was fixated and chest and belly were shaved and disinfected with 70 % (v/v) ethanol. The fur and the abdominal wall were opened and the organs rinsed twice with sterile Hanks solution, supplemented with 2.5 mM EGTA, 0.1 % (w/v) glucose, 0.1 U/mL penicillin, and 100 µg/mL streptomycin (Hanks I). An 18 gauge catheter was inserted into the portal vein and the liver was purged at a flow

rate of 8 mL/min with Hanks I solution supplemented with 0.3 mg/mL collagenase CLSII and 5 mM calcium chloride. Immediately after starting the inferior cava vein and the right heart ventricle were incised to permit a sufficient outflow from the liver. The organ was perfused until the tissue swelled and lost its flexibility (Fig. 11). The liver was excised, the gall bladder was removed and the liver capsule was opened to release the cells into Williams medium E w/o glutamine, supplemented with 100 nM L-hydrocortisone, 10 % (v/v) fetal calf serum, 1 μ M insulin, 2 mM glutamine, 0.1 U/mL penicillin, and 100 μ g/mL streptomycin. Hepatocytes were enriched by centrifugation for 2 min at 37.5x g and sieved by a 70 μ m cell strainer. 1×10^6 cells were seeded to a collagen coated 3.5 cm well. After 4 h the culture supernatant was removed and maintained as described in 4.1.2.

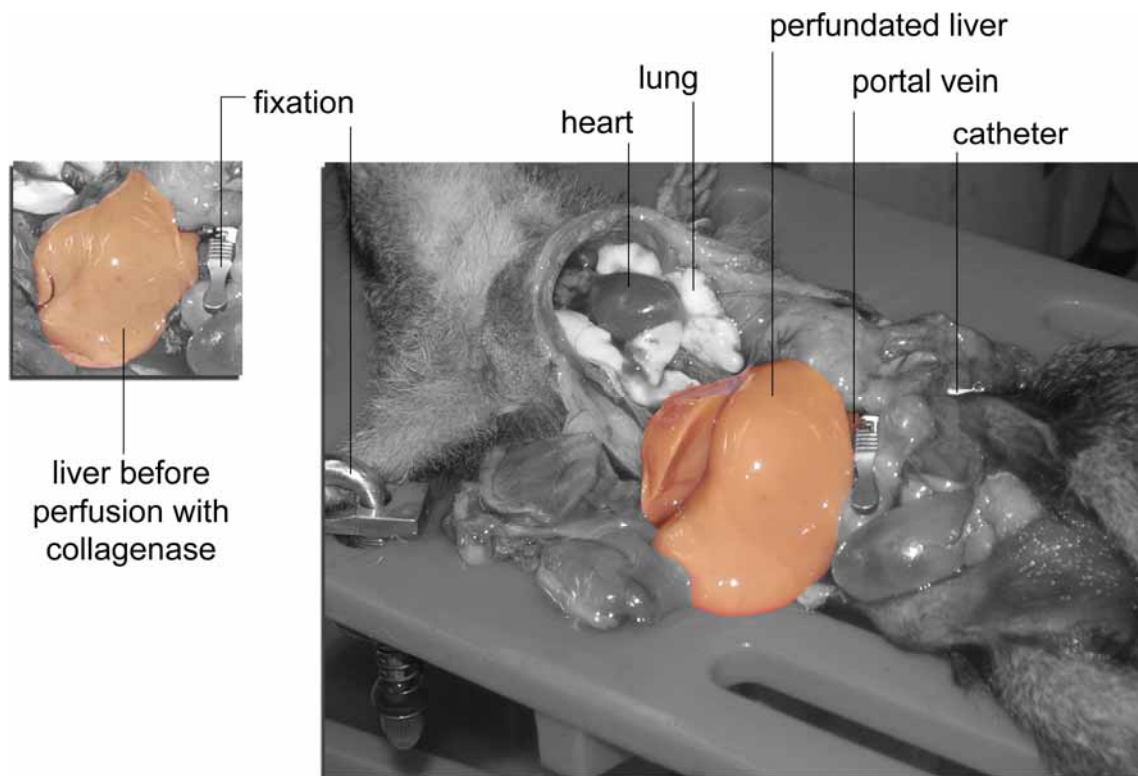


Figure 11: Collagenase perfusion of *Tupaia* liver tissue. The liver was purged with 8 mL/min by 0.3 mg/mL collagenase through a catheter in the portal vein until the tissue swelled and lost its flexibility.

4.2 RNA and DNA manipulation

4.2.1 RNA preparation

The RNA from eukaryotic cells was extracted using TriFast reagent according to the manufacturer's instructions. The RNA was stored at -80 °C in RNase free water.

4.2.2 Virus DNA preparation

4.2.2.1 Adsorber method

Viral DNA was prepared from 500 µL cell culture supernatant using High Pure Viral Nucleic Acid Kit according to manufacturer's instructions. The volumes of binding buffer and protease K solution at the first step were adapted to the increased sample volume. The virus DNA was stored in elution buffer at -20 °C.

4.2.2.2 Phenol/chloroform method

An equal volume of virus sample was mixed with lysis buffer (10 mM Tris-HCl, 6 M guanidine-HCl, 20 % (v/v) Triton X-100, 2.5 mg/mL proteinase K, pH 4.4) and incubated at 72 °C for 10 min.

The virus DNA extraction was performed by phenol/chloroform treatment and ethanol precipitation as described in standard protocols [Ausubel, et al., 2004]. The virus DNA was solved in TE buffer and stored at -20 °C.

4.2.3 Restriction enzyme reaction

For qualitative analysis 1-2 µg of plasmid DNA and for cloning purposes 0.5 µg of vector DNA was digested in a 10 µL reaction volume according to the enzyme

requirements listed by the manufacturer. The DNA fragments were analyzed by agarose electrophoresis.

4.2.4 *Dephosphorylation of vector DNA*

Prior to ligation with insert DNA, the 5'-ends of linearized vector DNA were removed by Antarctic phosphatase treatment to prevent self-ligation. The reaction was performed according to manufacturer's instructions in a 10 μ L reaction. The phosphatase was inactivated by 5 min heat denaturation at 65 °C.

4.2.5 *Ligation of DNA*

Ligations were performed in a volume of 10 μ L combining ~20 ng of linearized and dephosphorylated vector DNA and a 10 fold excess of insert DNA with compatible ends. The reaction was incubated overnight at 16 °C and finally heat inactivated for 10 min at 65 °C.

4.2.6 *Transformation of DNA*

DNA was introduced into *E. coli* by calcium chloride mediated transformation as described in Current Protocols of Molecular Biology [Ausubel, et al., 2004]. The chemically competent cells were prepared according to basic protocol 1, shock-frozen in liquid nitrogen and stored at -80 °C. The colonies were checked by PCR (4.2.8.1) for positive clones and correct ligations.

4.2.7 *Plasmid extraction*

Plasmid DNA was extracted from bacterial biomass using QIAprep Spin Miniprep Kit from a 3-5 mL overnight culture or QIAGEN Plasmid Maxi Kit from a 200-500 mL overnight culture. The extraction procedure was performed as described by Qiagen. The plasmid DNA was eluted in EB buffer and stored at -20 °C.

4.2.8 Polymerase chain reaction (PCR)

4.2.8.1 Standard PCR

Qualitative or preparative DNA analysis by PCR was performed in a reaction mix described in Tab. 8. The target DNA was amplified at 95 °C 6 min, 29x (95 °C 60 sec, 52 °C 60 sec, 72 °C 90 sec), 72 °C 10 min. For colony PCR a small portion of the bacterial colony was suspended in 20 µL deionized water. 2 µL of the bacteria suspension was used as sample for PCR.

Table 8: PCR reaction mixtures.

Reagents	Standard PCR	Mutagenesis	TaqMan PCR	Lightcycler PCR
<i>Reaction volume</i>	(50 µL)	(50 µL)	(50 µL)	(20 µL)
10x PCR buffer w/o MgCl ₂	5 µL		5 µL	2 µL
10x <i>Pfu</i> reaction buffer		5 µL		
MgCl ₂ (50 mM)	2.5 µL		4.5 µL	1.8 µL
TE buffer, pH 8.0			0.8 µL	0.24 µL
BSA (600 µg/mL)				0.24 µL
dNTP mix (25 mM each)	0.4 µL	0.25 µL	0.4 µL	0.32 µL
sense primer (10 µM)	1.25 µL	1.25 µL	1.25 µL	0.5 µL
antisense primer (10 µM)	1.25 µL	1.25 µL	1.25 µL	0.5 µL
probe (10 µM)			0.625 µL	0.25 µL
BIOTAQ polymerase	0.25 µL			
LunaTaq hotstart polymerase			0.25 µL	0.1 µL
<i>Pfu</i> hotstart polymerase		1 µL		
Sample	2 µL (≤20 ng plasmid)	1 µL (5-20 ng plasmid)	2 µL	1 µL

4.2.8.2 Quantitative PCR

For the quantification of target DNA molecules two systems were used: the high throughput TaqMan system Abi Prism 4000 and the faster low throughput Lightcycler 1.5 system. The principle of quantification is the detection of a third fluorescent linked oligonucleotide (probe), which binds in between the two binding sites of the primer set. In this study quantitative PCR systems were instrumental to quantify a 124 basepair

(bp) DNA sequence within the HBV genome. This HBV assay was first described 2003 by Stoeckl and co-workers [Stockl, et al., 2003].

The PCR reaction mixtures for the TaqMan and the Lightcycler formats are summarized in Tab. 8. The TaqMan temperature profile was 95 °C 5 min, 30x (95 °C 15 sec, 60 °C 60 sec) and the Lightcycler temperature profile was 95 °C 5 min, 30x (95 °C 15 sec, 60 °C 30 sec, 72 °C 30 sec).

4.2.8.3 Site directed mutagenesis

This PCR based method introduces site directed mutations in circular plasmid DNA by a set of reverse complementary oligonucleotides [Fisher and Pei, 1997]. The sequence alteration was coded in the central part of the backward and the forward primer, which was flanked upstream and downstream by at least 20 bp of complementary sequence. If possible a silent marker mutation was introduced near the crucial mutation, which did not affect the amino acid sequence but altered the restriction pattern of the plasmid.

A *Pfu* polymerase with proof reading activity amplified both strands of the plasmid starting at the same position in opposite directions. The reaction mix composition is described in Tab. 8. The template DNA was amplified at 95 °C 30 sec, 18x (95 °C 30 sec, 55 °C 60 sec, 2 min/kb of plasmid length). The annealing temperature in this method is set independently of the actual melting point of the primers because of the unusual length of the mutation primers (Tab. 5). Prior transformation in *E. coli* DH5 α the template DNA was digested with restriction endonuclease *DpnI*. Candidate plasmids were preselected by PCR and restriction analysis. Finally, the mutated plasmid was verified by sequence analysis.

4.2.9 Agarose electrophoresis

DNA fragments and PCR products were analyzed by agarose gel electrophoresis. Broad range agarose was dissolved in TAE buffer by heating. 0.1 μ g/mL ethidium bromide was added to the liquid agarose before it was casted into an electrophoresis tray. The density of the gel used was dependent on the expected DNA size. Fragments of

50-200 bp of size were analyzed in a 2 % (w/v) agarose gel and fragments larger than 200 bp in a 1 % (w/v) agarose gel. The samples were loaded with 1x agarose gel sample buffer and separated by electrophoresis at 50-80 V. For imaging the DNA was visualized on a UV table at 254 nm, for DNA preparation it was visualized at 365 nm. The fragment sizes were compared to molecular weight calibrators.

4.2.10 DNA extraction from agarose gels

The targeted DNA fragment was sliced from the agarose gel by a sharp and clean scalpel and extracted by QIAquick Gel Extraction Kit according to the manufacturer's instructions. The DNA was eluted in 30-50 μ L EB buffer and stored at -20 °C.

4.2.11 Sequencing and sequence analysis

DNA sequencing was performed by SeqLab Sequence Laboratories in Göttingen. DNA amounts were prepared as suggested by the service provider. DNA and protein sequence analysis was performed using Vector NTI Suite software provided by Invitrogen, Karlsruhe.

4.2.12 Northern blot

Northern blot analysis is based on the identification of target RNA by hybridization with a specific reverse complementary DNA probe. This method was performed according to standard procedures [Ausubel, et al., 2004]. Ten microgram of RNA was separated on a 1.2 % (w/v) agarose gel containing 10 % (v/v) formaldehyde and buffer NB. The RNA was transferred with 10x SSC buffer on Hybond-N uncharged nylon membrane and baked 20 min at 80 °C prior to probing.

The probe was generated by *Eco*RI and *Nco*I digestion of a HBV genome (subtype ayw, genotype D), which was labeled with [α -³²P]dATP using NEBlot kit according to the instructions of the manufacturer.

4.2.13 *Southern blot*

Southern blot analysis is based on the identification of target DNA by hybridization with a specific reverse complementary DNA probe. This method was performed according to standard procedures [Ausubel, et al., 2004]. The DNA was separated on 1.2 % (w/v) agarose gel and transferred onto Hybond-N uncharged nylon membrane with buffer SB. Prior to DNA transfer, the gel was treated for 15 min with 0.25 M hydrochloric acid to destroy the purine bases within the DNA. The membrane was baked for 20 min at 80 °C and probed with the same radioactively labeled DNA probe described in chapter 4.2.12.

4.2.14 *Endogenous Polymerase Assay (EPA)*

This assay is based on the detection of a radioactive tracer incorporated into the HBV genome by the encapsidated viral polymerase. 3×10^5 huh-7 cells were seeded in 6-well plates and transfected with 2 µg HBV DNA using Fugene 6. The enveloped viral particles were precipitated from the cell culture supernatant 5 d after transfection using a HBsAg-specific antibody (a kind gift from Klaus-H. Heermann, University of Goettingen, Dept. Virology, Germany) and swollen protein-A sepharose beads. The EPA reaction was performed as described [Koschel, et al., 2000] using 10 µCi [α - 32 P] dCTP for the labeling. The labeled DNA was separated by 1 % (w/v) agarose gel electrophoresis without ethidium bromide. The radioactive gel was dried in a vacuum dryer and analyzed by autoradiography.

4.3 **Cell lysis**

4.3.1 *Enzymatic cell lysis*

A bacterial cell pellet (2-4 g wet mass) was suspended in 30 mL TBS buffer containing a spatula tip lysozyme and protease inhibitors in effective concentrations (Tab. 7). The suspension was agitated for 20 min at room temperature and sonicated on ice for three

intervals of 50 watts intensity. The lysate was cleared by ultracentrifugation at 76,000x g for 1 h at 4 °C.

4.3.2 *Cell lysis using detergent*

Confluent adherent liver cells on a 6 cm cell culture dish were washed twice in PBS and lysed on ice in 500 µL low detergent lysis buffer (0.2 % (v/v) NP-40, 20 mM Tris, 150 mM sodium chloride, 1 mM EDTA, pH 7.5 and protease inhibitors at effective concentrations (Tab. 7)) or in 500 µL high detergent lysis buffer (RIPA; 20 mM Tris, 1 % (w/v) sodium deoxycholate, 1 % (v/v) Triton X-100, 0.1 % (w/v) sodium dodecyl sulfate, 150 mM NaCl, pH 7.2). The lysed cells were collected by a rubber policeman and cleared by ultracentrifugation at 76,000x g for 10 min at 4 °C.

4.3.3 *French Press*

A pellet of 2-4 g (wet weight) prokaryotic or eukaryotic cells was suspended in 30 mL TBS containing protease inhibitors in effective concentrations (Tab. 7). The suspension was cooled at 4 °C and disrupted at 20,000 psi differential pressure in a French Press. The disruption was repeated three times before the lysate was cleared by ultracentrifugation at 76,000x g for 1 h at 4 °C.

4.4 Protein chemistry

4.4.1 Protein quantification

4.4.1.1 Optical density

The amino acids tryptophan and tyrosine absorb light at a wavelength of 280 nm. Due to variable amino acid composition the absorption of 1 mg protein/mL is between 0.5-2 absorption units (AU). The molecular extinction coefficient of TP ($35,800 \text{ L} \times \text{mol}^{-1} \times \text{cm}^{-1}$) and the S domain ($25,800 \text{ L} \times \text{mol}^{-1} \times \text{cm}^{-1}$) was calculated by evaluation of the amino acid sequence using Vector NTI. Based on this calculation 1 AU equates 0.63 mg TP domain/mL or 0.73 mg S domain/mL, respectively.

4.4.1.2 Bradford assay

The binding of proteins to the dye Coomassie Brilliant Blue G-250 in the Bradford reagent stabilizes the anionic form of the dye. This shifts the light absorption maximum from 465 nm to 595 nm. Protein quantification was performed according to the manufacturer's instructions.

4.4.2 SDS-PAGE electrophoresis

This method separates a protein mixture dependent on its molecular weight (MW) composition. It was performed as described in standard protocols [Ausubel, et al., 2004]. The polymer density of the separation gel depends on the expected MW of the target protein (MW < 30 kDa = 15 % (w/v) PAGE gel, MW > 30 kDa = 10 % (w/v) PAGE gel). Proteins are denatured in SDS-PAGE sample buffer by 5 min heat denaturation at 95 °C prior to electrophoresis in SDS-PAGE buffer at 80-120 V.

4.4.3 Silver staining

This technique visualizes protein bands in a PAGE gel. It is based on the specific redox potential of proteins that is sufficient to reduce silver ions to its amorphous metallic state. The PAGE gel was incubated for 20 min in 50 mL of buffer S_{Fi} and S_{Ko} , washed 3x 10 min in deionized water and subsequently incubated for 20 min in 50 mL of buffer S_{Ke} . The PAGE gel was developed in 50 mL buffer S_E and the reaction was stopped by ~2 mL glacial acetic acid when the protein bands appeared in a proper resolution compared to the background staining. The gel was digitalized using a regular flat bed scanner.

4.4.4 Western blot

Separated proteins in a SDS-PAGE gel were transferred on a methanol pretreated PVDF membrane (Hybond-P) using a semi-dry blotting chamber as described in Fig. 12. The proteins migrate from the gel onto the membrane in an electric field of 1.3 mA/cm² for 1 h. Free membrane surface was coated using blocking solution (10 % (w/v) skim milk powder in buffer PBS-T). Antibodies were diluted in blocking solution as suggested by the manufacturer. Unbound antibodies were removed by washing with buffer PBS-T. For detection the membrane was incubated with peroxidase substrate reagent (ECL) as described by the manufacturer and exposed to a scientific imaging film.

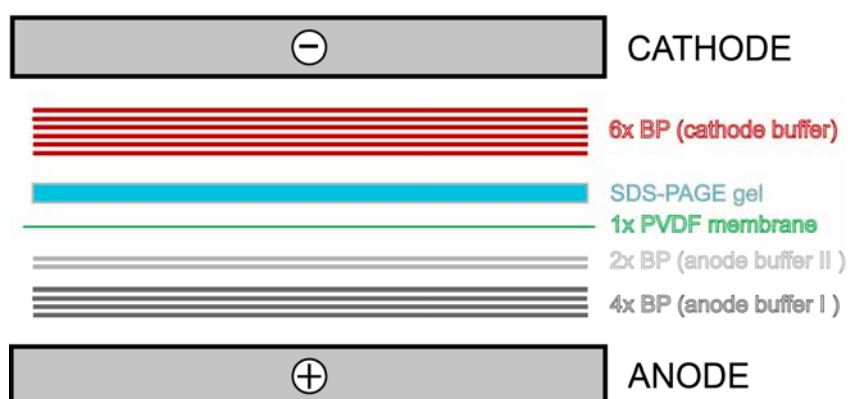


Figure 12: Scheme of a semi-dry blotting stack. Blotting paper (BP) in the size of the SDS-PAGE gel were soaked with anode I (light grey) /II (dark grey) or cathode buffer (red) and piled together with a PVDF membrane (green) and the gel (blue) to a semi-dry blotting sandwich in the order as indicated. The stack is held by the anode (bottom) and the cathode (top). Within 1 h and 1.3 mA/cm² the proteins migrate towards the anode onto the PVDF membrane.

4.4.5 *Immuno-histology*

Intracellular localization of proteins was determined by immuno-staining of permeabilized cells by fluorescence labeled antibodies. Eukaryotic cells were cultivated on a 15 mm glass cover slip in a 3.5 cm² cell culture dish. The cells were fixated for 15 min in -20 °C cold 100 % (v/v) ethanol including DAPI. All subsequent incubation steps were performed light protected at room temperature with slight agitation. The cell membrane was permeabilized by buffer PBS-T and the free surface was coated using blocking solution (10 % (w/v) bovine serum albumin in PBS-T). The primary and secondary antibodies were diluted in blocking solution as suggested by the manufacturer. Unbound antibodies were removed by washing with buffer PBS-T and the coverslip was sealed in mounting medium on a microscope slide. Slides were stored light protected at 4 °C prior to analysis in a confocal laser scanning microscope.

4.4.6 *In vitro phosphorylation*

E. coli produced terminal protein domain was dialysed (cut off 10,000 kDa) against 1x buffer K. The kinase reaction was initiated by addition of 10 µCi [γ -³²P] ATP and of 5-10 U of rat brain PKC (catalytical subunit) or recombinant human CKII, both purchased from Calbiochem. After 30 min incubation at 30 °C the reaction was stopped by addition of SDS-PAGE sample buffer and heat treatment (5 min, 95 °C). Proteins were separated by 12 % (v/v) SDS-PAGE, the gel was dried and incorporated radiation was detected by autoradiography.

4.5 Microscopy

4.5.1 *Confocal laser scanning microscopy*

Fluorescent labeled cells were analysed with a confocal laser scanning microscope. With this method the excitation of various fluorescence dyes can be focused to a defined layer within a cell. This offers the possibility to resolve a cell's fluorescence in a precise three-dimensional image and to investigate the co-localization of proteins within a cell. The analysis was performed using an Axioplan LSM-510 microscope.

4.5.2 *Electron microscopy*

HepG2.2.15 cells on Cytodex-3 were treated with 2.5 % (v/v) glutaraldehyde in 50 mmol/L HEPES buffer. After a brief washing step with deionized water the carriers were fixated with 1 % (w/v) osmium tetroxide for 1 h. Water was removed by washing with an increasing gradient of ethanol. The samples were dried by carbon dioxide using CPB-303 Critical Point Dryer. Finally, the samples were coated with a 10 nm layer of gold by a sputter coater and analyzed at 5 kV by a LEO 1530 field emission scanning electron microscope.

4.6 Antibody generation

E. coli derived antigen were purified under denaturated conditions and dialyzed against 50 mM Tris buffer at pH 9. Under these conditions the antigens precipitated during dialysis due to their weak solubility close to the isoelectric point. Prior to injection, about 1 mg of precipitated antigen was suspended in 0.5 mL PBS and emulsified with 0.5 mL of Freund's adjuvant through a 20 gauge injection needle (Fig. 13).

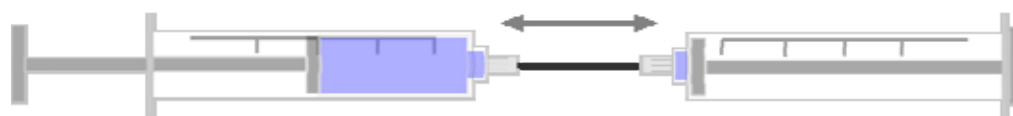


Figure 13: Generation of an antigen-adjuvant emulsion. The PBS/antigen suspension and the hydrophobic adjuvant were emulsified by a repeating passage through a 20 gauge injection needle, which empties in a syringe at both ends.

The injections were placed subcutaneously at three different sites near the lymph nodes of a rabbit. A typical immunization is summarized in Tab. 9. About two weeks after the last boost injection the rabbit was sacrificed. The blood serum was derived by centrifugation after coagulation at room temperature. The serum was stored at $-20\text{ }^{\circ}\text{C}$ until affinity purification.

Table 9: Typical time course for the immunization of rabbits. Incomplete Freund's adjuvant consists of mineral oil and an emulsifier substance like lanoline; complete Freund's adjuvant contains heat-inactivated *Mycobacterium tuberculosis*, additionally.

Injection	Time	Antigen	Adjuvant
1st	day 1	~1 mg	Freund's complete
2nd	2 weeks	~1 mg	Freund's incomplete
3rd	1-2 month	~1 mg	Freund's incomplete

4.7 Protein purification

All chromatographic protein purification methods were performed using the Äkta Purifier design.

4.7.1 Nickel-chelating chromatography

Recombinant proteins were expressed with a terminal extension of six histidine residues in a row. At $\text{pH} > 6.0$ this $(\text{His})_6$ -tag specifically binds nickel ions, which are immobilized by crosslinked nitrilotriacetic acid (NTA) to a gel matrix (Fig. 14).

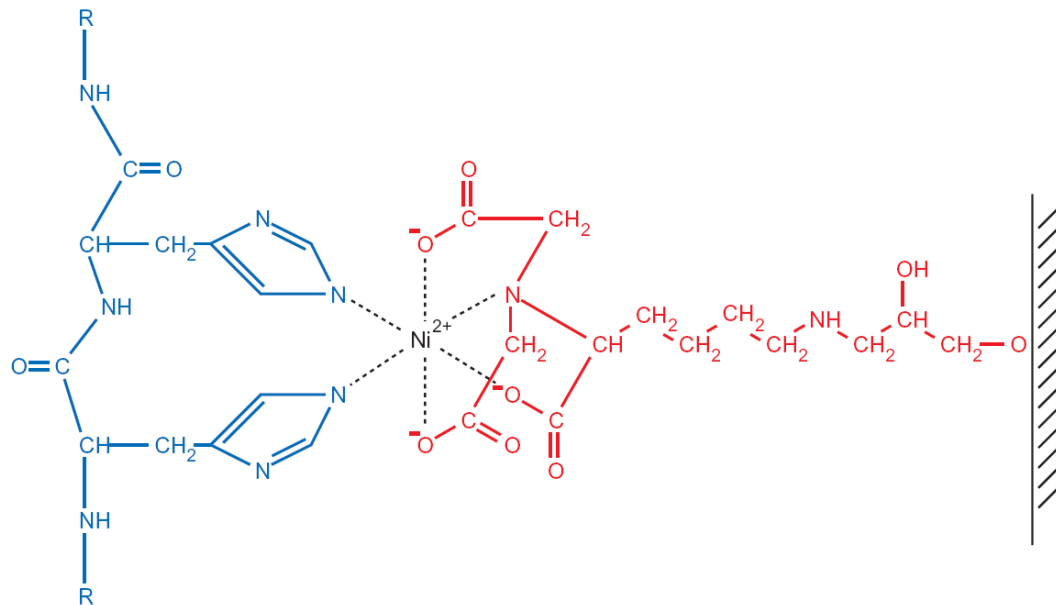


Figure 14: Purification principle of nickel-chelating chromatography. Terminal histidine extensions of a recombinant protein (blue) form a complex with nickel ions and immobilized nitrilotriacetic acid (red) at pH >6. Figure from Qiagen Expressionist.

The bound proteins can be eluted by addition of EDTA, a pH shift <6.0 or an excess of side chain analogue imidazole. The soluble (His)₆-tagged polymerase domains were extracted from 2-4 g of wet bacterial biomass. The cells were disrupted by a French Press and cleared by ultracentrifugation (4.3.3). The supernatant was diluted in buffer A_N to 50 mL and subjected to 1 mL column volume (cv) nickel-NTA sepharose. The column was washed for 10 cv with buffer W_N and proteins were eluted by buffer E_N. Fractions were examined by Western blot and the target protein was pooled and concentrated by ultrafiltration. The molecular weight cut off (MWCO) of the ultrafiltration unit was set to half of the molecular weight of the target protein.

Insoluble intracellular proteins were purified by denaturing nickel-NTA purification. The ultracentrifugation pellet after the cell disruption step was solved in 30 mL of chaotropic lysis buffer L_G by stirring gently for 1 h at room temperature. Occasionally, the suspension was homogenized through a 20-gauge injection needle. The suspension was cleared by ultracentrifugation (76,000x g, 1 h), diluted to 50 mL in buffer A_D and subjected to 1 mL nickel-NTA sepharose. The column was washed for 10 cv in buffer W_D and eluted in buffer E_D. The fractions containing target protein were pooled and further purified by cationic exchange chromatography.

4.7.2 *Cationic exchange chromatography*

This method separates a complex protein mixture due to net charge variation at a distinct pH. The denatured and prepurified recombinant polymerase domain was diluted to 50 mL with buffer A_{MS} and subjected to a MonoS cationic exchange column at pH 5.5. The bound proteins were separated by elution with a linear gradient of 20 cv to buffer A_{MS} including 1 M sodium chloride.

4.7.3 *Gel filtration*

Gel filtration columns separate molecules due to molecular weight differences. Defined pore sizes in the gel matrix increases the retention time for smaller molecules due to an increased molecule diffusion into the matrix. Bigger molecules pass the matrix faster and elute first. This method was used for the desalting of ammonium sulfate precipitated proteins. Therefore, a HiTrap Desalting gel filtration column with a cv of 5 mL was equilibrated with PBS or TBS buffer. 0.5 mL of a protein-salt mixture was injected and the early protein peak was separated from the late salt peak.

4.7.4 *Ammonium sulfate precipitation*

Soluble proteins were precipitated with solid ammonium sulfate (APPENDIX 2). The fine powder was added slowly to the gently agitated sample. The performed protein precipitation and the subsequent washing and centrifugation steps were performed at room temperature. When the targeted salt concentration was reached the sample was incubated for an additional 30 min and the precipitated proteins were removed by centrifugation at 10,000x g for 30 min. The protein pellet was washed twice with an ammonium sulfate solution with the same salt concentration as the proteins that were precipitated. The pellets were stored at 4 °C.

4.7.5 *Antibody affinity purification*

The generated polyclonal rabbit sera directed against the TP domain and the S domain of the HBV P protein were purified by antigen affinity chromatography. The affinity matrix was generated by N-hydroxysuccinimide (NHS)-activated sepharose, which covalently binds amino groups. The immobilization of denatured antigen was performed with variations to the instructions of the manufacturer as described below:

The purified antigen was dialyzed in PBS buffer at pH 8. Tris buffer would disturb the subsequent coupling reaction. About 1.5 mg of antigen precipitate was solved in 1 mL NHS-D buffer containing DMSO and the protein concentration was determined spectrophotometrically at 280 nm. Immediately before the coupling reaction ~2 mL of NHS-activated sepharose was prewashed by ~8 mL NHS-D buffer and added to the antigen solution. The suspension was incubated at room temperature with gentle agitation overnight. After that the suspension was separated by 500x g centrifugation, washed three times with 1 mL NHS-D and the supernatants were pooled for protein quantification. The remaining active NHS groups of the antigen-sepharose were inactivated by alternated washing with buffer NHS-A and NHS-B as described by the manufacturer.

The supernatants were pooled and mixed 1:2 with buffer NHS-G. The coupling efficiency for TP and S immobilization was calculated as described in (1).

$$(1) \quad \text{Coupling efficiency (\%)} = (A-B)/A * 100$$

A = optical density at 280 nm (antigen solution) * volume (antigen solution)

B = optical density at 280 nm (supernatant pool) * volume (supernatant pool)

10-13 mL rabbit blood serum was cleared by 0.45 μ m filtration and the pH was adjusted to pH 8 with 100 mM Tris buffer. The immunoglobulin content was enriched by fractionated precipitation in the 20-50 % (w/v) ammonium sulfate fraction. The antibody-salt pellet was solved in 800 μ L PBS and desalted by gel filtration. The antigen-affinity matrix was packed in an empty chromatography column and subsequently washed with 2 cv PBS, 3 cv buffer E_{AB} and equilibrated by 10 cv PBS. The desalted immunoglobulin fraction was diluted 1:1 in PBS and subjected to the

affinity column. Unspecific antibodies were removed by washing for 10 cv with PBS. The antigen-antibody binding was dissociated at pH 2.3 by a 5 cv step gradient with buffer E_{AB}. To prevent denaturation of the antibodies the pH was immediately neutralized by providing 20 % (v/v) 0.5 M potassium phosphate buffer (pH 8) to each fraction. The antibody fractions were pooled, concentrated by ultrafiltration and stored at -20 °C in 50 % (v/v) glycerol.

4.7.6 *TP binding partner fishing*

Recombinant terminal protein domain was purified and polished to injection grade as described in 4.7.1-2. The TP containing fraction of the cationic exchange run was adjusted to pH 8 and the protein content was quantified at 280 nm.

2 mL Ni-NTA agarose suspension was washed with 10 mL buffer A_{TP} and suspended in the TP domain solution. The sample was gently agitated for 1 h at room temperature. The agarose was washed twice with 1 mL buffer A_{TP}, the supernatants were pooled and the protein content was measured at 280 nm. The coupling efficiency was ~90 % as calculated similar to (1).

Same amounts of TP-agarose were loaded in two empty chromatographic columns and one column was loaded with an equal amount of 'empty' Ni-NTA Superflow (Fig. 15). The denatured TP was refolded by a slow linear gradient for 30 cv to buffer R. All three columns were equilibrated for 10 cv with CKII buffer. The same volume was injected into every column. Every injection contained 200 μM GTP, the injection for the TP* column contained an additional 2,500 U protein kinase CKII (Fig. 15). The columns were sealed and incubated for 3 h at 27 °C and washed with 5 cv CKII buffer.

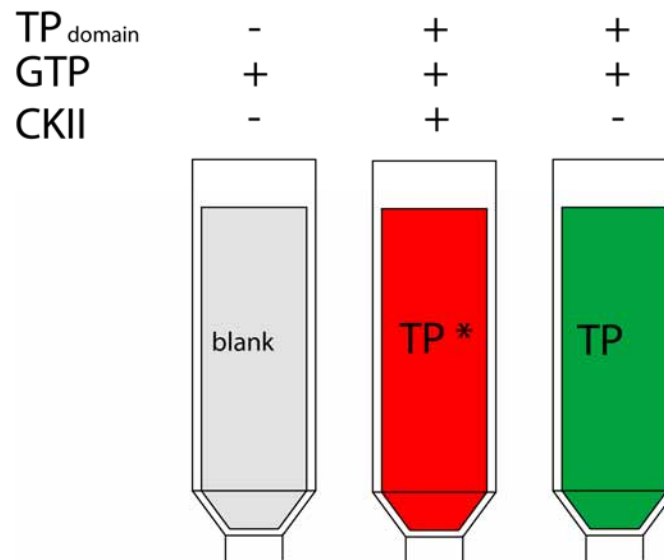


Figure 15: Immobilization and subsequent *in vitro* phosphorylation of TP domain on Ni-NTA Superflow. Same amounts of each reagent were applied to the (+) indicated columns: Terminal Protein domain of the HBV polymerase (TP domain), 200 μ M GTP, 2,500 U protein kinase CKII.

The huh-7 cell proteins were extracted from 1050 cm² confluent grown huh-7 by sonication in TBS buffer, including protease inhibitors and 1 mM EDTA. The soluble fraction of the cell lysate was cleared by centrifugation at 76,000x g, filtered through a 0.45 μ m membrane and adjusted to pH 8 with 100 mM Tris buffer. The protein content was precipitated with 75 % (w/v) ammonium sulfate according to chapter 4.7.4, washed with 75 % (w/v) ammonium sulfate solution and divided in 6 protein pellets. Each pellet was solved in 400 μ L TBS buffer and incubated for 15 min at room temperature and 800 rotations per minute (rpm). The protein solution was cleared by centrifugation (16,000x g, 15 min, and 4 °C) and desalted with TBS as described in chapter 4.7.3. The protein peak was pooled and diluted with 50 mL buffer A_{BP}, mixed and distributed evenly onto the three columns. Unbound sample was removed by washing with 5 cv buffer A_{BP} and binding partners were eluted with buffer A_{BP} including 1 M sodium chloride. The eluted fractions were stored at -80 °C.

5 RESULTS

5.1 Cultivation of HepG2.2.15 on Cytodex-3

5.1.1 *Identification of the optimal cell density*

Culture conditions for cultivation of HepG2.2.15 on Cytodex-3 were optimized in a culture volume of 10 mL including 50 mg dry weight (dw) of equilibrated Cytodex-3. Initial densities between 1×10^5 cells/mL and 1×10^6 cells/mL were evaluated for cell attachment and virus secretion 48 h post inoculation. If the number of cells used for inoculation was in the range of $3-9 \times 10^5$ cells/mL, a logarithmic correlation between the amount of inoculated cells and the level of extracellular HBV genome was observed (Fig. 16). Light and electron microscopy showed a negligible attachment of HepG2.2.15 for all cell densities below 1×10^5 cells/mL (Fig. 16*) and a good attachment above initial 5×10^5 cells/mL (Fig. 16**). The highest virus secretion after 48 h was observed at 9×10^5 inoculated cells per mL. At this density, cells and microcarrier formed extended three dimensional agglomerates after 48 h which were floating in suspension (Fig. 16***). Based on this in further experiments an initial cell density of 5×10^5 cells/mL was used because of an ideal cell attachment and growth to about 70-80 % confluence after 48 h. Moreover, this cell density allows a direct comparison to adherent HepG2.2.15 cultivation in T175 cm² culture flasks.

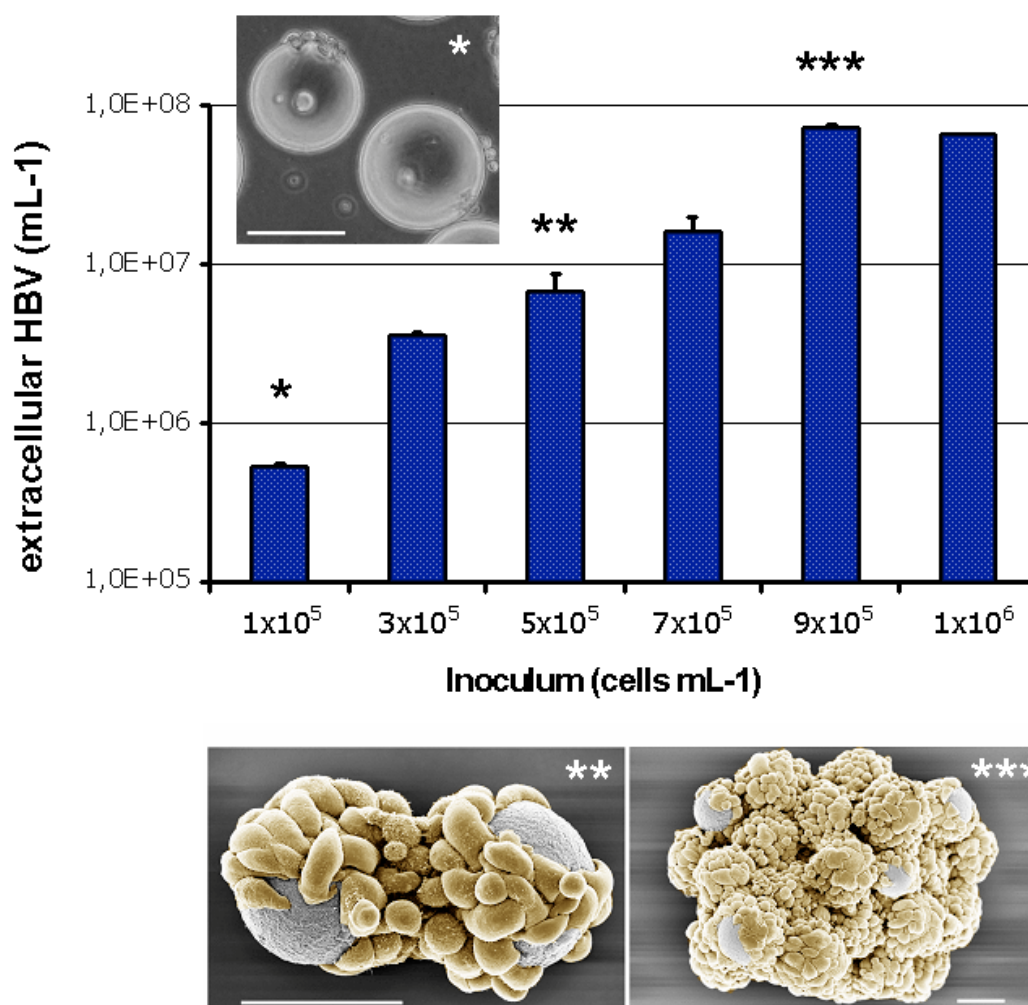


Figure 16: Optimal cell density for HBV production and cell attachment of HepG2.2.15 on Cytodex-3 after 48 h. 1-10x10⁵ cells/mL were inoculated in 10 mL culture media containing 50 mg (dry weight) Cytodex-3. Extracellular HBV genome was quantified by real-time PCR. (*) Light microscopy image of carrier suspension with initial 1x10⁵ cells/mL after 48 h of cultivation. (**) Raster electron microscopy (REM) image of carrier suspension with initial 5x10⁵ cells/mL and (***) REM image of 9x10⁵ cells/mL after 48 h of cultivation. Each white bar reflects 60 μ m of size. The REM images were colored by Photoshop CS [Lupberger, et al., 2006].

5.1.2 *HBV production and antigen secretion*

The HBV production and antigen secretion (HBsAg and HBeAg) was examined in two 20 mL microcarrier culture batches in comparison to two 20 mL stationary cultures. 5×10^5 cells/mL were cultured on 100 mg dw Cytodex-3 compared with the equal amount of cells grown in stationary culture flasks (T175 cm²) over 72 h. Each experiment was performed in two independent, identical batches and each parameter was determined in double. The cultivation on Cytodex microcarrier resulted in a significant higher HBeAg (Fig. 17A) and a reduced HBsAg (Fig. 17B) secretion as compared to the stationary flask culture.

In addition to the quantification of secreted viral proteins (HBsAg, HBeAg), the production of HBV particles was determined by quantifying the amount of extracellular HBV genome equivalents (GE) using real-time PCR (Fig. 17C). 48 h post inoculation we observed significantly more GE in the microcarrier cultures than in the stationary cultures. Under these conditions HepG2.2.15 secreted up to 18 fold more HBV particles as compared to the stationary cultures. Taken these results together in the Cytodex-3 cultures less HBsAg is secreted per extracellular HBV genome than in stationary cultures. These data indicate that the cultivation of HepG2.2.15 on microcarrier results (i) in an up to 18 fold increased amount of secreted viral particles and (ii) in a significantly increased ratio of secreted viral particles to subviral particles.

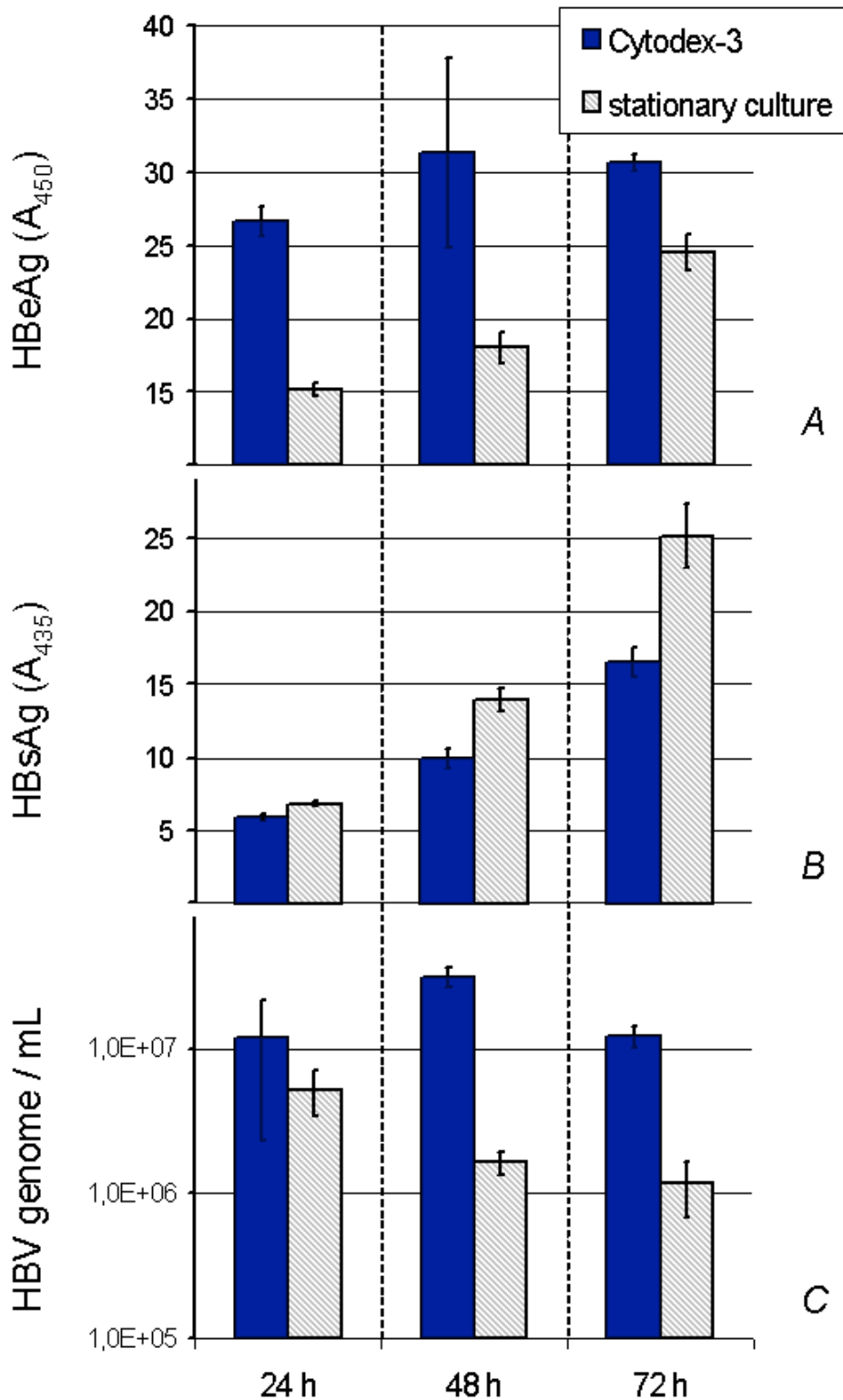


Figure 17: Comparison of HepG2.2.15 virus production on Cytodex-3 (dark bars) versus stationary culture flask (striped bars) over 72 h. Every 24 h the half of consumed culture medium was replaced. Aliquots of the replaced media were cleared and semi-quantified by ELISA for HBeAg (A) and HBsAg (B) and expressed as light absorption at 450 nm and 435 nm, respectively. In parallel, extracellular, encapsitated viral DNA was prepared and quantified by real-time PCR (C). Error bars were calculated as mean value/standard deviation. Differences between production levels were significant as assessed by Students *t*-test ($p < 0.05$) [Lupberger, et al., 2006].

To analyze whether the difference in the amount of secreted viral particles just reflects different numbers of cells the total amount of cells was estimated by Western blot analysis of cellular lysates using an actin-specific antiserum (Fig. 18). The Western blot reveals that in case of the carriers a significant smaller amount of cells produces obviously a higher amount of viral particles as compared to the cells grown in flasks. To investigate whether the different culture conditions affect the differentiation of the HepG2 cells the membrane was reprobed using an alpha-fetoprotein specific serum (Fig. 18). The Western blot shows that comparable amounts of the differentiation marker alpha-fetoprotein are produced in cells grown on carriers as compared to cells grown on flasks.

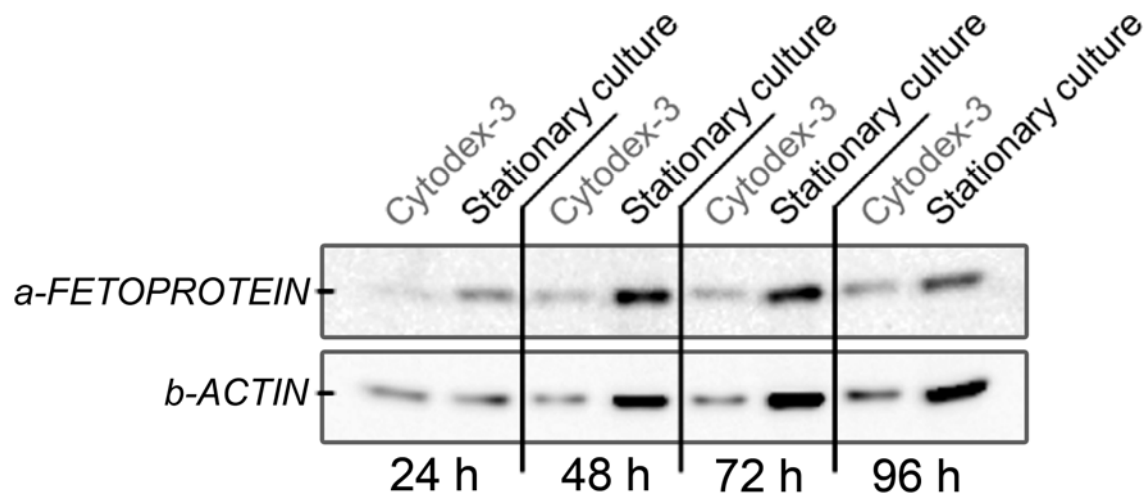


Figure 18: Analysis of cell number and cell differentiation of HepG2.2.15 cells grown on microcarrier or stationary culture. Identical amounts of cells (1×10^7) were used for inoculation of microcarrier and stationary flask culture. After 24 h, 48 h, 72 h and 96 h cells were harvested and lysed in identical volumes. Samples were analyzed by Western blotting using an actin-specific antiserum to evaluate relatively the amount of cells and using an alpha-fetoprotein-specific serum to analyze the differentiation state of the cells [Lupberger, et al., 2006].

5.1.3 Virus infectivity

The data described above indicate that cultivation of HepG2.2.15 cells on microcarrier results in an elevated amount of virus-specific DNA in the cell culture medium. To demonstrate that this increased amount of virus specific DNA is represented by complete viral genomes, DNA was isolated from the supernatant taken after 48 h and analyzed by Southern blotting (Fig. 19A). The Southern blot verifies that significant

higher amounts of viral genomes are found in the supernatant of cells grown on microcarrier as compared to the cultivation in flasks.

To exclude that this is due to an increased secretion of naked capsids the supernatants were adjusted to identical amounts of viral genomes and subjected to immunoprecipitation using an excess of HBsAg-specific serum (Fig. 19B). The quantitative PCR analysis of the precipitates demonstrates that the ratio of enveloped capsids to naked capsids is not affected if HepG2.2.15 cells were grown in flasks or on microcarrier.

To demonstrate unequivocally that the cultivation of HepG2.2.15 cells on microcarrier results in an increased number of infectious viral particles secreted into the supernatant identical volumes of supernatant from flasks and microcarrier were concentrated and applied for infection of primary *Tupaia* hepatocytes. Analysis of the HBeAg secretion of the infected *Tupaia* cells shows the significant higher infectivity of the supernatant in case of HepG2.2.15 cells grown on microcarrier as compared to cells grown in flasks (Fig. 19C). These experiments demonstrate that cultivation of HepG2.2.15 cells on microcarrier significantly improves the production of infectious viral particles. To investigate whether this is due to a change in the ratio between genomic and subgenomic RNA population identical amounts of RNA isolated from the two culture systems were analyzed by Northern blotting (Fig. 19D). The Northern blot shows that the different cultivation conditions do not affect the ratio between the genomic and subgenomic RNA populations.

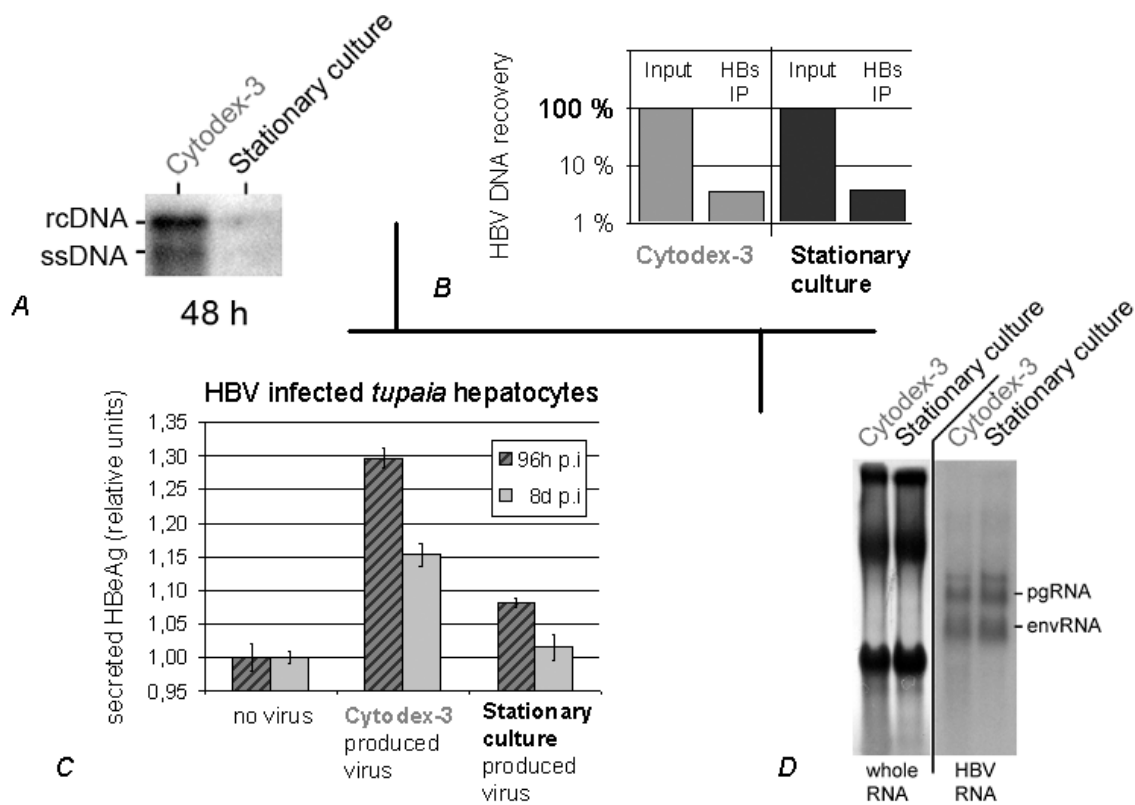


Figure 19: Comparative quantification of viral particles secreted from HepG2.2.15 grown on microcarrier and in stationary culture. (A) Southern blot analysis of DNA isolated from the supernatant of HepG2.2.15 cells grown for 48 h on microcarrier or in stationary culture. (B) Supernatants obtained after 72 h cultivation on microcarrier or in flasks were adjusted to identical genome equivalents as determined by quantitative PCR. The supernatants were subjected to immuno-precipitation using an excess of a HBsAg-specific serum (Dako; goat-derived anti-HBsAg) and the amount of precipitated genomes were determined by quantitative PCR. (C) Primary *Tupaia* hepatocytes were infected with concentrated supernatant obtained from the microcarrier or flask culture. To quantify the infectivity 96 h and 8 d post infection HBeAg secretion was quantified by ELISA. (D) 72 h after inoculation total RNA was isolated from HepG2.2.15 cells grown on microcarrier or in flasks. The RNA was adjusted to identical concentrations and analyzed by Northern blotting using a HBV-specific probe. The left panel shows the methylene blue staining of the membrane, indicating that comparable amounts of RNA were loaded. The right panel shows that the different culture conditions do not affect significantly the ratio between the different HBV-specific RNA species [Lupberger, et al., 2006].

5.1.4 Effect on cellular signaling

Recent reports describe a preference of HBV to replicate in quiescent cells [Friedrich, et al., 2005] and a dependence of HBV replication on the functionality of the c-Raf/MEK/ERK signaling cascade [Stockl, et al., 2003].

Cell proliferation was analyzed by quantification of *proliferating cell nuclear antigen* (PCNA) expression in HepG2.2.15. Cells grown on microcarrier and in T175 cm² flasks were lysed 72 h post inoculation and analyzed by Western blotting (Fig. 20). To control

the effect of cell proliferation on PCNA expression the fetal calf serum concentration in the culture medium of a parallel batch was shifted from 10 % to 5 %. All samples were normalized to intracellular beta-actin expression. The lower PCNA expression in the serum deprived cells reflected the decreased cell proliferation. But no significant difference of PCNA expression was observed between the two culture systems. This experiment showed that the increased HBV production of HepG2.2.15 cells cultivated on Cytodex-3 is not due to a decreased cell proliferation.

A potential activation of the c-Raf/MEK/ERK signaling pathway was examined by Western blot analysis using an anti-active MAP-specific antiserum (Fig. 20). The blot revealed an obvious higher level of the phosphorylated ERK-2 in cells cultivated on microcarrier as in those grown as stationary culture. The tendency of this finding was independent from the serum concentration in the culture medium.

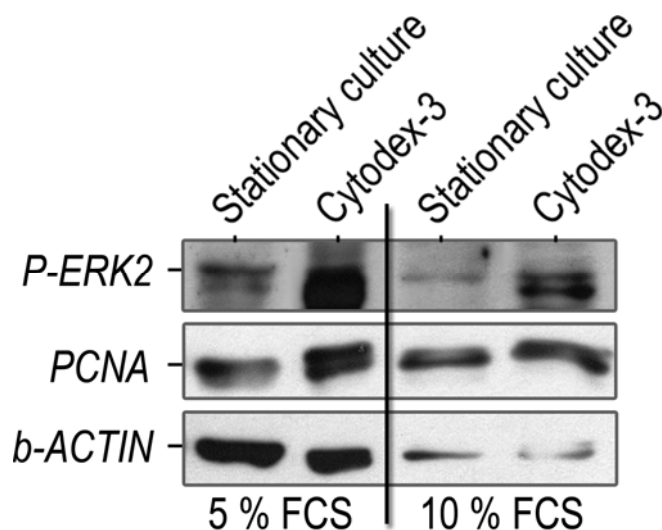


Figure 20: Comparison of cell proliferation and MAP kinase signaling activation in HepG2.2.15 grown on microcarrier versus stationary culture. 72 h post inoculation the level of *proliferating cell nuclear antigen* (PCNA) and activated form of *extracellular signal-regulated kinase 2* (P-ERK) was compared in HepG2.2.15 grown on Cytodex-3 to cells grown in T175 cm² cell culture flasks by Western blotting. In a simultaneous experiment the cell proliferation was limited by a reduction of the serum concentration in the culture medium from 10 % to 5 %. The protein amounts were normalized to beta-actin expression [Lupberger, et al., 2006].

5.2 Generation and purification of P directed antibodies

5.2.1 Purification and immobilization of recombinant TP and S domain

The TP domain (amino acid 1-181) and the S domain (amino acid 182-340) of the HBV polymerase (subtype ayw) were purified from recombinant bacterial expression systems based on the plasmid pJO2 (TP expression vector) and pJO3 (S expression vector). Both recombinant domains were produced with an C-terminal (His)₆-tag for affinity purification by Ni-NTA chromatography. A large amount of high pure protein was obtained when the isolation was performed under denaturing conditions (Fig. 21). This “injection” grade (Fig. 21, lane MS) was used for antibody generation (4.6), antibody affinity purification (4.7.5) and binding partner fishing (4.7.6).

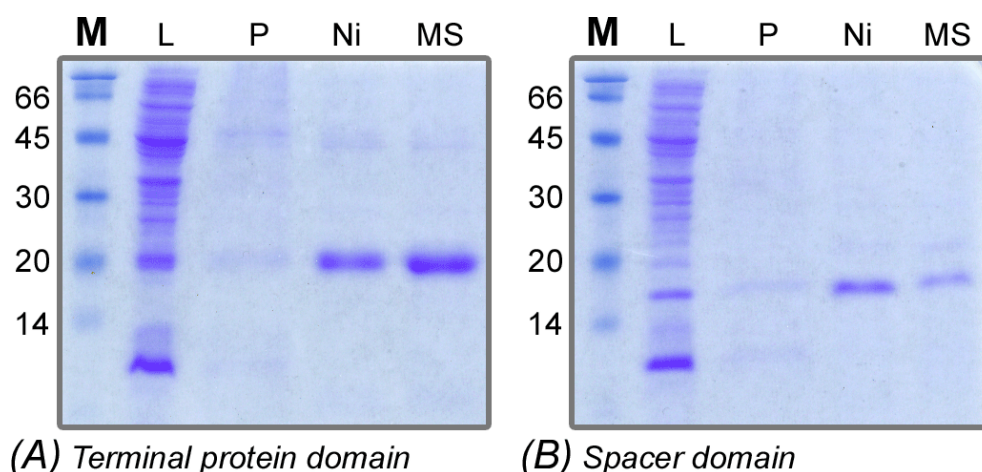


Figure 21: Isolation of highly purified terminal protein and spacer domain. M = low molecular weight marker, L = crude lysate, P = insoluble fraction, Ni = after Ni-NTA affinity purification, MS = after ionic exchange purification (injection grade). (A) Purified 21 kDa terminal protein domain. (B) Purified 17 kDa spacer domain. 15 % SDS-PAGE gel stained with Coomassie Brilliant Blue G250.

5.2.2 TP and S directed antibody

To generate HBV polymerase specific antibodies rabbits were immunized with precipitated injection grade TP domain and S domain, respectively. To minimize unspecific adsorption to secondary proteins the rabbit sera were affinity purified using the immobilized antigen. The antigen was immobilized to NHS-activated sepharose

with a coupling efficiency of about 50 % measured by optical density at 280 nm (1). The calculated coupling efficiencies were verified by comparison of the amounts of supernatant proteins before and after the coupling reaction (Fig. 22).

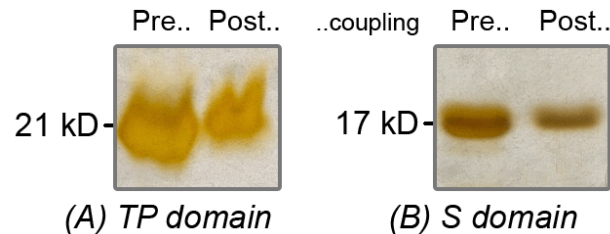


Figure 22: Coupling efficiency of TP and S domain to NHS-activated sepharose. 15 % SDS-PAGE gel stained with protein silver staining. The amount of supernatant protein was compared before (Pre..) and after (Post..) coupling to NHS-activated sepharose. Estimated 50 % of the TP domain (A) and of the S domain (B) immobilized to the sepharose.

Specificity and sensitivity of the purified antibodies were checked by Western blotting. Thereto the recombinant antigen (Fig. 21, lane MS) was diluted in equal amounts of liver cell lysate and detected by the respective affinity purified antiserum (Fig. 23).

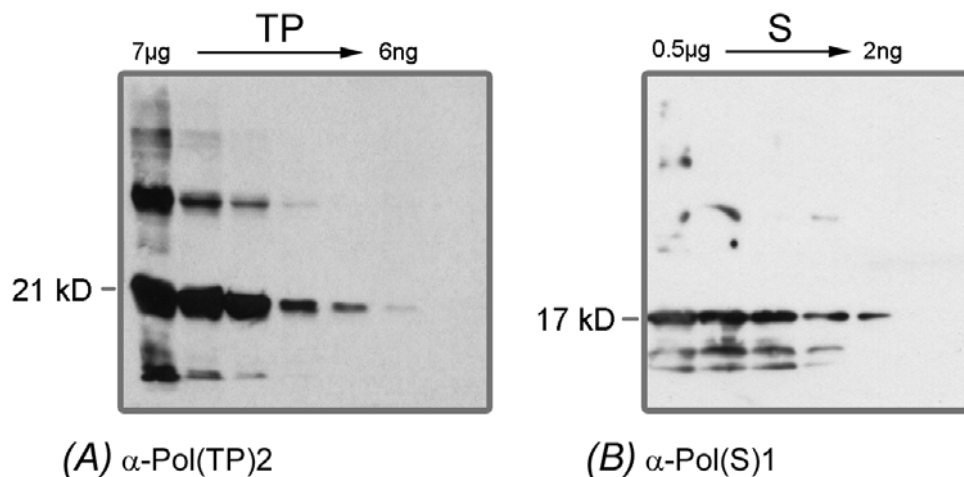


Figure 23: Determination of the sensitivity of the purified TP- and S-specific antisera. Proteins were separated on a 12 % SDS-PAGE gel. Recombinant antigen was diluted in a huh-7 cell lysate background and detected by (A) rabbit α-Pol(TP)2 (B) rabbit α-Pol(S)1. The detection level was about 6 ng of TP antigen and 2 ng of S antigen. Both antibodies were diluted 1:5000 in 10 % (w/v) skim milk powder in buffer PBS-T.

The antibodies generated against the TP domain and the S domain of the HBV polymerase did not show any cross reactivity with liver cell proteins because in this case bands would be visible in every sample with the same intensity. The TP domain derived rabbit α -Pol(TP)2 antibody was able to detect 6 ng of antigen in the cell lysate background (Fig. 23A). The S domain derived rabbit α -Pol(S)1 antibody was able to detect at least 2 ng of antigen in a cell lysate background (Fig. 23B). The antibodies could be diluted 1:8000 in 10 % (w/v) skim milk powder / PBS-T buffer without a loss of sensitivity.

The α -Pol(S)1 antibody immuno-precipitated HBV P protein from transfected huh-7 cells (Fig. 24), whereas the α -Pol(TP)2 antiserum failed to precipitate the polymerase, significantly (Fig. 24).

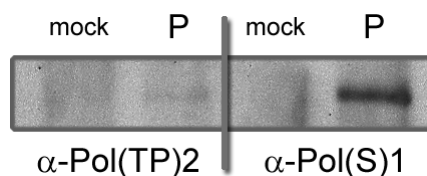


Figure 24: Immuno-precipitation of HBV P protein by the generated antibodies. Huh-7 cells were transfected with pcDNA3.1 (mock) and its descendent pJO13 (P), which codes a CMV promoter driven version of HBV P protein. Transfected cells on a 6 cm cell culture dish were lysed in 0.75x RIPA buffer and precipitated with 30 μ L protein A/G agarose beads and 3 μ L rabbit α -Pol(TP)2 and rabbit α -Pol(S)1, respectively. All precipitates were detected with antibody mouse α -Pol(3552).

The aptitude of the purified antibodies for immuno-histology analysis was evaluated by detecting of HBV polymerase (i) in baculovirus (*AcNPV::HBV P*) infected *Sf9* insect cells (Fig. 25) and (ii) in P protein producing huh-7 cells (Fig. 26). Both antibodies detected HBV polymerase in ethanol fixated *Sf9* and huh-7 cells. But the rabbit α -Pol(S)1 showed a higher sensitivity by visualizing lower P expression levels in transfected huh-7 cells.

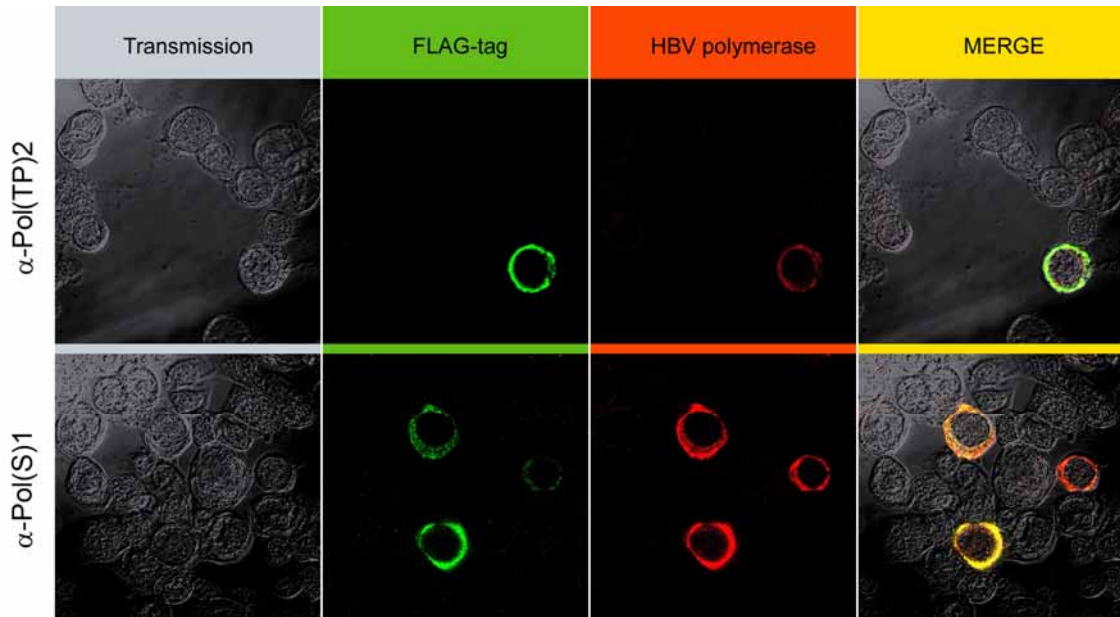


Figure 25: Immunofluorescence analysis of HBV P expressing *Sf9* cells with purified P directed antibodies. *Sf9* cells were infected with recombinant baculovirus *AcNPV::HBV P* harboring FLAG-tagged version of the human HBV P protein. After ethanol fixation (transmission) the cells were stained for human HBV P protein with α -Pol(TP)2 (upper red panel) and α -Pol(S)1 (lower red panel), respectively. The specificity of the generated antisera was verified by co-staining with α -FLAG M2 antibody (green panel). All measured wavelengths are merged in the yellow panel. The engineered baculovirus was kindly provided by Robert Lanford, University of Texas, USA.

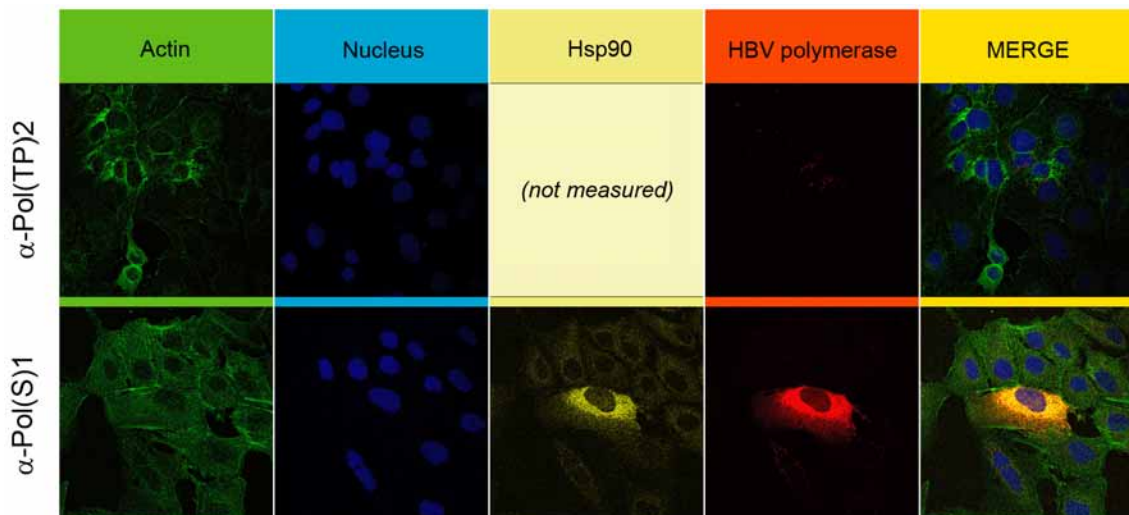


Figure 26: Immunofluorescence analysis of HBV P expressing huh-7 cells with purified P directed antibodies. Huh-7 cells were infected with HBV polymerase expression construct pJo13. After ethanol fixation the cells were stained for human HBV P protein (red) with α -Pol(TP)2 (upper panel) and α -Pol(S)1 (lower panel), respectively. The cytoskeleton was stained with phalloidin-FITC (green), the nucleus with DAPI (blue), and the chaperone protein Hsp90 with a specific antibody (light yellow). All measured wavelengths are merged in the yellow panel.

Taken this together two sets of antibodies were generated that are able to detect specifically HBV P protein in a hepatoma cell and insect cell background by immunohistology. In Western blot experiments the generated rabbit α -Pol(S)1 antibody was at least 3 times more sensitive and detected about 2 ng recombinant antigen on a SDS-PAGE gel. Only the α -Pol(S)1 antibody was able to detect the full length HBV P protein and was therefore used as antibody of choice for the further analysis of the HBV polymerase.

5.3 Nuclear import of the HBV polymerase

5.3.1 Identification of conserved motifs on the HBV polymerase

The primary amino acid sequence of HBV polymerases were aligned to find conserved motifs, which might be susceptible for host cell signaling. Therefore, the P protein of 18 *orthohepadna* viruses (human HBV genotypes A-H, two rodent hepatitis B viruses) and four *avihepadna* viruses (from Shanghai duck, ross goose, China duck and heron) were compared using the Clustal W algorithm (Fig. 27).

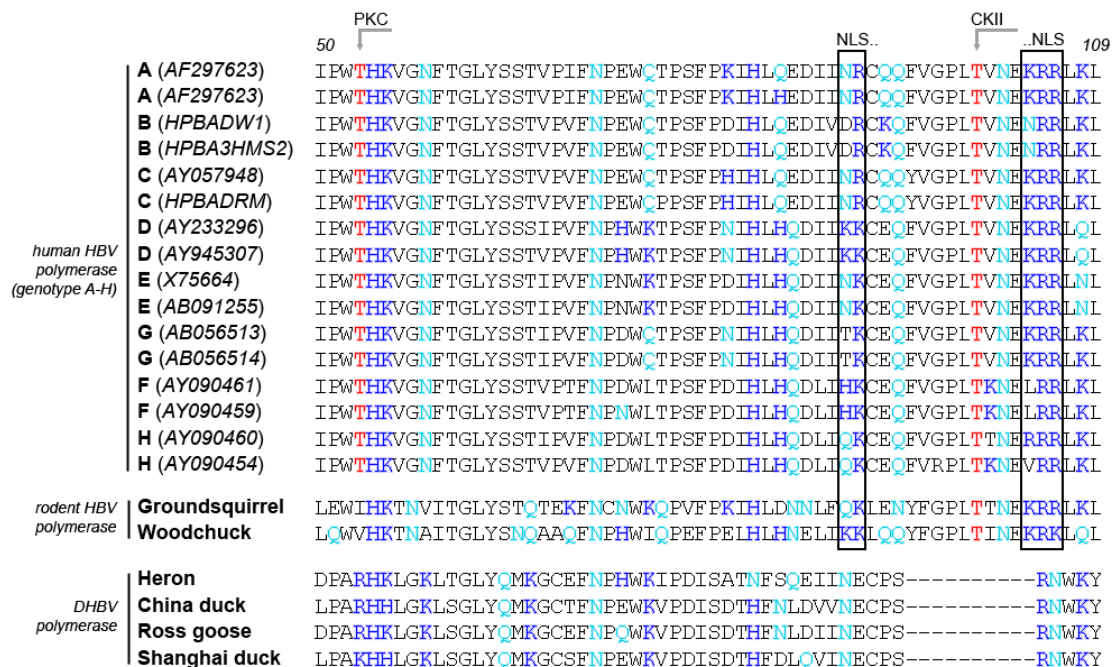


Figure 27: Sequence alignment of the HBV polymerase (P) from various virus genotypes and species. This figure shows amino acid alignment of 150-L109 referred to the sequence of genotype D, which was used in this study. Basic amino acids are highlighted in blue and polar (δ^+) amino acids are highlighted in turquoise. Conserved kinase recognition sites were identified (red) in human HBV genotypes at Thr53 (protein kinase PKC: T/S-X-K/R-X; X = any amino acid) and in *orthohepadnaviridae* at Thr100 (protein kinase CKII: T/S-X-X-E/D; X = any amino acid). A bipartite nuclear localization signal (black rectangles) was identified in *orthohepadnaviridae*, which is flanking the CKII recognition site by its two basic amino acid clusters. All identified putative motifs were not found in the aligned P proteins of the *avihepadnaviridae*.

Three conserved motifs were identified in the TP domain of the P protein: a putative protein kinase PKC recognition site at threonine 53 (amino acid counting referred to genotype D) a putative protein kinase CKII recognition site at threonine 100 and a putative bipartite nuclear localization signal (NLS) (Fig. 27). The CKII recognition site

is flanked by the two basic amino acid clusters K90-K91 and K104-R106 of the NLS. The CKII recognition site and the bipartite NLS were found in all *orthohepadnaviridae* but not in *avihepadnaviridae* whereas the PKC recognition site is only present in human HBV viruses.

5.3.2 TP domain is phosphorylated by protein kinases PKC and CKII

To control experimentally whether the predicted phosphorylation sites indeed can be phosphorylated by CKII and PKC *in vitro* phosphorylation was performed. Thereeto, highly purified recombinant TP domain was treated was treated with either PKC or CKII in the precence of $[\gamma\text{-}^{32}\text{P}]\text{ATP}$ (Fig. 28). To exclude any phosphorylation by contaminating kinases the purified TP domain was incubated as described above, but the recombinant kinases were omitted (Fig. 28, left lane). As an additional control the corresponding fractions of the Ni-NTA affinity chromatography from *E. coli* transformed with the empty expression vector were subjected to *in vitro* phosphorylation (Fig. 28, mock).

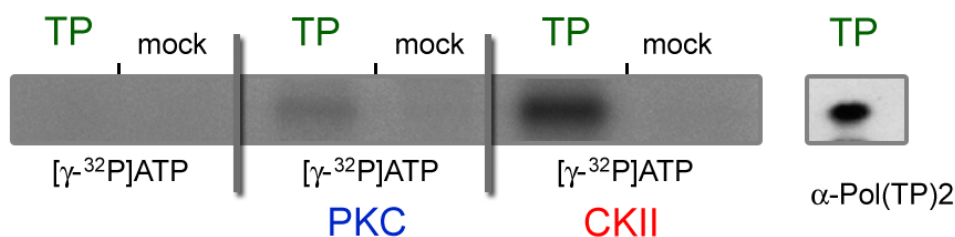


Figure 28: *In vitro* phosphorylation of recombinant TP domain by protein kinases CKII and PKC. Purified TP domain and mock purified proteins (empty vector products) were incubated with $[\gamma\text{-}^{32}\text{P}]\text{ATP}$ and the protein kinases PKC and CKII. To control auto-phosphorylation TP domain was incubated with $[\gamma\text{-}^{32}\text{P}]\text{ATP}$ in absence of a kinase. The protein specificity was verified by the TP specific antibody rabbit $\alpha\text{-Pol(TP)2}$ on a separate lane.

Fig. 28 shows a significant specific phosphorylation of the TP domain only if CKII or PKC is present. In case of the controls no significant phosphorylation was observed. To confirm the identity of the phosphorylated species with the TP domain Western blot analysis was performed (Fig. 28, right panel). This indicates that the predicted kinase recognition sites on the terminal protein are indeed accessible for phosphorylation.

5.3.3 PKC and CKII phosphorylation affect HBV replication

To study the relevance of CKII-dependent phosphorylation of the TP domain for HBV lifecycle primary *Tupaia* hepatocytes were infected with HBV particles (Fig. 29A). Five days after infection the hepatocytes were grown for 36 h in the presence of the cell permeable small molecular inhibitor DMAT and the virus replication was analyzed by Lightcycler PCR for quantification of secreted *de novo* synthesized viral particles and by Southern blotting for detection of intracellular cccDNA. In the HBV infected primary hepatocytes the inhibition of CKII during virus infection caused a strong and significant reduction of virus replication indicating that the inhibition of the protein kinase CKII impairs HBV replication (Fig. 29A). DMAT did not significantly reduce cell viability under these conditions, which was analyzed by DAPI staining of the cells at the end of the experiment (data not shown). This indicates that integrity of CKII is crucial for the infectivity of HBV.

To control the specificity of the observed effect the constitutively HBV expressing cell lines HepG2.2.15 and HepAD38 were instrumental. Both cell line harbor stably integrated HBV genomes. Due to the stable integration of the genome the re-import of *de novo* synthesized genomes plays a minor role for maintaining the pool of transcriptional templates. Therefore, inhibition of polymerase import should exert a small effect. HepG2.2.15 and HepAD38 cells were treated with DMAT and virus secretion was quantified by Lightcycler PCR (Fig. 29B). Under these conditions inhibition of CKII with DMAT did slightly but not significantly reduce virus secretion as compared to the solvent control (Fig. 29B). Differences in virus secretion was assessed by Students t-test ($p < 0.05$).

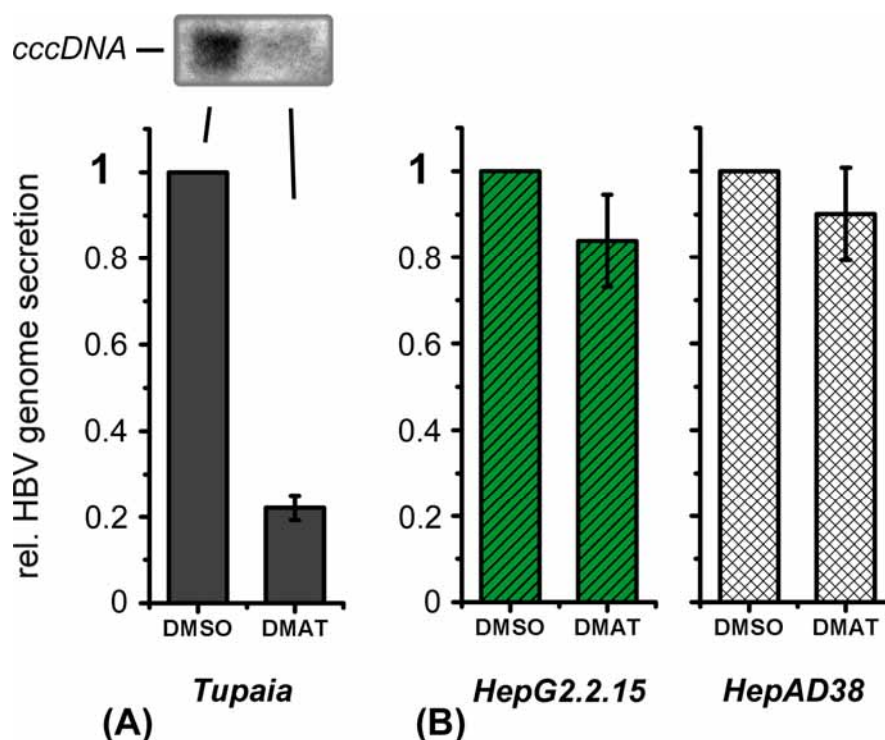


Figure 29: Effect of CKII inhibition on HBV secretion of infected hepatocytes. (A) Primary *Tupaia* hepatocytes were infected with HepAD38 derived HBV and five days post infection treated for 36 h with solvent DMSO or DMAT (10x IC₅₀). The HBV genome secretion was measured by Lightcycler PCR. The cccDNA content of infected *Tupaia* hepatocytes was visualized by Southern blot using a HBV specific probe. (B) After 2 h inhibitor pretreatment the stably HBV transfected cell lines HepG2.2.15 and HepAD38 were treated overnight with 10x IC₅₀ concentration of CKII inhibitor DMAT (IC₅₀ in rat liver = 150nM) and genome secretion was compared to the solvent control DMSO measured by Lightcycler PCR.

To investigate the role of PKC for the HBV lifecycle HepG2.2.15 and HepAD38 were treated overnight with PKC inhibitor Gö6976. To control whether DMSO exerts a stimulatory effect on the HBV replication the inhibitor was diluted in equal amounts of DMSO. After a 2 h pretreatment with the Gö6976 same amounts of cells were incubated with the PKC inhibitor overnight and virus secretion was measured by Lightcycler PCR. In contrast to CKII the inhibition of PKC led to a significant increase of HBV secretion, which was dose dependent (Fig. 30). This indicates that PKC has an inhibitory effect on the HBV lifecycle.

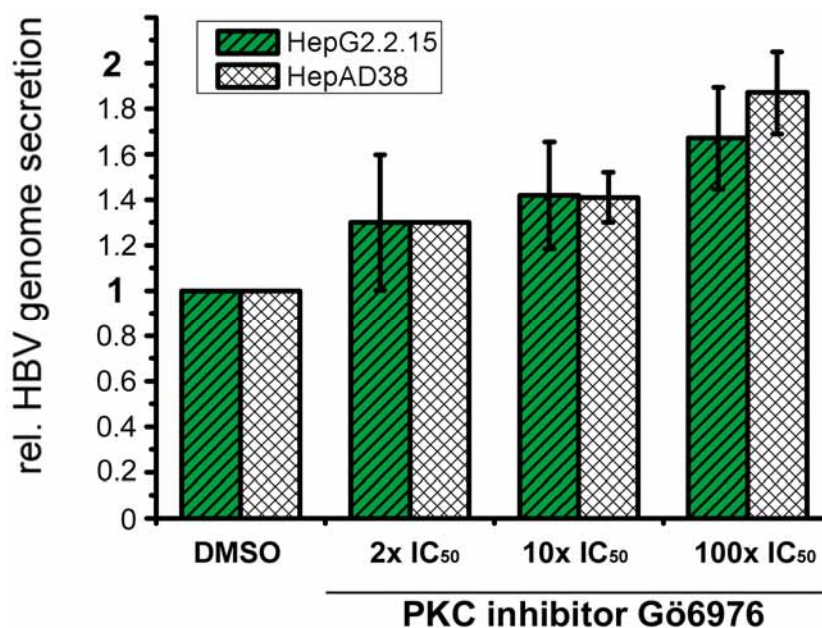


Figure 30: Effect of PKC inhibition on HBV secretion of infected hepatocytes. After 2 h inhibitor pretreatment the stably HBV transfected cell lines HepG2.2.15 and HepAD38 were treated overnight with 2x, 10x, and 100x IC₅₀ concentrations of PKC inhibitor Gö6976 (IC₅₀ for PKC α = 2.3 nM) and genome secretion was compared to the solvent control DMSO measured by Lightcycler PCR.

A treatment of hepatocytes with small molecule inhibitors can cause a variety of even opposite effects. Therefore, to learn more about the relevance of the putative kinase sites and the nuclear localization signal for the viral lifecycle, mutated HBV genomes were generated and examined for their ability to replicate in huh-7 (Fig. 31). To perform site directed mutations, a well characterized 2.5 fold HBV genome [Sells, et al., 1987] was truncated to generate a 1.2 fold descendent plasmid with only a single copy of the polymerase open reading frame. This genome harbored the minimal requirements for a productive viral replication.

To prevent the phosphorylation of a kinase recognition site the relevant threonine was substituted by an isoleucine (T53I, T100I). To simulate a phosphorylation the relevant threonine was replaced by an aspartate, which simulates the negative charge of a phospho-threonine (T53D, T100D). The putative bipartite NLS was inactivated by destroying one basic cluster of the motif (K105Q, K106S).

A polymerase-deficient HBV genome with an immediate transcriptional terminator sequence inserted in the open reading frame of the P protein was used as a control. This HBV (Δ P) construct was kindly provided by Dr. Alexander Pairan and Dr. Volker Bruss, University of Göttingen, Germany.

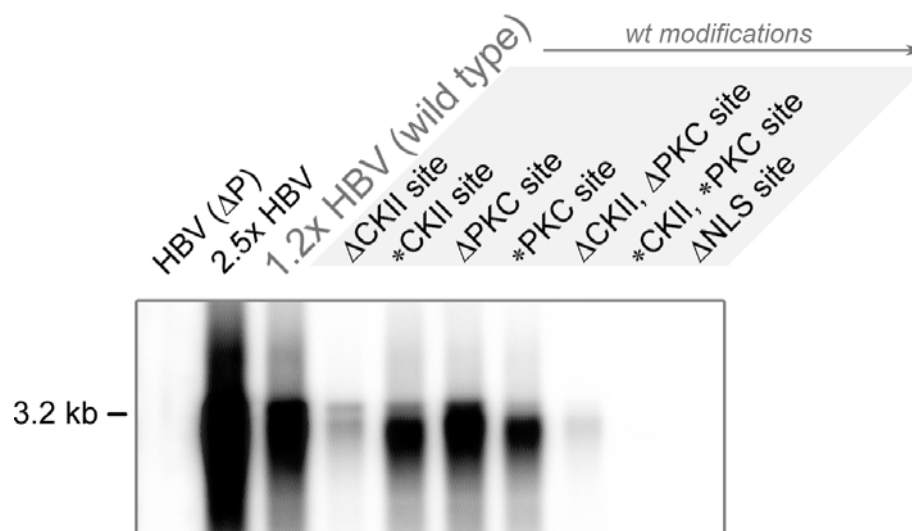


Figure 31: Effects of the identified motifs on virus replication. After immunoprecipitation with a HBsAg specific antibody the 3.2 kb HBV genomes were visualized by the radioactive tracer [α - 32 P]dCTP incorporated by the endogenous polymerase activity. In the 1.2 fold HBV wild type genome the unphosphorylated form of the CKII and the PKC recognition site in the P protein was simulated by a threonine to isoleucine substitution (Δ). The pseudo-phosphorylated kinase recognition site was simulated by a threonine to aspartate substitution (*). The NLS was inactivated by mutating the downstream basic cluster (K105Q and K106S) on the P protein. A 2.5x HBV genome and a P deficient genome (HBV (Δ P)) served as controls.

The secreted HBV particles were quantified by endogenous polymerase assay (EPA) 72 h post transfection of the genomes in huh-7 cells (Fig. 31). If a phosphorylation of the CKII recognition site on the P protein was prevented a decreased HBV secretion was observed (Δ CKII). The virus production was restored at the pseudo-phosphorylated CKII recognition site (*CKII). No significant difference to the wild type genome replication was observed if the PKC recognition site was inactivated by isoleucine (Δ PKC). But a significant decrease in virus secretion occurred by transfection of the corresponding pseudo-phosphorylated mutant (*PKC). When both kinase recognition sites were inactivated (Δ CKII, Δ PKC) the virus secretion was similar to the Δ CKII mutant genome. When both kinase recognition sites were pseudo-phosphorylated no virus secretion was detected. The NLS deficient mutant did not secrete active viral particles.

Taken these results together a CKII phosphorylation of the P protein maintains virus production and is crucial for virus replication. In contrast the phosphorylation of the HBV polymerase by PKC has an inhibitory effect on the virus production. No obvious functional connection of both phosphorylation sites was observed due to the dominant effect caused by the CKII pseudo-phosphorylation in the double isoleucine mutant.

5.3.4 *P protein harbors a functional bipartite NLS, which depends on phosphorylation*

The sequence analysis localized the CKII-phosphorylation site within a predicted bipartite nuclear localization signal (NLS). Based on this the resulting questions are (i) whether the predicted NLS indeed displays a NLS function and (ii) whether CKII-dependent phosphorylation affects the functionality of the TP-domain-derived NLS.

If the NLS is inactivated in a HBV genome by manipulating the basicity of the downstream cluster to K105Q and K106S the HBV genome is not able to replicate in huh-7 cells (Fig. 31, Δ NLS mutant). This indicates that the integrity of the putative NLS on the P protein is important for the viral lifecycle.

To study the functionality of the TP-derived putative bipartite NLS huh-7 cells were transfected with an expression plasmid encoding for a fusion protein of the putative NLS and GFP (NLS_{POL}-GFP). As a positive control served a 17 aa long prototype NLS (K142 to K158) derived from human nucleoplasmin (accession number gi114762) fused to the amino terminus of GFP (NLS_{NP}-GFP). The intracellular distribution of the GFP fluorescence was quantified by confocal laser scanning microscopy in living cells. Compared to wild type GFP expression, which was found even distributed within the cell (Fig. 32A), the level of NLS_{POL}-GFP was ~30 % higher in the nucleus than in the cytosol (Fig. 32C). In case of the positive control (NLS_{NP}-GFP) an about 75 % elevated level of GFP specific fluorescence in the nucleus was observed (Fig. 32B). This confirms that the predicted sequence indeed acts as a functional NLS. To analyze a putative relevance of CKII-dependent phosphorylation for the functionality of the TP-derived NLS, NLS_{POL}-GFP producing cells were incubated for 2 h with CKII inhibitor DMAT prior analysis by confocal microscopy. The quantification of GFP fluorescence revealed that presence of the CKII inhibitor prevented the directed nuclear enrichment

of the NLS_{POL}-GFP (Fig. 32D). Taken together these results indicate that the HBV polymerase harbors (i) a bipartite nuclear localization signal, (ii) which functionality depends on CKII mediated phosphorylation.

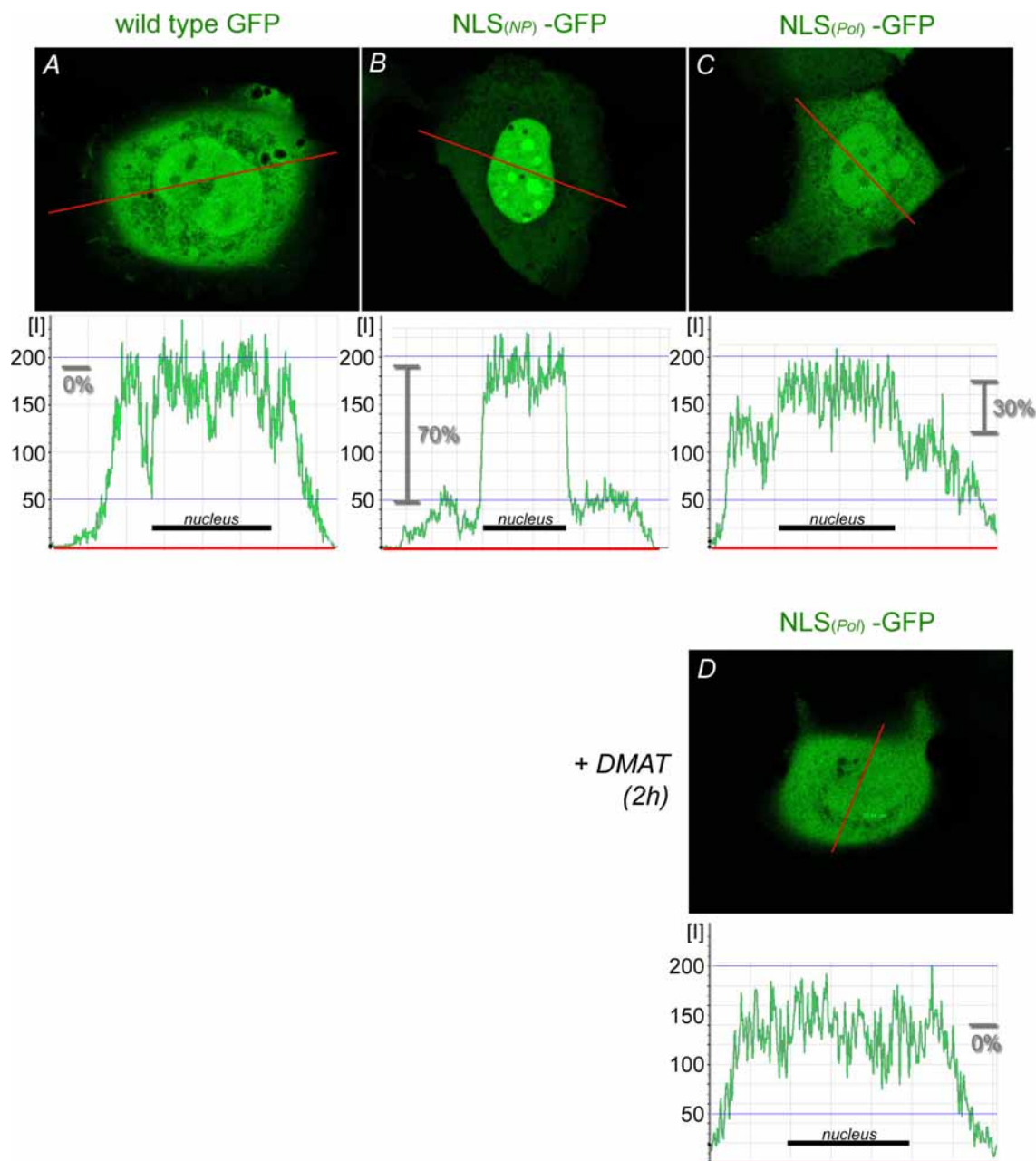


Figure 32: Subcellular localization of NLS-GFP fusion proteins. Huh-7 cells were transfected with (A) the negative control wild type GFP (pEGFP-N1), (B) a positive control: GFP fused to a prototype bipartite NLS of human nucleoplasmin, (C) GFP fused to the putative bipartite NLS of HBV P protein, (D) the same as (C) but cells were treated with 10x IC₅₀ of CKII inhibitor DMAT 2 h prior analysis. The fluorescence was measured in living cells by confocal laser scanning analysis. The central layer (out of 6) was quantified along the red indicated line and displayed in the corresponding graph of the lower panel as relative fluorescence intensity [I]. Differences of mean fluorescence intensities in the cytoplasm and within the nucleus (indicated as black line in the graph) were calculated and are indicated in percent.

5.3.5 Binding of karyopherin- α 2 to TP depends on CKII mediated phosphorylation

To verify these results and to characterize the functionality of the putative NLS the binding of endogenous PKC, CKII, and karyopherin- α 2 to immobilized TP domain was investigated. Karyopherin- α 2 (formerly known as importin- α 2) is a key adaptor protein for the directed nuclear import of proteins. Recombinant TP domain was bound to Ni-NTA columns and *in vitro* phosphorylated as described in chapter 4.7.6. The soluble protein fraction of huh-7 cells was purified by ammonium sulfate precipitation to remove endogenous phosphate donors like nucleotide triphosphates and subjected evenly to the three columns. Binding partners were eluted by a sodium chloride gradient. Elution fractions 2-4 were analyzed by Western blotting (Fig. 33).

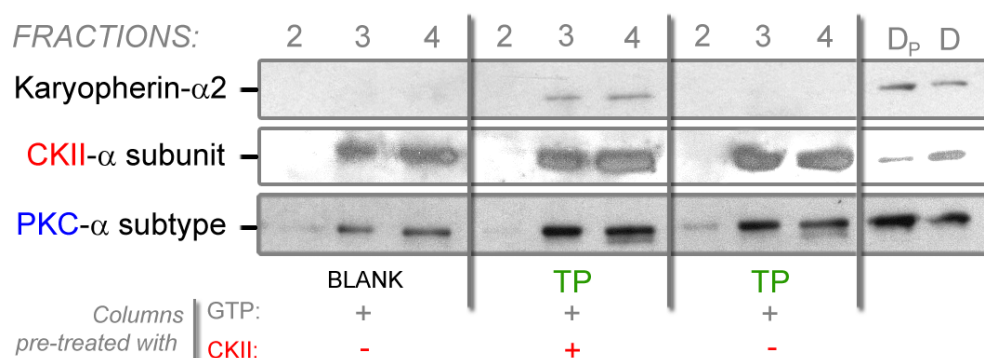


Figure 33: Binding of karyopherin- α 2, PKC, and CKII to immobilized TP domain. The interaction of soluble protein fraction of huh-7 cells to immobilized TP domain was investigated by Western blotting of the sodium chloride eluted fractions 2-4. Compared to the blank column w/o immobilized TP a significant binding of endogenous CKII (central panel) and PKC (lower panel) was observed. Karyopherin- α 2 bound only to the CKII pretreated TP column (upper panel). DP = flow through CKII treated TP column; D = flow trough of the untreated TP column.

A significant binding of endogenous protein kinases PKC and CKII to immobilized TP was detected compared to the blank column. Karyopherin- α 2 bound only to CKII/GTP treated TP but not to the blank column and to the GTP treated TP column (Fig. 33). An unspecific binding of karyopherin- α 2 to residual recombinant CKII from the pretreatment can be excluded due to similar amounts of endogenous CKII, which were found in the eluted fractions.

A binding of karyopherin- $\alpha 2$ to the NLS is a prerequisite for a directed nuclear import. This result implies a CKII-phosphorylation dependent nuclear import of the HBV polymerase within huh-7 cells.

5.3.6 *Ab initio modeling of the TP domain tertiary structure*

To calculate the accessibility of the nuclear localization signal in the TP domain of the HBV P protein an *ab initio* modeling was performed based on the ROSETTA protein folding program developed by Kim Simons, David Baker, Ingo Rudzinski, and Charles Kooperberg [Simons, et al., 1997]. The program cleaves a protein primary sequence virtually and calculates the conformations of the small fragments which are assembled to the five most probable versions of the tertiary structure of the target protein. It captures sequence dependent features of protein structures, such as the burial of hydrophobic residues in the core, as well as universal sequence independent features, such as the assembly of beta-strands into beta-sheets.

Fig. 34 shows the predicted tertiary structures of the wild type TP domain (T100) compared to a pseudo-phosphorylated TP mutant (T100D), where the threonine of the CKII recognition site is substituted by an aspartate. In this theoretical model the accessibility of the bipartite NLS motif (blue) in the wild type TP is blocked by a large beta sheet formed by the upstream part of the sequence (Fig. 34, left model). The substitution T100D within the CKII recognition site leads to a conformational change of the sequence upstream of the NLS. The consequence is the disclosure of the NLS by the protein bar, which causes the exposure of the NLS to the protein surface (Fig. 34, right model). In both models the protein primer tyrosine 63 is indicated and located at the opposite side of the theoretical model.

This folding pattern was similar in the four alternative tertiary structures predicted by ROSETTA. They differed only in minor folding variations (data not shown).

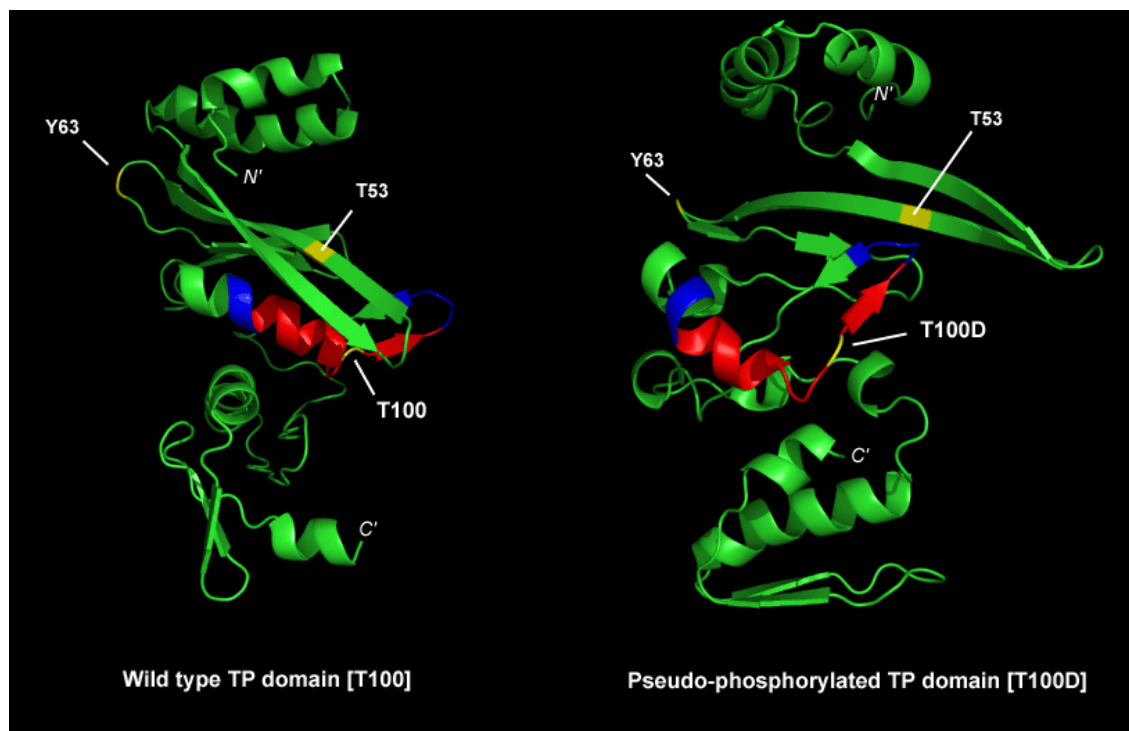


Figure 34: *Ab initio* modeling of TP domain (amino acid 1-181). Three dimensional models of wild type TP domain (T100, left panel) and a T100D CKII pseudo-phosphorylated version (T100D, right panel) were calculated using ROSETTA [Simons, et al., 1997]. The calculated PDB coordinates were visualized using PyMol. The amino acids of the bipartite NLS are highlighted in blue, the tyrosine-priming site Y63, the putative PKC recognition site T53 and the CKII recognition site T100 are highlighted in yellow. The amino acid spacer between the two NLS clusters are highlighted in red. The N-terminal (N') and the C-terminal (C') ends of the models are indicated.

6 DISCUSSION

An effective vaccine to prevent hepatitis B virus infection has been available since 1986, however HBV remains a major health problem with an estimated 400 million chronic infections worldwide [Hollinger and Liang, 2001]. HBV is a major causative agent for hepatocellular carcinoma, and perinatally infected children have an especially high risk of developing chronic HBV [de Franchis, et al., 2003]. In some highly endemic regions including China, Senegal, and Thailand the HBV infection rates in infants exceeds 25 % [Hollinger and Liang, 2001]. Currently, chronic HBV infections are treated with pegylated interferon-alpha in combination with nucleoside/nucleotide analogs [Buster and Janssen, 2006]. In the majority of cases this treatment suppresses the viral replication successfully, but there is a very low cure rate for chronic HBV infection. Another problem is the appearance of HBV escape mutants that are resistant to nucleos(t)ide-analogs after long term treatment. This emphasizes the need for additional therapy strategies to increase the success rate of the current chronic HBV treatments [Buster and Janssen, 2006].

Important parts of the viral lifecycle that could be potential targets for new antiviral drugs have yet to be fully characterized. For example, the viral surface proteins mediate binding of HBV to the hepatocyte, but the receptor complex that binds to the surface proteins is not known. Another poorly understood part of the viral lifecycle is the mechanism leading to the formation and amplification of viral cccDNA in the host cell nucleus. The stability and persistence of this episomal viral DNA during antiviral treatment remains an unsolved problem.

6.1 Cultivation of HepG2.2.15 on microcarrier increases HBV replication

Until recently, no adequate infection model for HBV was available. In 2001 Josef Kock and co-workers established a heterologous infection model that allows the study of HBV infection in primary hepatocytes of *Tupaia belangeri* [Kock, et al., 2001]. Primary hepatocytes are obtained by liver perfusion from the animals and can be efficiently

infected with human HBV. A few days post infection, *de novo* synthesized infectious viral particles are secreted and cccDNA is detectable within the *Tupaia* cells. Another novel HBV infection model was described by Philippe Gripon and co-workers in 2002 [Gripon, et al., 2002]. The highly differentiated hepatoma cell line HepRG appears to be susceptible to HBV infection when cultivated in the presence of corticoids and dimethyl sulfoxide. These new experimental systems require large amounts of infectious human HBV with a defined genome. The stably transfected cell line HepG2.2.15 serves as an HBV production system *in vitro* and is usually grown two-dimensionally under stationary conditions in a culture flask [Ganem, 1991]. Studies with various virus infected cell lines have shown that a variation of the cultivation substrate can alter virus replication and secretion [Wu and Huang, 2002; Wu, et al., 2002].

One aim of this study was to optimize HBV production by cultivation of the HepG2.2.15 cell line on the spherical microsubstrate, Cytodex-3, and to characterize the effects of this cultivation method on cellular signaling. To study this, equal amounts of HepG2.2.15 cells were cultivated on Cytodex-3 in suspension and compared to conventional cultivation in a T175 cm² flask. HBV production and viral protein secretion from the cells were compared. In these experiments a significantly higher level of secreted HBeAg was observed in the microcarrier cultures than in the stationary cultures (Fig. 17A). In accordance with this, an 18 fold higher HBV production in the microcarrier cultures was observed 48 h post inoculation by quantification of HBV genomes in the cell culture supernatants (Fig. 17C). The stationary cultures secreted significantly more HBsAg into the medium (Fig. 17B). 24 h post inoculation the HBsAg secretion was 13 % higher and after 72 h was 35 % higher than in the suspension cultures. When correlated with the extracellular genome equivalents, the data from the immuno-precipitation experiments as well as the data from the infection experiments (Fig. 19), it can be concluded that HepG2.2.15 cells cultivated on Cytodex-3 produce up to 18 fold more HBV virions and have simultaneously reduced secretion of subviral particles.

Electron microscopy was used to show that HepG2.2.15 cells grew in a more three dimensional manner on microcarrier compared to the stationary cultivation method (Fig. 16). Cells grown this way that floated in suspension may have better nutrient diffusion and altered cell-cell interactions than those grown in stationary culture.

Estimation of cell number using Western blot analysis with an actin-specific antiserum showed that significantly fewer cells are found when cultivated on microcarriers (Fig. 18). However, this smaller amount of cells produced a significantly higher amount of viral particles than cells grown in flask culture. This correlates with recent reports [Friedrich, et al., 2005; Ozer, et al., 1996] describing a preference of HBV to replicate in quiescent cells. After 72h, however, there seems to be no significant difference in the proliferation rate as determined by the PCNA-specific Western blot (Fig. 20). From this it can be concluded that the different productivity observed under these two culture conditions is not due to the proliferation rate of the cells, and that alternative mechanisms are responsible. It has been shown that HBV replication depends on the integrity of the c-Raf-1/MEK/ERK-2 signaling cascade [Stockl, et al., 2003]. In cells grown on microcarrier, an increased activation of ERK-2 was observed, as demonstrated by increased phosphorylation (Fig. 20). Increased ERK-2 activation favors HBV replication, and may cause the increased replication observed here [Stockl, et al., 2003].

Together this data suggests that a combination of better nutrient diffusion and increased cell-cell interaction may cause the enhanced activation of the c-Raf/MEK/ERK-2 signal cascade, leading to increased HBV replication. It is reported that enhanced integrin interactions on the cell surface activates MAP kinase signaling [Hughes, et al., 1997], and culture conditions may alter these integrin interactions. It is evident that cell culture conditions have a tremendous impact on infection and replication studies. In HepG2.2.15 cells, cultivation on the microcarrier substrate Cytodex-3 offers an advantageous cost-value ratio with a maximal effect on virus production.

6.2 PKC phosphorylation of HBV polymerase impairs virus replication

Host cell signal transduction plays a crucial role in the HBV lifecycle e.g. by stimulation of MAP kinase signaling by viral transactivator proteins resulting in enhanced gene transcription as described above. But on the other hand HBV replication is decreased in proliferating hepatocytes [Friedrich, et al., 2005; Ozer, et al., 1996]. This

correlates with the induction of rapid liver regeneration observed during acute HBV infection. Protein kinase C (PKC) isoforms positively regulate liver compensatory growth [Tessitore, et al., 1995]. If PKC is inhibited in HBV replicating cells using Gö6876, HBV secretion increases in a dose dependent manner up to 1.8 fold (Fig. 30). This shows that activation of PKC impairs HBV replication.

A highly conserved PKC recognition site was identified within the TP domain of human HBV genotypes using sequence alignment (Fig. 27). The HBV polymerase containing a pseudo-phosphorylated PKC recognition site (T53D) had impaired viral replication compared to the wild type polymerase, whereas when the PKC recognition site in TP was destroyed (T53I) no significant change in viral replication was observed (Fig. 31). Therefore PKC mediated phosphorylation of the HBV polymerase obviously impairs HBV replication.

One can speculate on the benefit to HBV of a highly conserved recognition sequence that enables its negative regulation. It is conceivable that tight regulation of HBV replication during the S-phase increases host cell survival, and hence survival of the virus.

6.3 Nuclear import of the HBV polymerase is mediated by a bipartite NLS and depends on CKII phosphorylation

The HBV polymerase is a key enzyme in viral genome replication and remains covalently attached to the HBV genome after its reverse transcription. Although pgRNA recognition, genome replication, and virus assembly are well studied, the fate of the HBV polymerase in other phases of the viral lifecycle remains enigmatic. Particular questions addressing the mechanism of nuclear delivery of the HBV genome and the role of the bound polymerase are discussed controversially [Brandenburg, et al., 2005; Kann, et al., 1997; Rabe, et al., 2003]. One open question concerns the subcellular localization of the HBV polymerase. According to its molecular weight of about 90 kDa, the HBV polymerase is too big to pass the nuclear pore complex by diffusion and be distributed equally between cytoplasm and nucleus. Yet, in duck HBV replication, non-encapsidated polymerase exists in addition to the encapsidated polymerase [Yao, et al., 2000]. The majority of the non-encapsidated duck HBV

polymerase is found in the cytoplasm, however a smaller fraction can be detected within the nucleus [Yao, et al., 2000]. Interestingly, in cells overexpressing HBV polymerase in the absence of other viral proteins, a fraction of HBV polymerase is found within the nucleus colocalized with the p11 protein of PML bodies [Choi, et al., 2003]. Furthermore, Michael Kann and co-workers showed that purified HBV polymerase is sufficient to mediate nuclear import of the bound viral genome in the absence of viral core proteins [Kann, et al., 1997].

This evidence opens the questions of (i) the mechanism of nuclear import, and (ii) its relevance to the HBV lifecycle. Therefore, the second objective of this study was to identify motifs on the HBV polymerase which determine the subcellular localization of the P protein during viral lifecycle.

By sequence alignment of HBV genotypes from different species we identified a potential protein kinase CKII recognition site in the TP domain of the HBV polymerase, which is flanked by the two basic clusters of a putative bipartite nuclear localization signal (NLS) (Fig. 27). More detailed analysis revealed that the predicted sequence indeed functions as a nuclear localization signal that when fused to GFP, leads to an enrichment of GFP in the nucleus compared to the even distribution of wild type GFP (Fig. 32). The NLS derived from the HBV polymerase has a weaker nuclear translocation capacity than the prototype bipartite NLS derived from nucleoplasmin [Dingwall, et al., 1982]. This correlates with the observation that only a minor fraction of HBV polymerase is localized within the nucleus (Fig. 26) [Choi, et al., 2003; Yao, et al., 2000]. Furthermore, a predominant nuclear localization would be fatal due to the fact that non-encapsidated polymerase has a key role during replication in the cytoplasm. It is very likely that additional factors regulate the HBV polymerase derived NLS functionality.

The functionality of the HBV polymerase derived NLS depends on CKII-mediated phosphorylation within the two basic clusters of the NLS (Fig. 31-33). CKII is a loosely regulated kinase [Litchfield, 2003]. It can therefore be assumed that CKII exerts a housekeeping phosphorylation function [Meggio and Pinna, 2003]. In accordance with this, mimicking of constitutive phosphorylation as demonstrated with the T100D mutant does not result in increased virus replication compared to the wild type control

(Fig. 31). If the subcellular localization and function of the HBV polymerase is indeed subjected to tight control, it is unlikely that CKII exerts this function.

CKII phosphorylation influences the subcellular localization of various nuclear proteins [Jans and Hubner, 1996]. For example CKII phosphorylation upstream of the NLS of simian virus 40 T-antigen enhances its nuclear import up to 40 fold [Jans and Jans, 1994], but phosphorylation of one or two amino acid immediately upstream of the crucial amino acid of classic monopartite NLS seems to have inhibitory effects on karyopherin binding due to a disturbance of the NLS basicity [Harreman, et al., 2004]. In the case of bipartite nuclear localization signals this correlation is not evident. For example the spacer region of the functional bipartite NLS from the *Agrobacterium tumefaciens* nopaline protein contains four negatively charged aspartates, one located immediately at the downstream basic cluster [Howard, et al., 1992]. On the other hand an increase in hydrophobicity of the 10-12 amino acid spacer seems to decrease its functionality [Robbins, et al., 1991].

No obvious functional connection between the identified PKC phosphorylation site and the NLS was found. If both CKII and PKC recognition sites were either destroyed (T53D, T100I) or pseudo-phosphorylated (T53D, T100D) the expected rescue effect on viral replication was not observed. Instead the T100I as well the T53D substitutions affected the virus replication in a predominantly negative manner (Fig. 31).

Phosphorylation can trigger changes in the tertiary structure of proteins. For example the reversible phosphorylation of the Na^+/K^+ -ATPase triggers a conformational change that mediates the active transport of bound ions through a membrane [Reyes and Gadsby, 2006]. The tertiary structure of the HBV polymerase is not known, however *ab initio* modeling of the terminal protein domain predicts the possibility that CKII mediated phosphorylation could stabilize a tertiary structure with an exposed NLS (Fig. 34). This hypothesis has not been verified experimentally.

The chaperone protein Hsp90 is an essential co-factor for pgRNA recognition by the HBV polymerase [Hu, et al., 2002]. The Hsp90 binding sites on the polymerase are localized within the TP domain and the RT domain [Cho, et al., 2000]. Interestingly, the identified NLS in the P protein is located within the Hsp90 binding site of the TP

domain. It is conceivable that the binding of Hsp90 to the HBV polymerase could mask the identified NLS, preventing nuclear translocation of the P protein prior to encapsidation. Furthermore, one can speculate that during nuclear import of the HBV genome, Hsp90 could reveal the NLS that trigger nuclear passage of the attached viral genome through the nuclear pore complex. This hypothesis is supported by the strong co-localization of Hsp90 and P protein that is observed in HBV polymerase expressing huh-7 cells (Fig. 26). Under these experimental conditions the majority of P protein is found in the cytoplasm colocalized with Hsp90, and only traces of P are found within the nucleus. The group of John Tavis found that the majority of non-encapsidated DHBV polymerase is bound to an unknown cytoplasmic structure [Yao, et al., 2000]. It is tempting to speculate that Hsp90, a binding partner of various cell structural proteins e.g. actin and tubulin, could mediate cytoplasmic retention of HBV polymerase. To prove this hypothesis, the straight forward experiment would be to measure the downregulation of Hsp90 in HBV polymerase expressing cells using an siRNA approach. This should increase the amounts of HBV polymerase in the nucleus. Unfortunately, this experiment was attempted but failed due to a dramatically enhanced Hsp90 expression in P protein expressing cells (Fig. 26). Also, the use of geldanamycin that inhibits the ATPase function of Hsp90 had no effects on the subcellular localization of the P protein in HBV polymerase expressing cells (data not shown).

Transfection experiments were used to show that virus replication is almost completely abolished if the NLS or the CKII-site is destroyed by site directed mutagenesis (Fig. 31). This clearly demonstrates that this structural motif plays a crucial role in the viral lifecycle. Nuclear import of the viral genome is essential for the establishment of viral infection after initial binding and entry of the virus into the target cell. Moreover, re-entry of viral genomes into the nucleus during the viral replication process is essential for maintenance of the pool of transcriptional templates [Tuttleman, et al., 1986]. An interesting aspect of this study is that inhibition of CKII activity, or destruction of the NLS or CKII site has a much stronger effect in infection or transient transfection experiments (Fig. 29 & 31) than in experiments performed with stably transfected cell lines (Fig. 29). In infection or transient transfection experiments only a very small pool of transcriptional templates exists to generate the 3.5 kb pgRNA. The re-entry of the viral genome is therefore essential to increase the intranuclear pool of transcriptional templates. In stable cell lines however, the pool of transcriptional

templates is increased by, but does not strictly depend on genome re-entry due to multiple integrations into the host genome.

There are conflicting results about the pathways that enable the import of viral genomes into the nucleus. Based on digitonin permeabilized cells [Rabe, et al., 2003] or lipofection of nucleocapsids into hepatoma cells [Rabe, et al., 2006] it was described that complete nucleocapsids are able to migrate through the nuclear pore complex into the nucleus. Other studies using cell permeable nucleocapsids showed that the nucleocapsids do not enter the nucleus. The disassembly and release of the viral genome occurs in a perinuclear domain [Brandenburg, et al., 2005] raising the question of the import mechanism of the polymerase associated viral genome. Michael Kann and co-workers reported in 1997 that the HBV polymerase is probably sufficient to mediate import of the bound viral genome into the nucleus of digitonin permeabilized huh-7 cells, whereas the protein free genome itself stayed in the cytosol [Kann, et al., 1997].

The conclusion from these data leads to the model that the HBV nucleocapsid dissociates in a perinuclear domain and that the polymerase plays an essential role for the import of the viral genome and the subsequent amplification of cccDNA levels in the nucleus. It can not be excluded that HBV polymerase exerts additional functions to those established here.

REFERENCES

- Aldrich, C. E.;** Coates, L.; Wu, T. T.; Newbold, J.; Tennant, B. C.; Summers, J.; Seeger, C. and Mason, W. S. (1989): In vitro infection of woodchuck hepatocytes with woodchuck hepatitis virus and ground squirrel hepatitis virus, *Virology* (vol. 172), No. 1, pp. 247-52.
- Allen, M. I.;** Deslauriers, M.; Andrews, C. W.; Tipples, G. A.; Walters, K. A.; Tyrrell, D. L.; Brown, N. and Condreay, L. D. (1998): Identification and characterization of mutations in hepatitis B virus resistant to lamivudine. Lamivudine Clinical Investigation Group, *Hepatology* (vol. 27), No. 6, pp. 1670-7.
- Allen, T. D.;** Cronshaw, J. M.; Bagley, S.; Kiseleva, E. and Goldberg, M. W. (2000): The nuclear pore complex: mediator of translocation between nucleus and cytoplasm, *J Cell Sci* (vol. 113 (Pt 10)), pp. 1651-9.
- Ausubel, F. M.;** Brent, R.; Kingston, R. E.; Moore, D. D.; Seidman, J. G.; Smith, J. A. and Struhl, K. (2004): *Current protocols of molecular biology*, John Wiley & Sons, New York.
- Bartenschlager, R.;** Junker-Niepmann, M. and Schaller, H. (1990): The P gene product of hepatitis B virus is required as a structural component for genomic RNA encapsidation, *J Virol* (vol. 64), No. 11, pp. 5324-32.
- Bouchard, M. J. and** Schneider, R. J. (2004): The enigmatic X gene of hepatitis B virus, *J Virol* (vol. 78), No. 23, pp. 12725-34.
- Bouchard, M. J.;** Wang, L. H. and Schneider, R. J. (2001): Calcium signaling by HBx protein in hepatitis B virus DNA replication, *Science* (vol. 294), No. 5550, pp. 2376-8.
- Brandenburg, B.;** Stockl, L.; Gutzeit, C.; Roos, M.; Lupberger, J.; Schwartlander, R.; Gelderblom, H.; Sauer, I. M.; Hofschneider, P. H. and Hildt, E. (2005): A novel system for efficient gene transfer into primary human hepatocytes via cell-permeable hepatitis B virus-like particle, *Hepatology* (vol. 42), No. 6, pp. 1300-9.
- Bruns, M.;** Miska, S.; Chassot, S. and Will, H. (1998): Enhancement of hepatitis B virus infection by noninfectious subviral particles, *J Virol* (vol. 72), No. 2, pp. 1462-8.

- Bruss, V.** (2004): Envelopment of the hepatitis B virus nucleocapsid, *Virus Res* (vol. 106), No. 2, pp. 199-209.
- Bruss, V.;** Lu, X.; Thomssen, R. and Gerlich, W. H. (1994): Post-translational alterations in transmembrane topology of the hepatitis B virus large envelope protein, *Embo J* (vol. 13), No. 10, pp. 2273-9.
- Buster, E. H.** and Janssen, H. L. (2006): Antiviral treatment for chronic hepatitis B virus infection--immune modulation or viral suppression?, *Neth J Med* (vol. 64), No. 6, pp. 175-85.
- Cho, G.;** Park, S. G. and Jung, G. (2000): Localization of HSP90 binding sites in the human hepatitis B virus polymerase, *Biochem Biophys Res Commun* (vol. 269), No. 1, pp. 191-6.
- Choi, J.;** Chang, J. S.; Song, M. S.; Ahn, B. Y.; Park, Y.; Lim, D. S. and Han, Y. S. (2003): Association of hepatitis B virus polymerase with promyelocytic leukemia nuclear bodies mediated by the S100 family protein p11, *Biochem Biophys Res Commun* (vol. 305), No. 4, pp. 1049-56.
- Conti, E.** and Kuriyan, J. (2000): Crystallographic analysis of the specific yet versatile recognition of distinct nuclear localization signals by karyopherin alpha, *Structure* (vol. 8), No. 3, pp. 329-38.
- Dandri, M.;** Volz, T. K.; Lutgehetmann, M. and Petersen, J. (2005): Animal models for the study of HBV replication and its variants, *J Clin Virol* (vol. 34 Suppl 1), pp. S54-62.
- Daub, H.;** Blencke, S.; Habenberger, P.; Kurtenbach, A.; Dennenmoser, J.; Wissing, J.; Ullrich, A. and Cotten, M. (2002): Identification of SRPK1 and SRPK2 as the major cellular protein kinases phosphorylating hepatitis B virus core protein, *J Virol* (vol. 76), No. 16, pp. 8124-37.
- de Franchis, R.;** Hadengue, A.; Lau, G.; Lavanchy, D.; Lok, A.; McIntyre, N.; Mele, A.; Paumgartner, G.; Pietrangelo, A.; Rodes, J.; Rosenberg, W. and Valla, D. (2003): EASL International Consensus Conference on Hepatitis B. 13-14 September, 2002 Geneva, Switzerland. Consensus statement (long version), *J Hepatol* (vol. 39 Suppl 1), pp. S3-25.
- Dingwall, C.;** Sharnick, S. V. and Laskey, R. A. (1982): A polypeptide domain that specifies migration of nucleoplasmin into the nucleus, *Cell* (vol. 30), No. 2, pp. 449-58.

- Dworetzky, S. I.**; Lanford, R. E. and Feldherr, C. M. (1988): The effects of variations in the number and sequence of targeting signals on nuclear uptake, *J Cell Biol* (vol. 107), No. 4, pp. 1279-87.
- Fisher, C. L.** and Pei, G. K. (1997): Modification of a PCR-based site-directed mutagenesis method, *Biotechniques* (vol. 23), No. 4, pp. 570-1, 574.
- Friedrich, B.**; Wollersheim, M.; Brandenburg, B.; Foerste, R.; Will, H. and Hildt, E. (2005): Induction of anti-proliferative mechanisms in hepatitis B virus producing cells, *J Hepatol* (vol. 43), No. 4, pp. 696-703.
- Ganem, D.** (1991): Assembly of hepadnaviral virions and subviral particles, *Curr Top Microbiol Immunol* (vol. 168), pp. 61-83.
- Gerok, W.**; Huber, C. and Meinertz, T. (2000): *Die Innere Medizin*, 10. ed., Schattauer, F.K. Verlag, ISBN: 3794518004.
- Goldfarb, D. S.**; Corbett, A. H.; Mason, D. A.; Harreman, M. T. and Adam, S. A. (2004): Importin alpha: a multipurpose nuclear-transport receptor, *Trends Cell Biol* (vol. 14), No. 9, pp. 505-14.
- Gong, Z. J.**; De Meyer, S.; Roskams, T.; van Pelt, J. F.; Soumillion, A.; Crabbe, T. and Yap, S. H. (1998): Hepatitis B virus infection in microcarrier-attached immortalized human hepatocytes cultured in molecularporous membrane bags: a model for long-term episomal replication of HBV, *J Viral Hepat* (vol. 5), No. 6, pp. 377-87.
- Gripon, P.**; Rumin, S.; Urban, S.; Le Seyec, J.; Glaise, D.; Cannie, I.; Guyomard, C.; Lucas, J.; Trepo, C. and Guguen-Guillouzo, C. (2002): Infection of a human hepatoma cell line by hepatitis B virus, *Proc Natl Acad Sci U S A* (vol. 99), No. 24, pp. 15655-60.
- Harreman, M. T.**; Kline, T. M.; Milford, H. G.; Harben, M. B.; Hodel, A. E. and Corbett, A. H. (2004): Regulation of nuclear import by phosphorylation adjacent to nuclear localization signals, *J Biol Chem* (vol. 279), No. 20, pp. 20613-21.
- Hildt, E.**; Munz, B.; Saher, G.; Reifenberg, K. and Hofschneider, P. H. (2002): The PreS2 activator MHBs(t) of hepatitis B virus activates c-raf-1/Erk2 signaling in transgenic mice, *Embo J* (vol. 21), No. 4, pp. 525-35.
- Hildt, E.**; Saher, G.; Bruss, V. and Hofschneider, P. H. (1996): The hepatitis B virus large surface protein (LHBs) is a transcriptional activator, *Virology* (vol. 225), No. 1, pp. 235-9.

- Hirsch, R. C.;** Lavine, J. E.; Chang, L. J.; Varmus, H. E. and Ganem, D. (1990): Polymerase gene products of hepatitis B viruses are required for genomic RNA packaging as well as for reverse transcription, *Nature* (vol. 344), No. 6266, pp. 552-5.
- Hollinger, F. B.** and Liang, T.J. (2001): Hepatitis B Virus, *Fields Virology*, 4th ed., pp. 2971-3036.
- Howard, E. A.;** Zupan, J. R.; Citovsky, V. and Zambryski, P. C. (1992): The VirD2 protein of *A. tumefaciens* contains a C-terminal bipartite nuclear localization signal: implications for nuclear uptake of DNA in plant cells, *Cell* (vol. 68), No. 1, pp. 109-18.
- Hu, J.;** Toft, D.; Anselmo, D. and Wang, X. (2002): In vitro reconstitution of functional hepadnavirus reverse transcriptase with cellular chaperone proteins, *J Virol* (vol. 76), No. 1, pp. 269-79.
- Hughes, P. E.;** Renshaw, M. W.; Pfaff, M.; Forsyth, J.; Keivens, V. M.; Schwartz, M. A. and Ginsberg, M. H. (1997): Suppression of integrin activation: a novel function of a Ras/Raf-initiated MAP kinase pathway, *Cell* (vol. 88), No. 4, pp. 521-30.
- Jans, D. A.;** Ackermann, M. J.; Bischoff, J. R.; Beach, D. H. and Peters, R. (1991): p34cdc2-mediated phosphorylation at T124 inhibits nuclear import of SV-40 T antigen proteins, *J Cell Biol* (vol. 115), No. 5, pp. 1203-12.
- Jans, D. A.** and Hubner, S. (1996): Regulation of protein transport to the nucleus: central role of phosphorylation, *Physiol Rev* (vol. 76), No. 3, pp. 651-85.
- Jans, D. A.** and Jans, P. (1994): Negative charge at the casein kinase II site flanking the nuclear localization signal of the SV40 large T-antigen is mechanistically important for enhanced nuclear import, *Oncogene* (vol. 9), No. 10, pp. 2961-8.
- Kalderon, D.;** Roberts, B. L.; Richardson, W. D. and Smith, A. E. (1984): A short amino acid sequence able to specify nuclear location, *Cell* (vol. 39), No. 3 Pt 2, pp. 499-509.
- Kann, M.;** Bischof, A. and Gerlich, W. H. (1997): In vitro model for the nuclear transport of the hepadnavirus genome, *J Virol* (vol. 71), No. 2, pp. 1310-6.
- Kann, M.;** Lu, X. and Gerlich, W. H. (1995): Recent studies on replication of hepatitis B virus, *J Hepatol* (vol. 22), No. 1 Suppl, pp. 9-13.

- Kann, M.;** Sodeik, B.; Vlachou, A.; Gerlich, W. H. and Helenius, A. (1999): Phosphorylation-dependent binding of hepatitis B virus core particles to the nuclear pore complex, *J Cell Biol* (vol. 145), No. 1, pp. 45-55.
- Kann, M.;** Thomssen, R.; Kochel, H. G. and Gerlich, W. H. (1993): Characterization of the endogenous protein kinase activity of the hepatitis B virus, *Arch Virol Suppl* (vol. 8), pp. 53-62.
- Kau, J. H. and** Ting, L. P. (1998): Phosphorylation of the core protein of hepatitis B virus by a 46-kilodalton serine kinase, *J Virol* (vol. 72), No. 5, pp. 3796-803.
- Kekule, A. S.;** Lauer, U.; Meyer, M.; Caselmann, W. H.; Hofschneider, P. H. and Koshy, R. (1990): The preS2/S region of integrated hepatitis B virus DNA encodes a transcriptional transactivator, *Nature* (vol. 343), No. 6257, pp. 457-61.
- Kidd-Ljunggren, K.;** Zuker, M.; Hofacker, I. L. and Kidd, A. H. (2000): The hepatitis B virus pregenome: prediction of RNA structure and implications for the emergence of deletions, *Intervirology* (vol. 43), No. 3, pp. 154-64.
- Kock, J.;** Nassal, M.; MacNelly, S.; Baumert, T. F.; Blum, H. E. and von Weizsacker, F. (2001): Efficient infection of primary tupaia hepatocytes with purified human and woolly monkey hepatitis B virus, *J Virol* (vol. 75), No. 11, pp. 5084-9.
- Koschel, M.;** Oed, D.; Gerelsaikhan, T.; Thomssen, R. and Bruss, V. (2000): Hepatitis B virus core gene mutations which block nucleocapsid envelopment, *J Virol* (vol. 74), No. 1, pp. 1-7.
- Kramvis, A.;** Kew, M. and Francois, G. (2005): Hepatitis B virus genotypes, *Vaccine* (vol. 23), No. 19, pp. 2409-23.
- Ladner, S. K.;** Otto, M. J.; Barker, C. S.; Zaifert, K.; Wang, G. H.; Guo, J. T.; Seeger, C. and King, R. W. (1997): Inducible expression of human hepatitis B virus (HBV) in stably transfected hepatoblastoma cells: a novel system for screening potential inhibitors of HBV replication, *Antimicrob Agents Chemother* (vol. 41), No. 8, pp. 1715-20.
- Lanford, R. E.;** Kim, Y. H.; Lee, H.; Notvall, L. and Beames, B. (1999): Mapping of the hepatitis B virus reverse transcriptase TP and RT domains by transcomplementation for nucleotide priming and by protein-protein interaction, *J Virol* (vol. 73), No. 3, pp. 1885-93.
- Lanford, R. E.;** Notvall, L. and Beames, B. (1995): Nucleotide priming and reverse transcriptase activity of hepatitis B virus polymerase expressed in insect cells, *J Virol* (vol. 69), No. 7, pp. 4431-9.

- Lanford, R. E.;** Notvall, L.; Lee, H. and Beames, B. (1997): Transcomplementation of nucleotide priming and reverse transcription between independently expressed TP and RT domains of the hepatitis B virus reverse transcriptase, *J Virol* (vol. 71), No. 4, pp. 2996-3004.
- Liao, W.** and Ou, J. H. (1995): Phosphorylation and nuclear localization of the hepatitis B virus core protein: significance of serine in the three repeated SPRRR motifs, *J Virol* (vol. 69), No. 2, pp. 1025-9.
- Lin, X.;** Yuan, Z. H.; Wu, L.; Ding, J. P. and Wen, Y. M. (2001): A single amino acid in the reverse transcriptase domain of hepatitis B virus affects virus replication efficiency, *J Virol* (vol. 75), No. 23, pp. 11827-33.
- Lin, Y. C.;** Brown, K. and Siebenlist, U. (1995): Activation of NF-kappa B requires proteolysis of the inhibitor I kappa B-alpha: signal-induced phosphorylation of I kappa B-alpha alone does not release active NF-kappa B, *Proc Natl Acad Sci U S A* (vol. 92), No. 2, pp. 552-6.
- Litchfield, D. W.** (2003): Protein kinase CK2: structure, regulation and role in cellular decisions of life and death, *Biochem J* (vol. 369), No. Pt 1, pp. 1-15.
- Lupberger, J.** and Hildt, E. (in press): Hepatitis B virus-induced oncogenesis, *World J Gastroenterol*.
- Lupberger, J.;** Mund, A.; Kock, J. and Hildt, E. (2006): Cultivation of HepG2.2.15 on Cytodex-3: higher yield of hepatitis B virus and less subviral particles compared to conventional culture methods, *J Hepatol* (vol. 45), No. 4, pp. 547-52.
- Mason, W. S.;** Seal, G. and Summers, J. (1980): Virus of Pekin ducks with structural and biological relatedness to human hepatitis B virus, *J Virol* (vol. 36), No. 3, pp. 829-36.
- Meggio, F.** and Pinna, L. A. (2003): One-thousand-and-one substrates of protein kinase CK2?, *Faseb J* (vol. 17), No. 3, pp. 349-68.
- Melegari, M.;** Wolf, S. K. and Schneider, R. J. (2005): Hepatitis B virus DNA replication is coordinated by core protein serine phosphorylation and HBx expression, *J Virol* (vol. 79), No. 15, pp. 9810-20.
- Mosammaparast, N.** and Pemberton, L. F. (2004): Karyopherins: from nuclear-transport mediators to nuclear-function regulators, *Trends Cell Biol* (vol. 14), No. 10, pp. 547-56.

- Nakabayashi, H.;** Taketa, K.; Miyano, K.; Yamane, T. and Sato, J. (1982): Growth of human hepatoma cells lines with differentiated functions in chemically defined medium, *Cancer Res* (vol. 42), No. 9, pp. 3858-63.
- Newbold, J. E.;** Xin, H.; Tencza, M.; Sherman, G.; Dean, J.; Bowden, S. and Locarnini, S. (1995): The covalently closed duplex form of the hepadnavirus genome exists in situ as a heterogeneous population of viral minichromosomes, *J Virol* (vol. 69), No. 6, pp. 3350-7.
- Orito, E.;** Mizokami, M.; Ina, Y.; Moriyama, E. N.; Kameshima, N.; Yamamoto, M. and Gojobori, T. (1989): Host-independent evolution and a genetic classification of the hepadnavirus family based on nucleotide sequences, *Proc Natl Acad Sci USA* (vol. 86), No. 18, pp. 7059-62.
- Ozer, A.;** Khaoustov, V. I.; Mearns, M.; Lewis, D. E.; Genta, R. M.; Darlington, G. J. and Yoffe, B. (1996): Effect of hepatocyte proliferation and cellular DNA synthesis on hepatitis B virus replication, *Gastroenterology* (vol. 110), No. 5, pp. 1519-28.
- Perlman, D. H.;** Berg, E. A.; O'Connor P, B.; Costello, C. E. and Hu, J. (2005): Reverse transcription-associated dephosphorylation of hepadnavirus nucleocapsids, *Proc Natl Acad Sci USA* (vol. 102), No. 25, pp. 9020-5.
- Peyssonnaud, C.** and Eychene, A. (2001): The Raf/MEK/ERK pathway: new concepts of activation, *Biol Cell* (vol. 93), No. 1-2, pp. 53-62.
- Picard, D.;** Kumar, V.; Chambon, P. and Yamamoto, K. R. (1990): Signal transduction by steroid hormones: nuclear localization is differentially regulated in estrogen and glucocorticoid receptors, *Cell Regul* (vol. 1), No. 3, pp. 291-9.
- Rabe, B.;** Glebe, D. and Kann, M. (2006): Lipid-mediated introduction of hepatitis B virus capsids into nonsusceptible cells allows highly efficient replication and facilitates the study of early infection events, *J Virol* (vol. 80), No. 11, pp. 5465-73.
- Rabe, B.;** Vlachou, A.; Pante, N.; Helenius, A. and Kann, M. (2003): Nuclear import of hepatitis B virus capsids and release of the viral genome, *Proc Natl Acad Sci USA* (vol. 100), No. 17, pp. 9849-54.
- Reyes, N.** and Gadsby, D. C. (2006): Ion permeation through the Na⁺,K⁺-ATPase, *Nature* (vol. 443), No. 7110, pp. 470-4.
- Robbins, J.;** Dilworth, S. M.; Laskey, R. A. and Dingwall, C. (1991): Two interdependent basic domains in nucleoplasmin nuclear targeting sequence:

- identification of a class of bipartite nuclear targeting sequence, *Cell* (vol. 64), No. 3, pp. 615-23.
- Schaefer, S.** (2005): Hepatitis B virus: significance of genotypes, *J Viral Hepat* (vol. 12), No. 2, pp. 111-24.
- Seeger, C.** and Mason, W. S. (2000): Hepatitis B virus biology, *Microbiol Mol Biol Rev* (vol. 64), No. 1, pp. 51-68.
- Sells, M. A.;** Chen, M. L. and Acs, G. (1987): Production of hepatitis B virus particles in Hep G2 cells transfected with cloned hepatitis B virus DNA, *Proc Natl Acad Sci U S A* (vol. 84), No. 4, pp. 1005-9.
- Shieh, M. W.;** Wessler, S. R. and Raikhel, N. V. (1993): Nuclear targeting of the maize R protein requires two nuclear localization sequences, *Plant Physiol* (vol. 101), No. 2, pp. 353-61.
- Simons, K. T.;** Kooperberg, C.; Huang, E. and Baker, D. (1997): Assembly of protein tertiary structures from fragments with similar local sequences using simulated annealing and Bayesian scoring functions, *J Mol Biol* (vol. 268), No. 1, pp. 209-25.
- Sprengel, R.;** Kaleta, E. F. and Will, H. (1988): Isolation and characterization of a hepatitis B virus endemic in herons, *J Virol* (vol. 62), No. 10, pp. 3832-9.
- Stockl, L.;** Berting, A.; Malkowski, B.; Foerste, R.; Hofschneider, P. H. and Hildt, E. (2003): Integrity of c-Raf-1/MEK signal transduction cascade is essential for hepatitis B virus gene expression, *Oncogene* (vol. 22), No. 17, pp. 2604-10.
- Stoeckl, L.;** Funk, A.; Kopitzki, A.; Brandenburg, B.; Oess, S.; Will, H.; Sirma, H. and Hildt, E. (2006): Identification of a structural motif crucial for infectivity of hepatitis B viruses, *Proc Natl Acad Sci U S A* (vol. 103), No. 17, pp. 6730-4.
- Takahashi, K.;** Machida, A.; Funatsu, G.; Nomura, M.; Usuda, S.; Aoyagi, S.; Tachibana, K.; Miyamoto, H.; Imai, M.; Nakamura, T.; Miyakawa, Y. and Mayumi, M. (1983): Immunochemical structure of hepatitis B e antigen in the serum, *J Immunol* (vol. 130), No. 6, pp. 2903-7.
- Tessitore, L.;** Perletti, G. P.; Sesca, E.; Pani, P.; Piccinini, F. and Dianzani, M. U. (1995): Protein kinase C isozymes during liver regeneration, *Biochem Biophys Res Commun* (vol. 214), No. 2, pp. 354-60.
- Tuttleman, J. S.;** Pourcel, C. and Summers, J. (1986): Formation of the pool of covalently closed circular viral DNA in hepadnavirus-infected cells, *Cell* (vol. 47), No. 3, pp. 451-60.

- Twu, J. S.** and Schloemer, R. H. (1987): Transcriptional trans-activating function of hepatitis B virus, *J Virol* (vol. 61), No. 11, pp. 3448-53.
- Vancurova, I.**; Paine, T. M.; Lou, W. and Paine, P. L. (1995): Nucleoplasmin associates with and is phosphorylated by casein kinase II, *J Cell Sci* (vol. 108 (Pt 2)), pp. 779-87.
- Walter, E.**; Keist, R.; Niederost, B.; Pult, I. and Blum, H. E. (1996): Hepatitis B virus infection of tupaia hepatocytes in vitro and in vivo, *Hepatology* (vol. 24), No. 1, pp. 1-5.
- Wang, G. H.** and Seeger, C. (1993): Novel mechanism for reverse transcription in hepatitis B viruses, *J Virol* (vol. 67), No. 11, pp. 6507-12.
- Wang, X.**; Sato, R.; Brown, M. S.; Hua, X. and Goldstein, J. L. (1994): SREBP-1, a membrane-bound transcription factor released by sterol-regulated proteolysis, *Cell* (vol. 77), No. 1, pp. 53-62.
- Wilson, J. N.**; Nokes, D. J. and Carman, W. F. (1999): The predicted pattern of emergence of vaccine-resistant hepatitis B: a cause for concern?, *Vaccine* (vol. 17), No. 7-8, pp. 973-8.
- Wollersheim, M.**; Debelka, U. and Hofschneider, P. H. (1988): A transactivating function encoded in the hepatitis B virus X gene is conserved in the integrated state, *Oncogene* (vol. 3), No. 5, pp. 545-52.
- Wu, S. C.** and Huang, G. Y. (2002): Stationary and microcarrier cell culture processes for propagating Japanese encephalitis virus, *Biotechnol Prog* (vol. 18), No. 1, pp. 124-8.
- Wu, S. C.**; Huang, G. Y. and Liu, J. H. (2002): Production of retrovirus and adenovirus vectors for gene therapy: a comparative study using microcarrier and stationary cell culture, *Biotechnol Prog* (vol. 18), No. 3, pp. 617-22.
- Yao, E.**; Gong, Y.; Chen, N. and Tavis, J. E. (2000): The majority of duck hepatitis B virus reverse transcriptase in cells is nonencapsidated and is bound to a cytoplasmic structure, *J Virol* (vol. 74), No. 18, pp. 8648-57.
- Zoulim, F.** (2005): New insight on hepatitis B virus persistence from the study of intrahepatic viral cccDNA, *J Hepatol* (vol. 42), No. 3, pp. 302-8.
- Zoulim, F.** and Seeger, C. (1994): Reverse transcription in hepatitis B viruses is primed by a tyrosine residue of the polymerase, *J Virol* (vol. 68), No. 1, pp. 6-13.

APPENDIX 1

Buffers and solutions

A_{BP}

20 mM Tris hydrochloride
 25 mM beta-glycerol phosphate
 1 mM sodium ortho-vanadate
 20 mM 2-mercaptoethanol
 0.1 % (v/v) Tween-20
 pH 7.5

A_D

100 mM Tris hydrochloride
 6 M urea
 pH 8.0

Agarose gel sample buffer (6x)

TAE (6x)
 30 % (v/v) glycerol
 0.1 mg/mL bromophenol blue

A_{MS}

20 mM sodium acetate
 6 M urea
 2 % (v/v) ethanol
 pH 5.5

A_N

TBS
 10 mM imidazole
 pH 8.0

Anode buffer I

0.3 M Tris base
 20 % (v/v) ethanol

Anode buffer II

25 mM Tris base
 20 % (v/v) ethanol

A_{TP}

100 mM Tris hydrochloride
 6 M urea
 20 mM 2-mercaptoethanol
 pH 8.0

Coomassie Brilliant Blue solution

0.25 % (w/v) Coomassie
 Brilliant Blue G250
 10 % (v/v) acetic acid
 45 % (v/v) ethanol

Coomassie Destain solution

10 % (v/v) acetic acid
 30 % (v/v) ethanol

CKII

20 mM Tris hydrochloride
 50 mM potassium chloride
 10 mM imidazole
 20 mM 2-mercaptoethanol
 20 mM beta-glycerol phosphate
 0.1 mM sodium ortho-vanadate
 0.1 % (v/v) Tween-20
 pH 7.5

E_{AB}

50 mM glycine
 150 mM sodium chloride
 pH 2.3

EB

10 mM Tris hydrochloride
 pH 8.5

E_D

100 mM Tris hydrochloride
6 M urea
pH 6.7

E_N

TBS
250 mM imidazole
pH 8.0

K (5x)

125 mM Tris hydrochloride
125 mM beta-glycerophosphate
50 mM MgCl₂
5 mM DTT
pH 7.5

Kathode buffer

40 mM 6-aminohexanoic acid

LB medium

10 g/L Bacto trypton
5 g/L yeast extract
5 g/L sodium chloride

L_G

100mM Tris hydrochloride
6 M guanidin hydrochlorid
pH 8.0

Mounting medium

100 mM Tris-HCl
10 % (w/v) Mowiol (polyvinyl alcohol)
25 % (w/v) glycerol
2.5 % (w/v) DABCO

NB

0.2 M Mops
50 mM sodium acetate
10 mM EDTA
pH 7.0

NHS-A

0.5 M ethanolamine
0.5 M sodium chloride
pH 8.3

NHS-B

0.1 M sodium acetate
0.5 M sodium chloride
pH 4.0

NHS-D

10 % (v/v) 10x PBS
ad DMSO

NHS-G

2 M glycine
pH 2.0

PBS

10 mM sodium phosphate dibasic
3 mM potassium phosphate monobasic
137 mM sodium chloride
pH 7.4

PBS-T

PBS incl. 0.05 % (v/v) Tween-20

R

20 mM Tris hydrochloride
134 mM sodium chloride
10 % (v/v) glycerol
10 % (w/v) sucrose
20 mM 2-mercaptoethanole
0.1 % (v/v) Tween-20
pH 7.5

RIPA

20 mM Tris hydrochloride
1 % (w/v) sodium desoxycholate
1 % (v/v) Triton X-100
0.1 % (w/v) sodium dedecyl sulfate
150 mM sodium chloride

SB medium

12 g/L Bacto trypton
 24 g/L yeast extract
 4 % (v/v) glycerol
 after autoclaving :
 170 mM potassium phosphate monob.
 720 nM potassium phosphate dibasic

SDS-PAGE buffer

25 mM Tris base
 0.2 M glycine
 0.1 % (w/v) sodium dodecyl sulfate

SDS-PAGE sample buffer (6x)

0.2 M Tris hydrochloride
 6 % (w/v) sodium dodecyl sulfate
 20 % (v/v) glycerol
 10 % dithiothreitol
 0.1 mg/mL bromophenol blue

S_E

2.5 % (w/v) sodium carbonate
 5.4 mM formaldehyde

S_{Fi}

25 % (v/v) ethanol
 10 % (v/v) glacial acetic acid

S_{KE}

0.1 % (w/v) silver nitrate
 3.4 mM formaldehyde

S_{KO}

0.4 M sodium acetate
 30 % (v/v) ethanol
 4.4 mM sodium thiosulfate
 pentahydrate
 0.5 % (v/v) glutaraldehyde

10x SSC

150 mM trisodium citrate dehydrate
 1.5 M sodium chloride
 pH 7.0

Stripping buffer

62.5 mM Tris hydrochloride
 2 % (w/v) sodium dodecyl sulfate
 100 mM 2-mercaptoethanol
 pH 6.7

TAE

30 mM Tris hydrochloride
 20 mM acetic acid
 1 mM EDTA
 pH 8.0

TBS

20 mM Tris hydrochloride
 134 mM sodium chloride
 pH 7.4

TE

10 mM Tris hydrochloride
 1 mM EDTA
 pH 8.0

W_N

TBS
 20 mM imidazole
 pH 8.0

W_D

100 mM Tris hydrochloride
 6 M urea
 pH 6.7

APPENDIX 2

Quantities of ammonium sulfate required to reach given degrees of saturation at +20 °C.

Starting percent saturation	Final percent saturation to be obtained																
	20	25	30	35	40	45	50	55	60	65	70	75	80	85	90	95	100
Amount of ammonium sulphate to add (grams) per liter of solution at +20 C																	
0	113	144	176	208	242	277	314	351	390	430	472	516	561	605	657	708	761
5	85	115	146	179	212	246	282	319	358	397	439	481	526	572	621	671	723
10	57	86	117	149	182	216	251	287	325	364	405	447	491	537	584	634	685
15	28	55	88	119	151	185	219	255	293	331	371	413	456	501	548	596	647
20	0	29	59	89	121	154	188	223	260	298	337	378	421	465	511	559	609
25		0	29	60	91	123	157	191	228	265	304	344	386	429	475	522	571
30			0	30	61	92	125	160	195	232	270	309	351	393	438	485	533
35				0	30	62	94	128	163	199	236	275	316	355	402	447	495
40					0	31	63	96	130	166	202	241	281	322	365	410	457
45						0	31	64	98	132	169	206	245	286	329	373	419
50							0	32	65	99	135	172	210	250	292	335	381
55								0	33	66	101	138	175	215	256	298	343
60									0	33	67	103	140	179	219	261	305
65										0	34	69	105	143	183	224	267
70											0	34	70	107	146	185	228
75												0	35	72	110	149	190
80													0	36	73	112	152
85														0	37	75	114
90															0	37	76
95																0	38

ACKNOWLEDGEMENT

My gratitude to all people, who contributed to this work and gave me mental and scientific support during the last years:

Thanks to my doctoral thesis supervisor Prof. Detlev Krueger from the Charité in Berlin for the opportunity to submit this work as dissertation at the Humboldt University in Berlin.

Thanks to Prof. Hubert Blum, head of the department Internal Medicine II of the University of Freiburg, and to the Robert Koch Institute in Berlin for providing excellent scientific environments and equipment.

Thanks to my scientific supervisor Dr. Eberhard Hildt, who made it possible to perform this work in his lab at the Robert-Koch Institute in Berlin and the University of Freiburg. You gave me the opportunity to work with you despite my unusual *vitae* and my persistent unshaven appearance. There was always an exceptional good personal and scientific climate in your group. I am looking forward to continue our good cooperation in future projects.

Thanks to Andreas Mund and Anja Luckow who supervised my supervision during their diploma thesis. Their dedicated and successful work had substantial impact on my doctoral thesis. Furthermore, many thanks to the countless trainees who participated on my projects and gave me a hand at the sometimes unpleasant routines.

Thanks to Dr. Alexander Pairan and Dr. Volker Bruss (University of Goettingen) for their help with the endogenous polymerase assay and the fruitful discussions, to Sabine Mac Nelly (University of Freiburg) the good fairy of the *Tupaia* hepatocytes, to Dr. Josef Kock (University of Freiburg) for the countless pristine blot hybridizations, to Dr. Muhsin Oezel and Freya Kaulbars (Robert-Koch Institute, Berlin) for the REM analysis of the microcarrier.

ACKNOWLEDGEMENT

Thanks to Kiyoshi Himmelsbach, Matthias Schmidt (University of Freiburg), and to Nadia Warner (University of Melbourne) for the careful revision of the manuscript.

And last but not least thanks to all the present and former members of Eberhard's lab, for all the fun during the days holding pipettes and during the nights holding beers, especially to Markus Moebis for our countless "homie de luxe" occasions performed in culinary bliss.

I wish you all the best for your future.

ASSURANCE of RESEARCH

I hereby assure that I composed my thesis autonomously, used no other resources or aids than stated and identified all quoted references.

Joachim Lupberger

(Freiburg im Breisgau, Germany, December 12th, 2006)

CURRICULUM VITAE

Joachim Lupberger, Feldmoos 5, D-88273 Fronreute, Germany

Phone: ++49 170 9819143, Email: joelupberger@hotmail.com

Nationality: German

EDUCATION AND QUALIFICATIONS

04/2003 – 12/2006

Dissertation (PhD), Humboldt University Berlin, Dr. E. Hildt, Germany

Thesis director: Prof. Dr. D. Krueger, Charité, Humboldt University, Berlin, Germany

Disputation: Spring 2007

10/1998 - 01/2003

Study of biotechnology, University of Applied Sciences (TFH-Berlin), Germany

Areas of concentration: (*basic study*) microbiology, biochemistry, molecular biology;
(*main study*) fermentation technology, process control, downstream processing,

biochemistry, immunology, genetic engineering

Degree: Diploma (Engineer of Biotechnology)

Grade: A

1991 - 1993

Technical school, Academy of Natural Sciences, Isny, Germany

Degree: Chemical- technical Assistant (CTA)

Grade: B

1985 - 1991

Intermediate school, Bildungszentrum St. Konrad, Ravensburg, Germany

Graduated with honors degree in chemistry

WORK EXPERIENCE

Starting 03/2007

**University Louis Pasteur, INSERM Unite 748, Prof. Dr. T. F. Baumert,
Strasbourg, France**

Postdoctoral fellow: Host cell interaction of hepatitis C virus (HCV)

Grant: "European Associated Laboratory" scholarship (Embassy of France)

01/2006 – 12/2006

University Hospital Freiburg, Dr. E. Hildt, Freiburg, Germany

PhD thesis objective: "Cultivation of Hepatitis B Virus Producing Cell Line HepG2.2.15 on Microcarrier and Functional Characterization of the Hepatitis B Virus Polymerase ". Identified two phosphorylation sites and a functional nuclear localization signal in the HBV polymerase, which has significant impact to the viral life cycle

04/2003 – 12/2005

Robert Koch-Institute, Dr. E. Hildt, Berlin, Germany

PhD thesis objective: "Cultivation of Hepatitis B Virus Producing Cell Line HepG2.2.15 on Microcarrier and Functional Characterization of the Hepatitis B Virus Polymerase". Established a novel cultivation method for adherent liver hepatoma cells to enhance HB virus production. (Group moved to Freiburg)

03/2002 - 11/2002

Massachusetts Institute of Technology, Prof. A.J. Sinskey, Cambridge, MA, USA

Diploma thesis: "Identification and Deletion of the Intracellular Poly[D-(-)-3-hydroxybutyrate] (PHB) Depolymerase Gene *phaZ2* in *Ralstonia eutropha* H16"

Grant: DAAD (German Academic Exchange Service)

01/1999 - 03/2002 and 01/2003 – 03/2003

**Charité, Humboldt University, Dr. K.A. Kreuzer, Dr. P. le Coutre,
Dr. C.A. Schmidt, Berlin, Germany**

Student employment: Developed real-time fluorescence PCR techniques in order to monitor housekeeping gene, Wilms tumor gene and *bcr-abl* gene transcription in CML positive patients during clinical phase study of STI571 "*Glivec*" (Novartis)

1994 - 1998

Institute of Lake Research, Hydrobiology, Dr. H. Güde, Langenargen, Germany

Position as CTA: Performed analysis of phosphorus, nitrogen, carbon and microscopy of bacteria; implemented metabolic measurements in algae with radioactive tracers (^{14}C and ^{32}P); responsible for lake monitoring with memory probes, GPS navigation on research ships and data processing

TEACHING

Supervised two diploma thesis projects focusing on the HBV polymerase.
Both students graduated with A.

SKILLS

Language: German (native language), English (excellent), French (basic)

Computer: LSM 510 (confocal laser scanning microscope), HTML, Illustrator, InDesign, Mac Vector, Microcal Origin, MSOffice, Photoshop, PyMol, Unicorn (Äkta purifier design), Vector NTI

REFERENCES

Dr. E. Hildt, Uniklinik, Hugstetter Str. 55, 79106 Freiburg, Germany;
eberhard.hildt@uniklinik-freiburg.de

Dr. P. le Coutre, Charite, Augustenburger Platz 1, 13353 Berlin, Germany;
philipp.lecoutre@charite.de

Prof. A.J. Sinskey, MIT, 77 Massachusetts Ave., Cambridge, MA 02139, USA;
asinskey@mit.edu

PUBLICATIONS

Lupberger, J.; Luckow, A.; Pairan, A.; Schmidt, M.; Schaedler, S. and Hildt, E. (submitted): Nuclear import of the hepatitis B virus polymerase is mediated by a bipartite NLS and depends on CKII phosphorylation.

Lupberger, J. and Hildt, E. (in press): Hepatitis B virus-induced oncogenesis. *World J Gastroenterol*.

Lupberger, J.; Mund, A.; Kock, J. and Hildt, E. (2006): Cultivation of HepG2.2.15 on micro carrier: Higher HBV production and less subviral particles in comparison to conventional cultivation methods, *J Hepatology* (vol. 45), No. 4, pp. 547-52.

Buerckstuemmer, T.; Kriegs, M.; **Lupberger, J.**; Pauli, E. K.; Schmittel, S. and Hildt, E. (2006): Raf-1 kinase associates with Hepatitis C virus NS5A and regulates viral replication, *FEBS Lett* (vol. 580), No. 2, pp. 575-80.

Brandenburg, B. and Stoeckl, L.; Gutzeit, C.; Roos, M.; **Lupberger, J.**; Schwartlander, R.; Gelderblom, H.; Sauer, I. M.; Hofschneider, P. H. and Hildt, E. (2005): A novel system for efficient gene transfer into primary human hepatocytes via cellpermeable hepatitis B virus-like particle, *Hepatology* (vol. 42), No. 6, pp. 1300-9.

Na, I. K.; Kreuzer, K. A.; **Lupberger, J.**; Dorken, B. and le Coutre, P. (2005): Quantitative RT-PCR of Wilms tumor gene transcripts (WT1) for the molecular monitoring of patients with accelerated phase bcr/abl + CML, *Leuk Res* (vol. 29), No. 3, pp. 343-345.

le Coutre, P.; Kreuzer, K. A.; Massenkeil, G.; Baskaynak, G.; Zschieschang, P.; Genvresse, I.; **Lupberger, J.**; Mapara, M.; Dorken, B. and Arnold, R. (2003): Autologous peripheral blood stem cell transplantation of stem cells harvested in imatinib-induced complete cytogenetic remission: an example of in vivo purging in CML, *Leukemia* (vol. 17), No. 12, pp. 2525-6.

le Coutre, P.; Kreuzer, K. A.; Na, I. K.; Schwarz, M.; **Lupberger, J.**, Holdhoff, M.; Baskaynak, G.; Gschaidmeier, H.; Platzbecker, U.; Ehninger, G.; Prejzner, W.; Huhn, D. and Schmidt, C. A. (2003): Imatinib in Philadelphia Chromosome Positive Chronic Phase CML Patients: Molecular and Cytogenetic Response Rates and Prediction of Clinical Outcome, *Am J Hematol* (vol. 73), No. 4, pp. 249-55.

York, G.M.; **Lupberger, J.**; Tian, J.; Lawrence, A. G.; Stubbe, J. and Sinskey, A. J. (2003): *Ralstonia eutropha* H16 Encodes Three Intracellular Poly[D-(-)-3-hydroxybutyrate] (PHB) Depolymerase Genes, *J Bacteriol* (vol. 185), No. 13, pp. 3788-94.

Lupberger, J.; Kreuzer, K. A.; Baskaynak, G.; Peters, U. R.; le Coutre, P. and Schmidt C. A. (2002): Quantitative analysis of beta-actin, porphobilinogen deaminase and beta-2-microglobulin mRNA and their comparison as control transcripts for RT-PCR, *Mol Cell Probes* (vol. 16), No. 1, pp. 25-30.

le Coutre, P.; Kreuzer, K. A.; **Lupberger, J.**; Na, I. K.; Müller, C.; Gambacorti-Passerini, C.; Appelt, C.; Bonnet, R.; Platzbecker, U.; Holdhoff, M.; Ehninger, G. and Schmidt, C. A. (2002): Role of a-1 acid glycoprotein in patients with Ph+ Chronic Myeloid Leukemia under treatment with STI571: determination of plasma protein and mRNA levels during the first 10 weeks of therapy, *Blood Cells Mol Dis* (vol. 28), No. 1, pp. 75-85.

Kreuzer, K. A.; Saborowski, A.; **Lupberger, J.**; Appelt, C.; Na, I. K.; le Coutre, P. and Schmidt, C. A. (2001): Fluorescent 5'-exonuclease assay for the absolute quantitation of Wilms tumour gene (WT1) mRNA: Implications for monitoring human leukaemias. *Br J Haematol* (vol. 114), No. 2, pp. 313-8.

Kreuzer, K. A.; Bohn, A.; **Lupberger, J.**; Solassol, J.; le Coutre, P. and Schmidt, C. A. (2001): Simultaneous absolute quantification of target and control templates by real-time fluorescence RT-PCR using 4-(4'-dimethylamino-phenylazo) benzoic acid (DABCYL) as a dark quencher dye, *Clinical Chemistry* (vol. 47), No. 3, pp. 486-490.

ORAL PRESENTATIONS

Lupberger, J.; Luckow, A.; Pairan, A. and Hildt, E. (2006): Nuclear import of the hepatitis B virus polymerase is mediated by a bipartite NLS and depends on CKII phosphorylation. *International Meeting on HBV Viruses*, Vancouver, Canada.

Lupberger, J.; Luckow, A. and Hildt, E. (2005): HBV polymerase harbors a bipartite nuclear localization signal, which is subjected to tight regulation. *Fourth workshop of the study group: "Cell biology of Viral Infections" of the German Society for Virology*, Deidesheim, Germany.

POSTER

Brandenburg, B.; Gutzeit, C.; Koeck, J.; **Lupberger, J.** and Hildt, E. (2006): Entry and post-entry-trafficking of HBV in primary tupaia hepatocytes require the integrity of the actin cytoskeleton. *International Meeting on HBV Viruses*, Vancouver, Canada.

Lupberger, J.; Luckow, A. and Hildt, E. (2005): HBV polymerase harbors a bipartite nuclear localization sequence, which is tight regulated by protein kinases CKII and PKC. *International Meeting on HBV Viruses*, Heidelberg, Germany.

Mund, A.; **Lupberger, J.** and Hildt, E. (2005): Cultivation of HepG2.2.15 on spherical microcarrier: A significant higher yield of HBV and less subviral particles. *Annual Meeting of the German Society for Virology*, Hanover, Germany.

Lupberger, J.; Mund, A.; Salewsky, B.; Kieselmann, O. and Hildt, E. (2004): The HBV Polymerase: Recombinant RT Domain is Active. *In vitro* Phosphorylation of Terminal Protein and Spacer. *International Meeting on HBV Viruses*, Woods Hole, MA, USA.

Lupberger, J.; Schneider, M.; Eckhardt, J.; Quiroga, A.; Brandenburg, B. and Hildt, E. (2004): The Functional Characterization of the HBV Polymerase: Colocalization with the Promyelocytic Leukemia Protein (PML). *Annual Meeting of the German Society for Virology, Joint Meeting with "Società Italiana di Virologia"*, Tübingen, Germany.

Lupberger, J.; York, G. M.; Kok, P.; Tian, J.; Liu, P.; Lawrence, A. G.; Stubbe, J. and Sinskey, A. J. (2002): Identification and Characterization of the Intracellular Poly[D(-)-3-Hydroxybutyrate] Depolymerases *phaZ2* and *phaZ3* in *Ralstonia eutropha*. *Meeting of International Symposium on Biological Polyesters*, Muenster, Germany.

le Coutre, P.; Kreuzer, K. A.; **Lupberger, J.**; Na, I. K.; Müller, C.; Gambacorti-Passerini, C.; Appelt, C.; Bonnet, R.; Platzbecker, U.; Holdhoff, M.; Ehninger, G. and Schmidt, C. A. (2001): Role of a-1 acid glycoprotein in patients with Ph⁺ Chronic Myeloid Leukemia under treatment with STI571: determination of plasma protein and mRNA levels during the first 10 weeks of therapy. *43rd Meeting of the American Society of Hematology*, Orlando, USA.

Kreuzer, K. A.; le Coutre, P.; Na, I. K.; **Lupberger, J.**; Appelt, C.; Saborowski, A. and Schmidt, C. A. (2001): Assessment of minimal residual disease (MRD) by quantitation of Wilms tumor gene (WT1) mRNA in acute myelogenous and lymphatic as well as chronic myelogenous leukemia. *Acute Leukemias IX - Prognostic Factors and Treatment Strategies*, München, Germany.

Kreuzer, K. A.; le Coutre, P.; Na, I. K.; **Lupberger, J.**; Saborowski, A. and Schmidt, C. A. (2001): Wilms tumor gene (WT1) mRNA quantitation by real time fluorescence RT-PCR is a powerful tool to monitor the disease course of acute myelogenous and lymphatic as well as chronic myelogenous leukemia. *27th Annual Meeting European Group for Blood and Marrow Transplantation (EBMT)*, Maastricht, Netherlands; *Bone Marrow Transplant* (2001), (vol. 27), No. S1, pp. 29.

Kreuzer, K. A.; le Coutre, P.; Saborowski, A.; **Lupberger, J.**; Appelt, C.; Na, I. K.; Bohn, A. and Schmidt, C. A. (2000): In vitro treatment of chronic myeloid leukemia cells with STI571 leads to an equal reduction of Wilms tumor gene (WT1) and bcr/abl mRNA transcripts. *42nd Meeting of the American Society of Hematology*, San Francisco, USA.